THE AMERICAN PHYSICAL SOCIETY

OFFICERS OF THE SOCIETY

President	K. T. Compton	Princeton University, Princeton, N.J.
Vice-President	Henry G. Gale	University of Chicago, Chicago, Ill.
Secretary	H. W. Webb	Columbia University, New York City.
Treasurer	G. B. Pegram	Columbia University, New York City.
Editor	Jesse T. Tate	University of Minnesota, Minneapolis, Minn.
Assistant Secretary for the Pacific Coast	D. L. Webster	Stanford University, Calif.

THE PHYSICAL REVIEW

Published monthly — Two volumes annually

First series. From July 1, 1893 to January 1, 1913 the Review was conducted by Edward L. Nichols, Ernest Merritt and Frederick Bedell, with the financial support of Cornell University. The first four volumes were issued annually; subsequent volumes, semi-annually; thirty-five volumes in all.

Second series. On January 1, 1913 the Review was transferred to the American Physical Society as announced on the first page of the new series which was then begun. Since then it has been conducted by a Board of Editors elected by the Society. Semi-annual volumes begin in January and July.

Contributors are referred to page 2 of the advertisements for further information.

General Subscription, throughout the Postal Union, $5.00 in advance.

Single Copies, $.65.

General Index, 1893-1920, $4.00, in advance.

Back Volumes, $4.50 per volume; Back Numbers, $.65 per copy. Postage is free if remittance accompanies order; otherwise postage is extra. No bound volumes can be supplied. The Review offers to purchase a limited number of First Series, Vol. 1, No. 1 ($1.50 each); Second Series, Vol. 7, No. 1, January 1916; Vol. 7, No. 2, February 1916; Vol. 7, No. 4, April 1916; and Vol. 7, No. 5, May 1916 (at $1.50 each).

Advertisements. Rates will be supplied by the Editor on request. Copy for each number must be received at Minneapolis before the 1st of the preceding month; old copy is used until new copy is received. Send electrotypes direct to the printers, George Banta Publishing Co., Menasha, Wisconsin.

Discount of 20% percent is allowed subscription agencies and members of the American Physical Society.

Changes of address and Complaints of failure to receive the Review, in the case of members of the Physical Society, should be addressed to the Treasurer; otherwise, to the Editor. *New copies will be sent free only if complaint is received within three months of date of issue.*

Communications should be addressed to the Physical Review, 1300 University Ave. S.E., Minneapolis, Minn.

Entered at the postoffice at Minneapolis, Minn., as second class matter.
Acceptance for mailing at special rate of postage provided for in section 1103, Act of October 3, 1917, authorized September 2, 1919.

Second Series *April, 1927* *Vol. 29, No. 4*

THE

PHYSICAL REVIEW

THE CARBON ATOM MODEL AND THE STRUCTURE OF DIAMOND

By R. B. Lindsay

Abstract

Electron orbits in the neutral carbon atom.—The atomic model of carbon used is assumed to have four 2_1 orbits. The dimensions of these orbits are computed by a method outlined in a previous paper using various assumptions as to screening, viz.: (a) spherical distribution of charge about the nucleus; (b) orientation in orbital planes with random phase relations; (c) orientation in orbital planes with definitely assigned phase relations. All the methods yield a value of the aphelion distance in the close vicinity of $2.00a_0$, where $a_0 = .532$A, agreeing well with the "radius" as obtained from the atomic volume, i.e. $2.06a_0$. The orbital energies, however, vary from $0.36\ e^2/a_0$ to $0.76\ e^2/a_0$ according to the screening assumption used, the largest value being obtained under hypothesis (c).

Approximate calculation of the lattice energy of diamond.—The atom models as computed under assumption (c) are distributed in the diamond lattice, and the field on any electron due to the rest of its own atom and to neighboring atoms is calculated as a function of the distance from the nucleus assuming that: (1) the orbital plane of the electron is oriented in a certain symmetrical way relative to the lines joining its nucleus to those of the neighboring atoms; (2) for a first approximation only the four nearest atoms need be considered as effective; (3) the effect of the electrons in the neighboring atoms is that of a time distribution of their charges in their orbital planes, disregarding definite phase relations such as have been assumed by previous writers. An approximate expression for the increase in energy of the electron due to the neighboring atoms is developed, and the calculation of the lattice energy per electron for various values of a, the lattice constant, is carried out. It is found that a has an upper limit of $3.00a_0$. In particular the lattice energy for $a = 2.74a_0$ comes out to be $0.55Rh$, and the corresponding heat of sublimation is 171 k. cal. per mol. The experimental value for a is $2.90a_0$ and for the heat of sublimation from 168 to 177 k. cal. per mol. The limitations of the method employed are emphasized.

Introduction

THE Bohr model of carbon consists of a nucleus with six positive charges surrounded by six electrons. Two of these electrons move in 1_1 orbits relatively near to the nucleus, while the original assumption of Bohr was that the four outer electrons move in 2_1 orbits whose planes are arranged in tetrahedral symmetry. This arrangement was suggested by the peculiar chemical behavior of carbon. Recent work by Fowler[1] on the spectrum of

[1] A. Fowler, Proc. Roy. Soc. **A105**, 299 (1924).

singly ionized carbon has seemed to cast doubt on this scheme. Fowler finds that the analysis of this spectrum points to the presence of a 2_2 orbit in ionized carbon. This might indicate in neutral carbon two 2_1 and two 2_2 orbits instead of the four 2_1 orbits previously assumed. The present writer is not yet sure that this is a necessary result of Fowler's work. Moreover there appear to be difficulties in fitting a 2_2 orbit of the energy required by Fowler's results in the field of the two 1_1 and two 2_1 orbits. These difficulties are not so great in the case of the possible two 2_2 orbits in neutral carbon; nevertheless simple preliminary calculations for such a model result in orbits too large to agree well with the dimensions of the neutral carbon atom as estimated from crystal structure and other sources. The writer hopes to discuss this matter fully in a later paper. In the present paper however, calculations on the orbits in the carbon atom and on the crystal structure of diamond will be carried out on the assumption that neutral carbon has four 2_1 orbits.

I. Orbits in the Carbon Atom Model

The first task in making any calculations on the carbon crystal structure is to estimate the orbits in the neutral carbon atom. The 1_1 orbits provide no difficulty for the electrons moving in them are so close to the nucleus that their influence on the other electrons of the same atom and on the electrons of other atoms may be accounted for merely by deducting two units from the charge on the nucleus. As a matter of fact, simple calculation based on assumptions made by the author in previous work[2] shows that the radius of the 1_1 orbits is about $0.2\,a_0$, where a_0 is the radius of the smallest orbit in hydrogen and equals 0.532×10^{-8} cm.

The estimation of the 2_1 orbits may be carried out in a number of ways. First, we may use the general method suggested by the writer in previous work on the models of the alkali atoms[2] wherein the assumption is made that the screening on any given electron due to all the others is the same as that due to a spherical distribution in shells about the nucleus. This scheme takes no account of the possible existence of definite phase relations among electrons in the same group, and it also neglects the orientation of orbital planes. Moreover, it makes the effective nuclear charge on each electron at aphelion in a 2_1 orbit equal to one unit. Since the computation procedure using this method has been fully described in the papers of the writer above referred to, it will be unnecessary to discuss it further here. In what follows it is referred to as Method I.

A second method makes the assumption that there is orientation of orbital planes, and in particular that the planes of the four 2_1 orbits are arranged so as to be perpendicular respectively to the lines from the center to the vertices of a regular tetrahedron. The screening of a given electron due to the others in the same group is then assumed to be that of time distributions of the charges of the other electrons throughout their planes,

[2] R. B. Lindsay, Jour. Math. and Phys., Mass. Inst. of Tech. 3, 191 (1924). See also: Jour. Opt. Soc. of Amer., 11, 17 (1925).

thus still neglecting phase relations. Since this method is used in Part Two in the calculation of field values in the case of the diamond, it will be well to indicate it at some length here.

The problem here is to determine the average screening potential V^s at a point in one plane due to a time mean distribution of the charges of the other three electrons in their planes. The procedure will be first to compute the potential due to a circular ring of charge and then to integrate over all such rings from perihelion to aphelion.

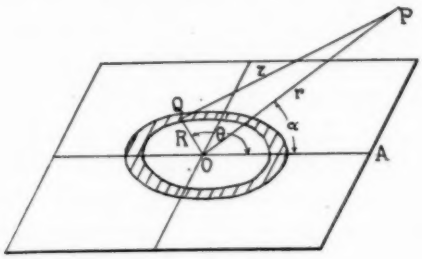

Fig. 1.

Consider the orbital plane shown in Fig. 1. Let O be the nucleus of the atom. It is desired to find the potential energy of an electron at P. If the charge per unit length of the ring is $q_0 e$ (e being the charge on the electron, or "unit" charge, as it has been called above), then

$$V^s_{R,R+dR} = e^2 q_0 \oint ds/z \tag{1}$$

$$= 2e^2 q_0 R \int_0^\pi (r^2 + R^2 - 2rR\cos\alpha\cos\theta)^{-1/2} d\theta$$

$$= 2e^2 q_0 R f(r, R) \tag{2}$$

where $f(r, R)$ is used to denote the integral. Now $q_0 = q/2\pi R$, where q is the total fraction of e which lies between R and $R+dR$. If the time spent by the electron between R and $R+dR$ is dt, and the total period of revolution of the electron is T, then $q = dt/T$. We therefore have

$$V^s_{R,R+dR} = (e^2 dt/\pi T) f(r, R)$$

and the potential energy of an electron at P due to the complete orbit will be

$$V^s = \int_{R(\min)}^{R(\max)} (e^2/\pi T) f(r, R) dt \tag{3}$$

Our next task is to evaluate $f(r, R)$. Making the substitution $2\psi = \pi - \theta$ and letting $b = (r^2 + R^2)/2rR \cos\alpha$, this reduces to the well known form

$$f(r, R) = (rR\cos\alpha)^{-1/2} \int_0^{\pi/2} 2[\tfrac{1}{2}(b+1)]^{-1/2} [1 - 2\sin^2\psi/(b+1)]^{-1/2} d\psi$$

$$= kK(rR\cos\alpha)^{-1/2} \tag{4}$$

where K is the complete elliptic integral of the first kind, and

$$k=[2/(b+1)]^{1/2}.$$

From the time equation of the orbit, derived by the Hamilton-Jacobi method, we have[3]

$$dt=mdR[2m(E-V)-k'^2h^2/4\pi^2R^2]^{-1/2} \tag{5}$$

where E and V denote respectively the total energy of the orbit and the potential energy of the electron at the distance R from the nucleus. The mass of the electron is indicated by m and k' is the azimuthal quantum number, h being Planck's constant. On substitution into the formula (3) we finally have for the screening potential at P:

$$V^s=\frac{(e^2/\pi a_0)\int_{R(\min)}^{R(\max)} Kk[Rr\cos\alpha/a_0^2]^{-1/2}[2(E-V)-k'^2a_0^2/R^2]^{-1/2}d(R/a_0)}{\int_{R(\min)}^{R(\max)}[2(E-V)-k'^2a_0^2/R^2]^{-1/2}d(R/a_0)} \tag{6}$$

where a_0 is as before the radius of the smallest orbit in hydrogen, which forms the natural unit of distance for this kind of calculation.

On introducing now the assumption of tetrahedral symmetry, it is clear that if the point P lies in any one of the other three orbital planes, the angle α in the expression for V^s may take on values from a certain minimum value $\alpha_0\equiv$arc cos (1/3) to a maximum value arc cos 1, depending on where P is taken in its orbital plane. The natural thing to do here, then, would be to take an average of V^s over this range of values. Actually it is found by computation to be accurate enough to consider this average as given by V^s for $\alpha=$arc cos (0.8). Since this average will be the same for each of the other three electrons (because of the tetrahedral symmetry), to get the total screening potential at the point P, we need only multiply the value obtained in (6) by three.

In the calculation of V^s by (6) it is of course necessary to proceed by approximations, since the true orbit is not known to begin with. For this purpose it will be convenient to begin with an orbit which we have reason to believe is a first approximation to the true orbit, such as an elliptic orbit or better the orbit calculated according to Method I. For this orbit we know the value of the expression $[2(E-V)-k'^2/(R/a_0)^2]^{1/2}$ as a function of R/a_0, and hence the computation of V^s for any value of r can be carried out. From this we get a new V as a function of r and proceed to calculate the new orbit. Therefrom we can make a new time distribution leading to a new calculation of V^s and so get a second approximation. As was found in previous work of the writer,[2] this does not prove so tedious as might be imagined. The actual procedure in computing the orbit follows so closely the lines amply worked out by the author in the papers above referred to that it will be unnecessary to speak further of it here. In what follows

[3] Loc. cit., see page 203 ff.

this second method of working out the orbit will be referred to as Method II.

A third possible method goes a step further and to the assumption of the orientation of the orbital planes in tetrahedral symmetry adds the hypothesis that the electrons move in their orbits in definite phases with respect to each other. It should at once be emphasized that this step involves the abandonment of the cubical symmetry characteristic of the previous methods, both as regards instantaneous and time average positions of the electrons. This introduces a further element of arbitrariness into the work which is justified only by the interest which has been aroused by the discussion of phase phase relation assumptions in atomic model calculations.[4] There are a variety of hypotheses which may be made. Three particularly simple schemes suggest themselves, as follows. (I) The four electrons are at any instant all equidistant from the nucleus (i.e. they form a pulsating system). (II) The four electrons are grouped in two pairs, the electrons of each pair being equidistant from the nucleus at any instant and one pair being the other in phase by $T/2$ where T is the period of revolution. In this case there are two electrons at perihelion while the other two are at aphelion, etc. (III) The four electrons pass through perihelia at successive intervals of time equal to $T/4$. Of these schemes the first is extremely unlikely, as has been pointed out by the present writer in a previous paper.[2] Moreover, simple calculations based on it show that it would necessitate orbits which are far too large to fit reasonably any experimental data. The second and third plans are, however, worthy of consideration. In making calculations on any phase-relation scheme we can use two general methods of procedure, one of which is more arbitrary than the other.

In the first place we can suppose that each electron at any instant screens the others as a uniformly charged ring with radius equal to its distance from the nucleus at that instant. In this case, then, to calculate the screening potential on any electron due to the others at a given instant we determine from the assumed phase relation the position of the other electrons in their orbital planes at that instant and apply Eq. (2) above. This involves a knowledge of the time distribution of the charge on each electron orbit which is given by equation (5). On this plan the particular position of the orbit in its plane has no significance. The fact that the orbits rotate in their planes indicates that this is not a very arbitrary assumption. Calculations carried out under this plan using either of the two phase-relation hypotheses II and III will be referred to in what follows under A_1 and A_2 respectively.

Another way of applying the phase-relation assumptions will be to fix definitely not only the orientation of the orbital planes, but also the orientation of the orbits in their planes with respect to each other. This plan is

[4] In this connection one of the Editors has kindly pointed out that the actual schemes which the author has devised for introducing phase relations (see discussion on page 502) are equivalent to; (1) an arrangement with twofold rotational symmetry about one of the original fourfold axes of the cube with no plane of symmetry and (2) an arrangement with twofold symmetry about one of the original fourfold axes of the cube with two planes of symmetry meeting at right angles in this axis and with no other symmetry.

arbitrary in that it affords wide room for choice. The fact, however, that in all this work we are retaining the basic assumption that each electron moves in an effectively central field of force helps to narrow the possibilities to some extent. In other words, it is desirable to arrange the orbits with respect to each other in such a way that the screening potential for any electron at a given distance r_0 from the nucleus is the same as that for any one of the other electrons when the latter is at distance r_0 from the nucleus. This acts to introduce a kind of symmetry into the orientation of the orbits. The writer has tried two modes of arrangement under this plan. In both of these the assumption is made that the four orbits are divided into pairs in such a way that the major axes[5] of each pair lie in the plane formed by the normals through the nucleus to the planes of the orbits of that pair. The distinction between the two modes lies in the choice of angle between the major axes of a given pair. This angle can be either arc cos (1/3) or arc cos (−1/3). The former possibility is chosen in the first mode and the latter in the second mode. To make matters somewhat clearer, let us consider Fig. 2 in which *O* represents the nucleus and *OA*, *OB*, *OC*, *OD* represent the lines from the center to the vertices of a regular tetrahedron.

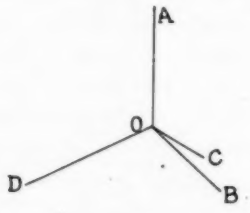

Fig. 2.

Then if we number the 2_1 electrons 1, 2, 3, 4, respectively, the orbital planes 1, 2, 3, 4 will be normal respectively to *OA*, *OB*, *OC*, *OD*. Table I indicates the specific arrangements corresponding to the first and second modes.

TABLE I

Arrangement of orbital planes in carbon atom.

Mode I				Mode II			
Major axis of orbit	Normal to	Lies in plane	Directed away from	Major axis of orbit	Normal to	Lies in plane	Directed
1	*OA*	*AOD*	*OD*	1	*OA*	*AOB*	as *OB*
2	*OB*	*BOC*	*OC*	2	*OB*	*AOB*	from *OA*
3	*OC*	*BOC*	*OB*	3	*OC*	*COD*	as *OD*
4	*OD*	*AOD*	*OA*	4	*OD*	*COD*	from *OC*

From the table it follows that in the first mode electron orbits 1,4 and 2,3 form pairs with angle between the major axes of the components of each

[5] In the case of these orbits which are not real ellipses the major axis is defined as the line joining the nucleus and the electron when the latter is at aphelion, and its positive direction is away from the nucleus.

pair equal to arc cos (1/3), while in the second mode electron orbits 1,2 and 3,4 form pairs with the corresponding angle equal to arc cos $(-1/3)$.

In applying each of these modes of arrangement it is necessary to develop formulas for the distance between any two electrons at any instant. From these the screening potential on an electron at a given distance from the nucleus can at once be calculated using the assumed phase relations. If we denote the polar coordinates of the four electrons in their orbital planes by (r_1, ϕ_1), (r_2, ϕ_2), (r_3, ϕ_3), (r_4, ϕ_4)[6] and the distance from electron 1 to electron j at any instant as r_{1j}, we have

$$r_{1j}^2 = r_1^2 + r_j^2 - 2r_1 r_j \cos(r_1, r_j) \tag{7}$$

where j takes the values 2, 3, 4 in rotation. To use this expression, it is necessary to have formulas for cos (r_1, r_j). These are developed by the use of the analytic geometry formula for the cosine of the angle between two lines, viz.

$$\cos(r_1, r_j) = \cos\alpha_1 \cos\alpha_j + \cos\beta_1 \cos\beta_j + \cos\gamma_1 \cos\gamma_j \tag{8}$$

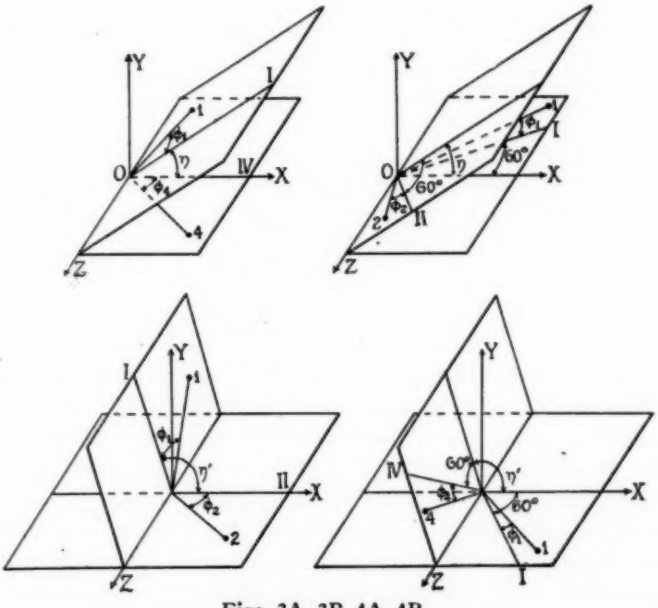

Figs. 3A, 3B, 4A, 4B.

where α_1, β_1, γ_1 are the direction angles of r_1 with respect to an appropriately chosen set of rectangular axes and α_j, β_j, γ_j are the corresponding angles for r_j. The following diagrams (Figures 3A, 3B, 4A, 4B) will serve to indicate the method chosen for the derivation of the values of cos (r_1, r_j), and will also make clear the cardinal features of each mode of arrangement. Figures 3A and 3B (top) refer to the first mode of arrangement and Figures 4A and 4B refer to the second. In each case *OI*, *OII*, *OIII*, *OIV* represent the major axes

[6] It is to be understood that the angle ϕ is in each case the angle made by the radius vector with the positive direction of the major axis.

of electrons 1, 2, 3, 4 respectively. The angles η and η' are arc cos (1/3) and arc cos $(-1/3)$ respectively. In the first mode of arrangement it is unnecessary to provide a separate diagram for 03 because the symmetry enables us to deduce cos (r_1, r_3) from the expression for cos (r_1, r_2). A similar explanation holds in the case of the second mode. Applying formula (8) to these diagrams, we deduce the following expressions: For the first mode of arrangement

$$\begin{aligned}
\cos(r_1,r_2) &= (1/3)\cos(60^\circ+\phi_1)\cos(60^\circ-\phi_2)-\sin(60^\circ+\phi_1)\sin(60^\circ-\phi_2)\\
\cos(r_1,r_3) &= (1/3)\cos(60^\circ-\phi_1)\cos(60^\circ-\phi_3)-\sin(60^\circ-\phi_1)\sin(60^\circ-\phi_3)\\
\cos(r_1,r_4) &= (1/3)\cos\phi_1\cos\phi_4-\sin\phi_1\sin\phi_4
\end{aligned} \tag{9}$$

For the second mode of arrangement

$$\begin{aligned}
\cos(r_1,r_2) &= -(1/3)\cos\phi_1\cos\phi_2-\sin\phi_1\sin\phi_2\\
\cos(r_1,r_3) &= \ (1/3)\cos(60^\circ+\phi_1)\cos(60^\circ+\phi_3)-\sin(60^\circ+\phi_1)\sin(60^\circ+\phi_3)\\
\cos(r_1,r_4) &= -(1/3)\cos(60^\circ-\phi_1)\cos(60^\circ-\phi_4)+\sin(60^\circ-\phi_1)\sin(60^\circ-\phi_4)
\end{aligned} \tag{10}$$

Calculations have been carried out using phase relation assumption III (page 501) with the two arrangements corresponding to (9) and (10). In what follows these will be referred to as B_2 and B_2' respectively. In making the calculations it has been assumed that electrons 2 and 3 are at $r_{T/4}$ (i.e. the distance from the nucleus corresponding to $t = T/4$) when electrons 1 and 4 are at perihelion and aphelion respectively; the sense of rotation for each orbit is taken to be counterclockwise to one looking inward toward O from A, B, C, D, respectively.[7]

In the case of any of the above specified methods of using definite phase relations, the fixation of the orbit after the determination of V as a function of r proceeds as in the previous cases. After V^s and therefrom V have been calculated from a first approximation to the orbit, a properly quantized orbit in this field is developed by the method of approximations above indicated. In what follows any plan involving the use of phase relations will be referred to under Method III with the appropriate subdivision indicating the special scheme under which the method is applied.

The results of the calculations based on the foregoing assumptions are presented in Table III which gives the values of the aphelial distances, orbital energies, and effective quantum numbers of the 2_1 orbits in neutral carbon according to the various methods used. The orbital energy is defined by the formula

$$E = -2\pi^2 N^{*2} e^4 m / h^2 n^{*2} \tag{11}$$

where e, m, and h have the usual significance, while N^* is the effective nuclear charge at aphelion and n^* is the effective quantum number.[8] The values of E are given in multiples of e^2/a_0.

[7] For mode B_2' this is varied by having electrons 1 and 3 revolve counterclockwise while 2 and 4 revolve clockwise.

[8] Loc. cit., see page 192.

TABLE III

	Method I	Method II	Method III			
			A_1	A_2	B_2	B_2'
r_{max}/a_0	2.08	2.12	2.15	1.95	1.85	1.95
E	−.36	−.49	−.40	−.50	−.69	−.76
n	1.17	1.28	1.22	1.23	1.32	1.41

In examining the results, it is interesting to note that the dimensions of the 2_1 orbit come out very nearly the same by all the methods, nor is there any systematic divergence. The actual values computed for r_{max} agree rather well with the "radius" of the carbon atom as calculated from the atomic volume. For diamond this latter value is $2.06a_0$. The great divergences noted come in the energy values, the various ways of applying Method III yielding in general higher values than the simpler assumption of the first two methods. We might expect the model yielding the greatest numerical value for the energy and therefore being energetically more stable to be more nearly right. However, the arbitrary nature of the assumptions underlying plans B_2 and B_2' in particular makes it unwise to assume that these yield necessarily the most stable models. What we can be fairly sure of is the size and general time distribution for the 2_1 orbit, since these do not seem to depend very largely on the particular arrangement chosen.

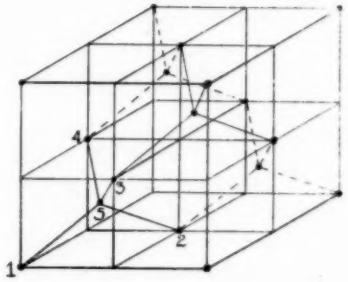

Fig. 5.

II. THE STRUCTURE OF DIAMOND

The crystal structure of diamond is well known to be the tetrahedral type indicated in Fig. 5. Each atom lies at the mid-point of a regular tetrahedron with four others at its vertices, the closest distance between neighboring atoms being designated by a, which has the experimental value 1.54A or $2.90a_0$.

The object of the present investigation is to replace the atoms in the diamond lattice by the models worked out in Part I, and with suitable simplifying assumptions to compute the lattice energy and the heat of sublimation. To carry this out it is necessary first to calculate the potential on any electron in a given atom due to the nucleus and the other electrons in the same atom as well as the nuclei and electrons in the neighboring atoms. For this calculation we must know not only the arrangement of the electron

system in a given atom but also the orientation of the system with respect to the neighboring systems. For the former we have a considerable range of choice, namely the various models worked out in Part I. It is essential, of course, to choose a model wherein the electrons move in definitely oriented orbital planes. As the basis of the present computations the writer has chosen arbitrarily plan B_2' under Method III. To see how the individual atoms are oriented with respect to each other, let us consider atom 5 in Fig. 5. The orbital planes of the 2_1 electrons in this atom are normal respectively to 51, 52, 53, 54, and we assume that the orbits are arranged in these planes according to plan B_2' above. Similarly the orbital planes of the electrons in atom 2 are normal respectively to 52, 53, 54, 51, since they are normal to lines parallel to these lines respectively. And so on in rotation for the others.

We shall not assume, however, definite orientation in their orbital planes of the orbits in atoms 1, 2, 3, 4, but shall consider the effect of the electrons in these atoms on any electron in atom 5 as that due to a time distribution of their charges in their orbital planes. In contrast to the work of other authors who have attacked the same or similar problems, notably Landé,[9] we thus disregard any possible phase relations existing among the electrons

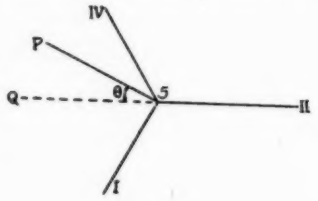

Fig. 6.

in different atoms. It is a matter of some interest, in the opinion of the present writer, to investigate the effect of disregarding such phase relations.

Because of the symmetry it will be necessary to compute V^s as a function of r for a single 2_1 electron in atom 5. For this we must then derive expressions for the distances from this electron to the nuclei of the other atoms and for the angles between these lines and the orbital planes of the electrons in the other atoms. The method of calculation of V^s and V is then identical with that described in full under Method II (pages 499 ff above). In other words we use formula (6), where α now takes a single definite value for each orbital plane considered, and r is replaced by u, the distance from the electron to the nucleus corresponding to that orbital plane. Since the calculation is designed to be only a first approximation it will be sufficient to consider only the four atoms nearest atom 5 in computing V^s. The determination of the distances u and the angles α is a problem in analytic geometry. Consulting for this purpose Fig. 6, let the plane of the paper represent the plane through 5 normal to the line 35, that is, be the plane of the orbit of the electron in atom 5 for which we are to compute V^s. Let 5I, 5II, 5IV, represent the projections on this plane of the lines (see Fig. 5) 51, 52, and 54. Then $r(=5P)$

[9] A. Landé, Zeits. f. Physik. 4, 410 (1921).

and $\theta(=P5Q)$ will be the polar coordinates of the electron considered. Remembering that the angle between each of the lines 51, 52, 54, and its projection is $\phi=\text{arc sin } (1/3)$, and denoting by u_1, u_2, u_3, u_4, the distances from the electron to the nuclei of the four surrounding atoms, we find by application of formula (7):

$$\begin{aligned} u_1^2 &= r^2+a^2+2ar\cos\phi\sin(\theta-30^\circ) \\ u_2^2 &= r^2+a^2+2ar\cos\phi\cos\theta \\ u_3^2 &= r^2+a^2 \\ u_4^2 &= r^2+a^2-2ar\cos\phi\sin(\theta+30^\circ) \end{aligned} \tag{12}$$

If next we denote by α_{jk} the angle between the line u_j and the plane of the kth electron in atom j, we find that

$$\left.\begin{aligned} \sin\alpha_{11} &= -[a+r\cos\phi\sin(\theta-30^\circ)]/u_1 \\ \sin\alpha_{12} &= [a/3+r\cos\phi\sin(\theta+30^\circ)]/u_1 \\ \sin\alpha_{13} &= a/3u_1 \\ \sin\alpha_{14} &= [a/3-r\cos\phi\cos\theta]/u_1 \end{aligned}\right\} \tag{13 A}$$

$$\left.\begin{aligned} \sin\alpha_{21} &= [a/3+r\cos\phi\sin(\theta+30^\circ)]/u_2 \\ \sin\alpha_{22} &= -[a+r\cos\phi\cos\theta]/u_2 \\ \sin\alpha_{23} &= a/3u_2 \\ \sin\alpha_{24} &= [a/3-r\cos\phi\sin(\theta-30^\circ)]/u_2 \end{aligned}\right\} \tag{13 B}$$

$$\left.\begin{aligned} \sin\alpha_{31} &= [a/3-r\cos\phi\sin(\theta-30^\circ)]/u_3 \\ \sin\alpha_{32} &= [a/3-r\cos\phi\cos\theta]/u_3 \\ \sin\alpha_{33} &= a/u_3 \\ \sin\alpha_{34} &= [a/3+r\cos\phi\sin(\theta+30^\circ)]/u_3 \end{aligned}\right\} \tag{13 C}$$

$$\left.\begin{aligned} \sin\alpha_{41} &= [a/3-r\cos\phi\cos\theta]/u_4 \\ \sin\alpha_{42} &= [a/3-r\cos\phi\sin(\theta-30^\circ)]/u_4 \\ \sin\alpha_{43} &= a/3u_4 \\ \sin\alpha_{44} &= [-a/3+r\cos\phi\sin(\theta+30^\circ)]/u_4 \end{aligned}\right\} \tag{13 D}$$

The above formulas (13 *A*, *B*, *C*, *D*) are deduced by the application of the formula (8) to the diamond space lattice shown in Figure 5. To make this derivation somewhat clearer, Figure 7 illustrates diagrammatically the situation for the angles α_{3j}. The plane there represented is the plane normal to 53. The angles which $P3$ makes with the orbital planes of the electrons in atom 3 (viz. α_{31}, α_{32}, α_{33}, α_{34}) are complementary respectively to those[10] which $P3$ makes with the normals to the orbital planes (viz. 31′, 32′, 35,

[10] The smaller angles of course are chosen in each case.

34′ respectively). Now 31′, 32′, 35, 34′ are parallel respectively to 51, 52, 53, 54. We need therefore only use the method set forth in Part One (page 503) to deduce the equations (13*C*). The derivation of the others follows similarly.

The usual procedure at this point would be to assume a definite orbit as a first approximation; then, taking a definite value of a to begin with, to compute the values of V^* and V as functions of r. The fixation of the orbit would then follow the method outlined in Part One. Since, however, we are interested principally in the lattice energy, we can get a first approximation to this quantity without going through the above work. The method is as follows. The new 2_1 orbit, i.e. the orbit in the crystal lattice, will be

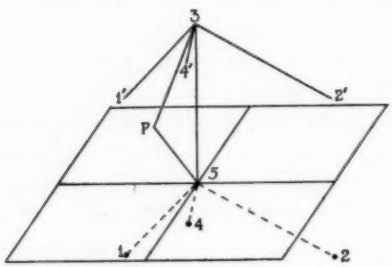

Fig. 7.

quantized with the same quantum number as the 2_1 orbit in the neutral atom. But V^* and V will be different functions of r and the orbital energy will be different. These facts are subsumed in the following equation.

$$\oint [2(E-V)+2(\Delta E-\Delta V)-k'^2/r^2]^{1/2}dr = \oint [2(E-V)-k'^2/r^2]^{1/2}dr \quad (14)$$

where ΔE is the change in energy of the 2_1 orbit due to its presence in the lattice structure and ΔV is the change in V due to the same cause. The integration is taken from r_{min} to r_{max} and back again to r_{min}. Expanding the radical on the left hand side, we have to a first approximation

$$\Delta E = \oint [2(E-V)-k'^2/r^2]^{-1/2}\Delta V dr \Big/ \oint [2(E-V)-k'^2/r^2]^{-1/2}dr \quad (15)$$

In (15) ΔV is, of course, a function of r which can be computed by the method outlined in the immediately preceding pages. The integration can then be carried out and a first approximation to ΔE obtained. It should be emphasized that in calculating (15) the values of $[2(E-V)-k'^2/r^2]^{1/2}$ used are those computed according to plan B_2' explained in Part I. These values will, of course, change slightly for changes in a, the lattice constant, but from the way the radical enters the formula, it is clear that this will not lead to material error.

The lattice energy per atom is given by[11] $\Phi = 4\Delta E$. The corresponding heat of sublimation per molecule which we may denote by H, is given by

[11] A. Landé, loc. cit., page 420.

$H=\Phi L/Q$ where L is the Avogadro number and Q the mechanical equivalent of heat. Here Φ is expressed in multiples of $e^2/2a_0=Rh$, where R is the Rydberg number.

Table IV gives the calculated values of Φ and the corresponding heats of sublimation in k. cal. per mol for various values of a in the vicinity of the experimental value.

TABLE IV

a/a_0	3.0	2.9	2.8	2.74
Φ/Rh	.12	.23	.41	.55
H	38	71	126	171

From these results we may note in the first place that the values of H are of the right order of magnitude. Indeed, the experimental value of a is about $2.90a_0$ and the experimental value of H is about 170 k. cal. per mol. Unfortunately the curve giving H as a function of a does not show a maximum for a value of a in the vicinity of $2.90a_0$. In other words, the method chosen is incompetent to fix the equilibrium value of the lattice constant. That is due to the fact that it breaks down completely as a approaches values in the neighborhood of the aphelial distance of the 2_1 orbits in the carbon atom, viz. $2.0a_0$. Nevertheless it is clear that the method sets an upper limit to the value of a which is approximately $3.0a_0$. For values of a less than $2.5a_0$ the interpenetration of the orbits of the various atoms tends to render our average calculations meaningless, and it seems probable that it will be necessary to fall back to assuming definite phase relations among electron motions in the different atoms when such interpenetration takes place to a great extent.

SLOANE PHYSICS LABORATORY,
YALE UNIVERSITY,
August, 1926.

SERIES SPECTRA OF IONIZED PHOSPHORUS, P_{II}

By I. S. Bowen

Abstract

One hundred and ten of the strong lines of P_{II} have been classified as arising from various combinations between thirty-two terms of the triplet system. The observed terms are exactly those demanded by the Hund theory.

IN previous papers[1] by Professor Millikan and the author the series spectra of one, two, and three-valence-electron atoms of phosphorus (P_{III}, P_{IV}, and P_V) have been analyzed. The present paper is an extension of the same methods, combined with the predictions of the Hund theory, to the analysis of the spectra arising from the four-electron atom of phosphorus, (P_{II}).

According to the Hund theory the various configurations of a four-electron system such as P_{II} should give rise to terms as shown in Table I.

TABLE I

Spectroscopic terms in a four-electron system, according to the Hund theory.

Configuration	Designation	Types of Terms
s^2p^2	a	^3P, ^1S, ^1D
sp^3	b	^5S, ^3S, ^3P, ^3D, ^1P, ^1D
$s^2p \cdot s$	k	^3P, ^1P
$s^2p \cdot p$	m	^3S, ^3P, ^3D, ^1S, ^1P, ^1D
$s^2p \cdot d$	n	^3P, ^3D, ^3F, ^1P, ^1D, ^1F

In Table II which gives the results of this analysis of P_{II} the terms arising from any configuration are designated by the letter appearing opposite it in the second column of Table I. In the case of terms due to the last three configurations of Table I the total quantum number of the excited electron is indicated in the usual way by a numeral preceding the designation of the term. Of course for P_{II} all electrons in the a and b configurations and all electrons except the excited one in the k, m, and n configurations are in three-total-quantum-number orbits.

While five terms arising from the $s^2p \cdot 4d$ configuration have been located, it has been impossible to determine the inner quantum numbers of these terms and consequently to sort them into components of the ^3P, ^3D, ^3F terms that are demanded by the Hund theory for this configuration. This is because certain of the possible lines, the knowledge of whose presence or absence is necessary for the determination of the inner quantum number, so nearly coincide with other strong lines that they could not be detected, even if present. For this reason all of these terms have been indicated by an X.

[1] Bowen and Millikan, Phys. Rev. **25**, p. 295, p. 591, p. 600 (1925).

TABLE II

Triplet series lines of P_{II}

Int.	λI.A.Vac.	ν	Designation	Int.	λI.A.Vac.	ν	Designation	Term Values	
1	782.550	127787.4	aP_1–$4nX_0$	5	3473.86	28786.4	$3nP_2$–$4mP_2$	aP_2	160497.7
0	782.642	127772.3	aP_1–$4nX_2$	3	3479.73	28737.9	$3nP_1$–$4mP_2$	aP_1	160332.4
1	782.960	127720.4	aP_1–$4nX_1$	5	3503.99	28538.9	$3nP_2$–$4mP_1$	aP_0	160027.8
2	783.739	127593.5	aP_2–$4nX_1$	4	3519.60	28412.3	$3nP_1$–$4mP_0$		
0	784.464	127475.6	aP_2–$4nX_{2,0}$	4	3716.90	26904.1	$3nP_2$–$4mD_2$		
1	784.808	127419.7	aP_2–$4nX_2$	3	3762.87	26575.5	$3nP_2$–$4mD_3$	bP_1	50243.8
1	786.146	127202.8	aP_1–$4nX_0$	4	3769.76	26526.9	$3nP_1$–$4mD_2$	bP_0	50205.2
0	810.28	123414.1	aP_2–$5kP_2$	2	3787.76	26400.8	$3nP_2$–$4mD_1$		
1	906.996	110254.1	aP_2–bP_2	4	3794.67	26352.8	$3nP_1$–$4mD_1$		
2	908.046	110126.6	aP_1–bP_2	3	3796.16	26342.4	$3nP_2$–$4mD_1$		
2	908.356	110089.0	aP_1–bP_1	3	4034.81	24784.3	$4mD_1$–$4nX_2$	bD_1	56443.1
2	910.554	109823.3	aP_2–bP_2	3	4037.35	24768.7	$4mD_1$–$4nX_0$	bD_2	56394.7
2	910.884	109783.5	aP_2–bP_1	4	4063.22	24611.0	$4mD_2$–$4nX_0$	bD_0	56301.3
2	961.024	104055.7	aP_0–bD_1	4	4065.78	24595.5	$4mD_2$–$4nX_2$		
3	962.124	103936.7	aP_1–bD_2	5	4073.27	24550.3	$4mD_2$–$4nX_1$		
3	962.568	103888.8	aP_1–bD_1	5	4092.68	24433.9	$4mD_1$–$4nX_1$		
2	964.074	103726.5	aP_2–bD_2	4	4118.24	24282.2	$4mD_2$–$4nX_0$	$4kP_2$	73900.0
3	964.932	103634.2	aP_2–bD_2	2	4121.93	24260.5	$4mD_2$–$4nX_1$	$4kP_1$	73753.6
3	965.400	103584.0	aP_2–bD_1	6	4128.65	24221.0	$4mD_2$–$4nX_2$	$4kP_0$	73372.9
4	1149.970	86958.8	aP_1–$4kP_2$	4	4131.93	24201.8	$4mD_1$–$4nX_0$		
4	1152.825	86743.4	aP_0–$4kP_1$	1	4403.19	22710.8	$4mP_0$–$4nX_1$		
5	1153.995	86655.5	aP_2–$4kP_2$	6	4415.52	22647.4	$4mP_1$–$4nX_0$	$5kP_2$	37153.3
4	1155.020	86578.6	aP_1–$4kP_1$	5	4418.54	22631.9	$4mP_1$–$4nX_2$	$5kP_1$	37042.0
4	1156.985	86431.5	aP_1–$4kP_0$	4	4427.18	22587.7	$4mP_1$–$4nX_1$	$5kP_0$	36606.5
4	1159.105	86273.5	aP_2–$4kP_1$	6	4464.19	22400.5	$4mP_2$–$4nX_0$		
3	1301.865	76812.9	aP_2–$3nP_2$	4	4467.35	22384.6	$4mP_2$–$4nX_2$		
3	1304.485	76658.6	aP_1–$3nP_2$	6	4469.22	22375.3	$4mP_2$–$4nX_1$		
2	1304.655	76648.6	aP_1–$3nP_1$	8	4476.51	22338.8	$4mP_2$–$4nX_2$	$4mS$	54496.2
2	1305.505	76598.7	aP_1–$3nP_0$	4	4484.91	22297.0	$4mP_1$–$4nX_1$		
3	1309.890	76342.3	aP_2–$3nP_1$	7	4532.04	22065.1	$4mP_1$–$4nX_0$		
4	1310.720	76293.9	aP_2–$3nP_0$	2	4535.07	22050.4	$4mP_0$–$4nX_1$		
3	1532.49	65253.3	aP_2–$3nD_1$	7	4556.08	21948.7	$4mS$–$4nX_1$	$4mP_2$	55273.2
3	1535.86	65110.1	aP_1–$3nD_2$	7	4559.31	21933.1	$4mS$–$4nX_0$	$4mP_1$	55195.1
2	1536.38	65088.1	aP_1–$3nD_1$	5	4629.99	21598.3	$4mS$–$4nX_1$	$4mP_0$	54947.8
3	1542.29	64838.6	aP_2–$3nD_2$	6	4680.25	21366.4	$4mS$–$4nX_0$		
2	1543.08	64805.5	aP_2–$3nD_2$	0	4825.18	20724.6	$4mD_1$–$5kP_2$		
1	2455.21	40729.7	$3nD_2$–$4mS$	4	4865.73	20551.9	$4mD_2$–$5kP_2$	$4mD_2$	57332.0
3	2482.71	40278.6	$3nD_2$–$4mP_2$	4	4928.53	20290.0	$4mD_1$–$5kP_1$	$4mD_1$	57158.5
5	2484.90	40243.1	$3nD_2$–$4mP_1$	7	4944.79	20223.3	$4mD_2$–$5kP_2$	$4mD_0$	56829.8
3	2496.70	40052.9	$3nD_1$–$4mP_1$	5	4955.70	20178.8	$4mD_1$–$5kP_0$		
4	2498.08	40030.7	$3nD_2$–$4mP_1$	7	4971.02	20116.6	$4mD_2$–$5kP_1$		
4	2501.68	39973.1	$3nD_1$–$4mP_0$	4	5153.63	19403.8	$4kP_0$–$4mS$		
2	2604.49	38395.2	$3nD_2$–$4mD_2$	6	5192.84	19257.3	$4kP_1$–$4mS$	$3nP_2$	83674.7
3	2606.79	38361.4	$3nD_2$–$4mD_3$	9	5297.55	18876.7	$4kP_2$–$4mS$	$3nP_1$	83685.5
3	2625.54	38087.4	$3nD_1$–$4mD_2$	8	5317.54	18805.7	$4kP_1$–$4mP_2$	$3nP_0$	83733.9
4	2626.94	38067.1	$3nD_2$–$4mD_2$	9	5346.20	18704.9	$4kP_0$–$4mP_1$		
2	2629.33	38032.5	$3nD_1$–$4mD_2$	8	5388.36	18558.5	$4kP_1$–$4mP_1$		
3	2637.56	37913.8	$3nD_1$–$4mD_1$	7	5411.15	18480.4	$4kP_1$–$4mP_0$	$3nD_3$	95246.0
2	2638.97	37893.6	$3nD_2$–$4mD_1$	10	5427.42	18425.0	$4kP_2$–$4mP_2$	$3nD_2$	95225.7
6	3420.21	29238.0	$3nP_2$–$4mS$	7	5501.23	18177.8	$4kP_2$–$4mP_1$	$3nD_1$	95191.0
6	3425.84	29189.9	$3nP_1$–$4mS$	4	5379.60	18588.7	$4mP_1$–$5kP_2$		
4	3427.16	29178.7	$3nP_0$–$4mS$	8	5452.16	18341.4	$4mP_2$–$5kP_2$		
				5	5485.06	18231.3	$4mP_0$–$5kP_1$		
				6	5508.66	18153.2	$4mP_1$–$5kP_1$	$4nX_0$	33130.0
				6	5542.72	18041.7	$4mP_1$–$5kP_0$	$4nX_1$	32897.9
				6	5584.88	17905.5	$4mP_2$–$5kP_1$	$4nX_2$	32608.4
				6	5589.80	17889.7	$4mS$–$5kP_2$	$4nX_3$	32563.0
				2	5729.27	17454.2	$4mS$–$5kP_1$	$4nX_4$	32547.6

As in N_{II}[2] the lines arising from the jump from the sp^3 configuration to the s^2p^2 configuration are present but they are relatively much weaker than in that element, apparently because the term values of the sp^3 configuration lie much closer to the ionization energy of the atom in P_{II} than in N_{II}. The spectrum is also similar to that found by Fowler[3] for Si_I. Just as in Si_I the $3nP$ term is inverted while all others are normal. In this respect the elements of the second row of the periodic table differ from the corresponding elements of the first row. For the lighter elements the $3nD$ term is normal while the bD and the bP terms are inverted.

From the table it is evident that all triplet lines which should be expected to appear strongly have been located. This is still another confirmation of the Hund theory and its great utility in the prediction of spectra.

In the table all wave-lengths above 2400A are taken from Geuter[4] and corrected to I.A. Vac. The term values are determined by making the $4kP_0$ and the $5kP_0$ terms follow a Rydberg formula.

NORMAN BRIDGE LABORATORY OF PHYSICS,
CALIFORNIA INSTITUTE OF TECHNOLOGY.
JANUARY 14, 1927.

[2] Bowen, Phys. Rev. **29**, 231 (1927).
[3] Fowler, Phil. Trans. **225**, p. 1 (1925).
[4] Kayser, Handbuch der Spektroskopie, Vol. VI, p. 246.

THE DIFFUSION OF IMPRISONED RESONANCE RADIATION IN MERCURY VAPOR

By Mark W. Zemansky

Abstract

The rate of diffusion of imprisoned resonance radiation in mercury vapor.—The imprisonment of resonance radiation in mercury vapor was studied by measuring the rate at which resonance radiation emerged from one face of a slab of vapor after the exciting light, incident upon the other face, was cut off. The radiation was found to fall off exponentially, and the exponential constant of decay was measured for vapor densities ranging from 0.77×10^{15} atoms per cc to 29×10^{15} atoms per cc, corresponding to temperatures ranging from 60°C to 130°C. Slabs of two different thicknesses were studied, one 1.95 cm, and the other 1.30 cm. It was found that for vapor densities lower than about 4×10^{15} atoms per cc, the exponential constant varied approximately inversely as the square of the thickness of the slab, in qualitative agreement with the theory of the diffusion of imprisoned radiation as worked out by Milne.

Extension of Milne's theory: broad exciting line; collisions of second kind.—In this region of vapor densities it was found also that the exponential constant decreased with the vapor density. The failure of Milne's results to give quantitative agreement with this result is discussed and it is suggested that this discrepancy is due to the fact that the exciting light in this experiment was a very broad spectral line, and that postulated by Milne of very narrow width. A rough method of extending Milne's theory to include the absorption and imprisonment of frequencies larger and smaller than the heart of the 2536.7 line is discussed, and it is shown that the experimental results can be explained on this basis. At higher vapor densities, the decay constant increased almost linearly with the number of absorbing atoms per cc. It is shown that this result is in accordance with the theory of imprisonment when extended to include impacts of the second kind. The probability of an impact of the second kind between a normal and an excited mercury atom is calculated from the experimental data and found to be approximately 9×10^{-4}.

Introduction

IT IS well known that the fluorescence excited in some solids and liquids persists for a short time after the excitation has been cut off. Wood,[1] and later, Gottling[2] and Wawilow[3] studied the visible fluorescence excited in fluorescine, rhodamine, uranium glass, etc., and found that fluorescence persists after the cut-off of the exciting light for a time, which, in some cases, is as long as 10^{-2} secs.

Phillips[4] investigated the visible fluorescence excited in mercury vapor, and showed that it was carried by a moving column of the vapor a considerable distance past the point of excitation. Since this fluorescence, consisting of a violet and a green band, depends upon the absorption of the

[1] R. W. Wood, Proc. Roy. Soc. **A99**, 362 (1921).
[2] P. F. Gottling, Phys. Rev. **22**, 566 (1923).
[3] S. J. Wawilow and W. L. Lewschin, Zeits. f. Physik. **35**, 920 (1926).
[4] F. S. Phillips, Proc. Roy. Soc. **A89**, 39 (1913).

mercury resonance line 2536.7 this experiment implies that mercury vapor is capable of holding resonance radiation in it for a short time. It does not determine, however, whether this is accomplished by metastable atoms or by repeated atomic absorptions and re-emissions, nor is it suitable to decide this question, since the origin of the visible fluorescent bands is so much in doubt.

The most direct experiment on persistent resonance fluorescence was made by Miss Hayner,[5] who studied the actual resonance radiation emitted by mercury vapor after the excitation was cut off. Miss Hayner used a quartz mercury arc provided with a hot cathode so that it could be struck and cut off very rapidly by a commutator. Light from this arc was incident on one face of a small cylindrical quartz cell containing mercury vapor, and the rate at which the resonance radiation escaped from the other face, after the arc was cut off, was measured. She obtained the result that the resonance radiation fell off exponentially, with an exponential constant that was independent of the density of the vapor, and approximately inversely proportional to the thickness of the slab of vapor. She found also that the resonance radiation did not persist after the cut-off, if the absorption cell was sealed off after evacuation.

In 1912, Wood[6] observed that resonance radiation excited in one portion of a mass of mercury vapor spread to other portions, and, by introducing a small quartz window, established the fact that this diffusion was not due to the movement of atoms. He concluded that the resonance radiation spread by repeated atomic absorptions and re-emissions. This idea was extended by K. T. Compton[7] to explain certain peculiarities in the behavior of the arc. He suggested that resonance radiation becomes imprisoned within a mass of vapor because of the fact that a quantum of radiation is absorbed and re-emitted by many atoms before it finds its way out of the enclosing vessel. Calculations on the basis of this theory were made by Compton and by Webb[8] who used the differential equation of diffusion to calculate the number of excited atoms in a mass of vapor and the rate at which radiation arrives at one boundary.

Recently this problem has received a more rigorous solution by Milne[9] who used the Einstein radiation hypotheses to obtain the differential equation of the diffusion of imprisoned resonance radiation. Considering the vapor enclosed between two infinite planes, and monochromatic radiation incident upon one face, he obtained an exact expression for the radiation arriving at the other face after the exciting radiation was cut off. According to his result, the radiation should fall off exponentially with an exponential constant inversely proportional to: (1) The square of the number of absorbing atoms per cc; (2) The square of the thickness of the slab of vapor.

[5] L. J. Hayner, Phys. Rev. **26**, 364 (1925).
[6] R. W. Wood, Phil. Mag. **23**, 689 (1912).
[7] K. T. Compton, Phys. Rev. **20**, 283 (1922); Phil. Mag. **45**, 752 (1923).
[8] H. W. Webb, Phys. Rev. **24**, 113 (1924).
[9] E. A. Milne, Journ. Lon. Math. Soc. No. 1 (1926).

This result does not agree with Miss Hayner's experimental results, nor has it been possible to account for her results on the basis of any theory. Consequently it was thought worth while to repeat her experiment under better conditions. The following paper contains a description of such experiments and a theoretical discussion of the results.

METHOD AND APPARATUS

The method was essentially the same as that used by Miss Hayner. The total radiation from a water cooled, magnetically deflected quartz mercury arc A (see Fig. 1) passed through a horizontal slit S, 0.5 mm wide,

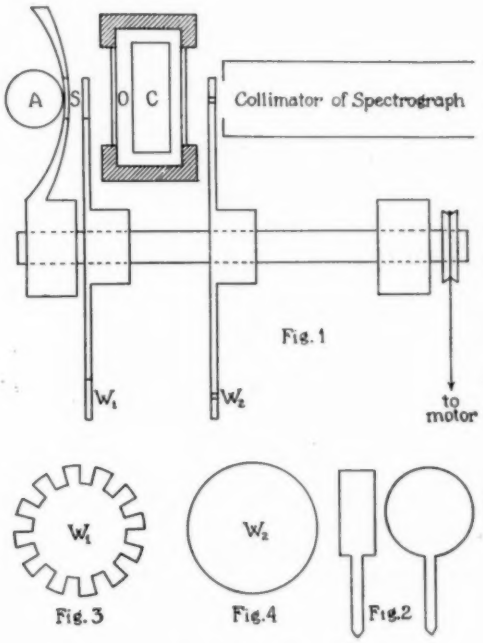

Fig. 1

Fig. 3 Fig. 4 Fig. 2

Figs. 1, 2, 3, 4

into a cylindrical cell C containing mercury vapor. The cell was of clear fused quartz with circular faces 5.1 cm in diameter, (see Fig. 2) which was baked out, evacuated and sealed off with a drop of mercury remaining in the stem. An electric oven O with quartz windows kept the faces and the stem of the cell at constant temperature. Between the oven and the slit there was a rotating wheel W_1 with twelve teeth. (see Fig. 3) The face of the wheel was very close to the slit and the edges of the teeth were parallel to the slit. This arrangement alternately transmitted the light and cut it off twelve times per revolution. Mounted on the same shaft as W_1 was a second wheel W_2 containing two sets of holes, (see Fig. 4) twelve holes in the outer set, and nine in the inner. The diameter of each hole was 0.3 mm. These holes acted as moving slits for a Hilger quartz spectrograph placed as is shown in Fig. 1, causing pairs of curved traces on the photographic

plate, each pair corresponding to one of the mercury arc lines. (see Fig. 5) The two wheels were so adjusted that, just as a tooth on W_1 was about to cover the slit S, a hole in W_2 presented itself in front of the collimator of the spectrograph. After a trace on the plate a few millimeters long (distance AB in Fig. 5) had been made, the tooth cut the exciting light off, and the persistent radiation produced a continuation of the trace (distance BC in Fig. 5). The small, rounded portion at the point B represents the interval of time required for the tooth to cover the breadth of the slit, usually about 10^{-5} secs.

The history of the radiation emitted from the cell after the exciting light was cut off was obtained by measuring the photographic density at different points along each trace; each point corresponding to a known interval of time after the cut-off. Density-time curves were plotted for both traces on the same graph. Since one trace was produced by twelve exposures per

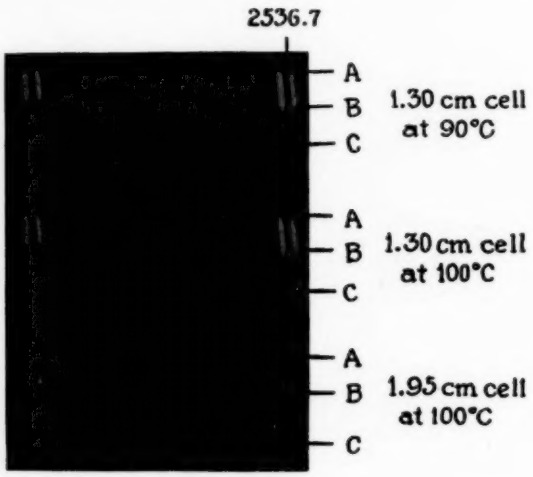

Fig. 5

revolution and the other by nine, corresponding densities represent exposure times in the ratio of 1 to 3/4. In order to determine the intensity relation between corresponding points on the two traces, two photographs were taken on the same plate, one with the usual spectrograph diaphragm, and one with a diaphragm which cut out 1/4 of the light. The trace representing full intensity and 3/4 time, was then compared with the trace representing 3/4 intensity and full time, and it was found that the two traces were identical when the photographic densities were between 0.4 and 0.8; that is, in the linear region of the curve of blackening of the plate. Thereafter, within these limits, the trace produced by nine exposures per revolution was used as a comparison trace representing 3/4 the intensity of the other trace.

On each plate three separate exposures were taken corresponding to three different sets of conditions. One of these was produced by the persistent radiation emerging from the 1.95 cm cell at 100°C. This pair of traces

was used as a standard of comparison and appears as the lowest pair of traces in Fig. 5. The trace representing full intensity is on the left. From these two traces the constant of contrast of the plate, γ, and the exponential constant, $1/T$, for the persistent radiation at 100°C were obtained in the following manner:

The two traces were placed in turn over the circular slit of the densitometer and the photographic densities of all points ten minutes of arc apart were measured. Translating angular distance into time, and plotting all values of photographic density that lay between 0.4 and 0.8 against the time, two curves were obtained, one for the full intensity trace and the other for the 3/4 intensity trace. Each curve consisted of a rapidly decreasing portion, representing a small period during the cut-off of the exciting light, and a linear region representing the persistent radiation. The intersection of these two portions was taken as the instant of cut-off. Calling the density of this intersection point on the full intensity curve D, and the density of the corresponding point on the 3/4 intensity curve D', we have

$$\begin{aligned} D &= \gamma \log I + \text{const.} && (0.4 < D < 0.8) \\ D' &= \gamma \log \tfrac{3}{4} I + \text{const.} && \text{"} \end{aligned} \qquad (1)$$

Whence

$$\gamma = (D - D')/\log_{10}(4/3) = (D - D')/0.125$$

Now, let I be the intensity of the persistent radiation that gives rise to the full-intensity trace, t seconds after the cut-off of the exciting light. Then $I = I_0 e^{-t/T}$ where $1/T$ is the exponential constant to be measured. Combining this equation with Eq. (1) we obtain

$$D = -\gamma t/2.30T + \text{const.}$$

which expresses the fact that the density-time curve is a straight line, when D is between 0.4 and 0.8 with a slope S equal to $\gamma/2.30T$. The exponential constant for the persistent radiation at 100°C was then obtained from $1/T = 2.30S/\gamma$ and that corresponding to any other trace on the plate, from the relation $TS = T'S'$ where T' and S' refer to the second trace.

Procedure and Results

Before exposing the plate, the stem of the cell which contained the drop of mercury was heated to the desired temperature, and the faces to a temperature about 5°C higher. In this way condensation of mercury on the faces of the cell was avoided. The wheels rotating so close to the oven which contained the cell caused a draft which tended to cool the oven, so that, at least three-quarters of an hour had to be allowed for the whole system to attain constancy. The temperature of the stem of the cell and the speed of the wheels remained constant within two percent during an exposure which lasted in most cases about one hour.

No difficulty was found at any time in obtaining imprisonment of resonance radiation in a sealed-off cell. It was evidently not necessary to have

freshly evaporating mercury present, since the liquid mercury remained in the stem of the cell throughout an exposure. Only that pair of traces corresponding to wave-length 2536.7 showed any trace on the plate *after* the cut-off of the exciting light. Although all the mercury arc lines were present in the exciting light, there was never any evidence of absorption and consequent re-emission of any wave-length other than 2536.7. It is, therefore, believed that whatever absorption of other wave-lengths occurred it played a negligible rôle in the imprisonment of the resonance radiation.

The exponential constant of decay of the persistent radiation from the 1.95 cm cell and the 1.30 cm cell at temperatures ranging from 60°C to 130°C (about a 30-fold increase in vapor density) was measured. The saturation vapor pressures of mercury at the temperatures employed were taken from Landolt and Börnstein's tables and the number of atoms per cc corresponding to the different vapor pressures calculated.

The results are presented in Table I. The first and second columns give temperatures and corresponding vapor densities respectively. The third

TABLE I

Rate of decay of resonance radiation emerging from a slab of mercury vapor after the exciting light, incident on other face, is cut off.
T is the time constant in the equation $I = I_0 e^{-t/T}$.

Temp. °C	No. of Atoms per cc $N \times 10^{-15}$	1.95 cm cell		1.30 cm cell	
		$(1/T) \times 10^{-3}$	$T \times 10^{4}$	$(1/T) \times 10^{-3}$	$T \times 10^{4}$
60	0.770	26.6	0.376		
70	1.40	14.2	0.704	28.1	0.356
80	2.50	8.81	1.13	19.3	0.518
90	4.40	7.07	1.41	12.1	0.827
100	7.26	6.89	1.45	9.47	1.06
110	11.8	7.72	1.30	9.00	1.11
120	18.8	9.64	1.04	10.6	0.944
130	29.0	13.2	0.757	13.5	0.740

and fourth columns give the corresponding values of the exponential constant $1/T$ and the time constant T for the cell 1.95 cms thick, and the fifth and sixth columns give the same quantities for the 1.30 cm cell. In Fig. 6 these results are plotted for both cells with the exponential constant as ordinate and the number of atoms per cc as abscissa.

DISCUSSION

In Fig. 6 it is seen that the curves for the two cells are of the same general character. At low vapor densities, the exponential constant of decay of the persistent radiation decreases very rapidly with increasing vapor density; and at high vapor densities, the exponential constant rises nearly linearly with the vapor density. That is, as the number of absorbing atoms increases, the resonance radiation remains imprisoned for a longer and longer time, until a maximum time is reached, after which, any increase in the number of absorbing atoms causes a diminution in the time of imprisonment of the radiation in the vapor.

Let us compare these results with those obtained by Milne. Assuming that one face of an infinite slab of vapor perpendicular to the x axis, is exposed to radiation of very narrow spectral width, and, neglecting molecular motion and impacts, Milne finds that the number of excited atoms per cc, n_2, is given by the equation

$$\frac{\partial n_2}{\partial t} = \frac{1}{4\alpha^2 N^2 \tau} \frac{\partial^2}{\partial x^2}\left(n_2 + \tau \frac{\partial n_2}{\partial t}\right) \tag{2}$$

where τ represents the duration of the excited state produced by absorption of the radiation, N the number of atoms per cc, and α the atomic absorption

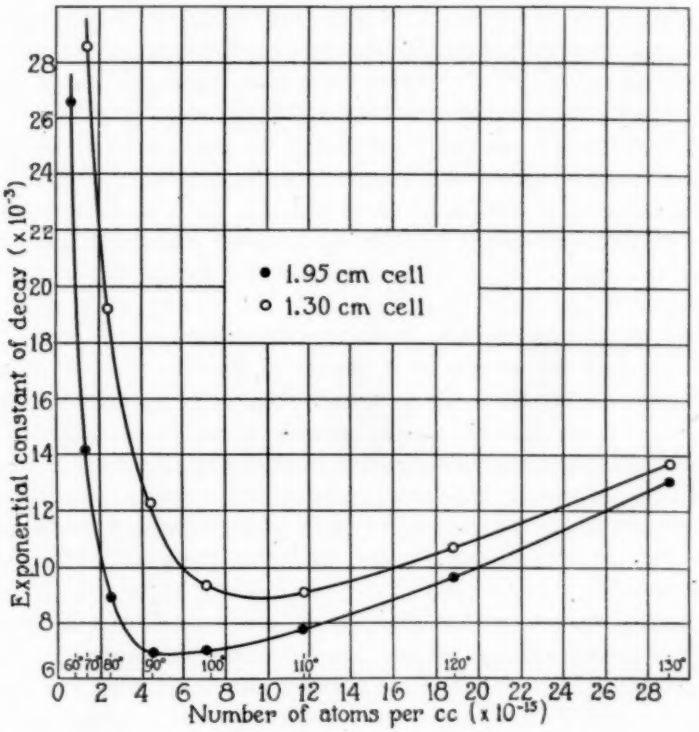

Fig. 6

coefficient for the exciting radiation. The solution of this equation yields the result that the radiation emerging from the far face of the slab after the exciting light, incident on the front face, is cut off, falls off exponentially, with a time constant T given by

$$T = \tau(1 + 4l^2\alpha^2 N^2/\pi^2) \tag{3}$$

where l stands for the thickness of the slab. The duration of the 2^3P_1 state ($2p_2$ state, in the old notation), τ, for mercury is known to be 10^{-7} seconds.[10]

[10] W. Wien, Ann. d. Physik. **73**, 483 (1914); Eldridge, Phys. Rev. **23**, 772 (1924); Phys. Rev. **24**, 234 (1924); Hanle, Zeits. f. Physik. **30**, 93 (1924); Turner, Phys. Rev. **23**, 464 (1924); Tolman, Phys. Rev. **23**, 693 (1924); Breit and Ellett, Phys. Rev. **25**, 888 (1925).

Malinowski[11] and Orthmann[12] measured the absorption coefficient of mercury vapor at a density of about 3×10^{13} atoms per cc for the radiation from a mercury resonance lamp at room temperature, and found a value of approximately 3. This gives for the atomic absorption coefficient a value of approximately 10^{-13} which can be regarded as reliable in order of magnitude at least.

Since, in this experiment, N, the number of atoms per cc, ranged from 0.77×10^{15} to 29×10^{15} and l was 1.95 cm for the thicker slab, and 1.30 cm for the thinner, $4l^2\alpha^2N^2/\pi^2>>1$ and we can write Eq. (3) more simply

$$1/T=\pi^2/4\tau l^2\alpha^2N^2 \tag{4}$$

which is the expression for the exponential constant that would result if, in the original differential equation, Eq. (2), the term $\partial^3n_2/\partial x^2\partial t$ were neglected. Consequently in the region of vapor densities employed in this experiment we may neglect the last term in Eq. (2).

If now, we consider the left-hand part of the experimental curves in Fig. 6 for which $N<4\times10^{15}$ atoms per cc, we see, at first, that the way in which $1/T$ varies with l is in good agreement with Eq. (4) which requires that $1/T$ be inversely proportional to l^2. The ratio of the squares of the thicknesses of the two slabs is 2.2. At 70°C the inverse ratio of the exponential constants is 2.0, at 80°C it is 2.2 and at 90°C, 1.7.

A quantitative comparison, however, between Eq. (4) and the experimental values of the exponential constant for the thicker cell shows a large discrepancy. At 60°C for which $N=0.77\times10^{15}$ atoms per cc, Eq. (4) gives $1/T=1100$ as against the experimental value of 26600. At 70°C, Eq. (4) gives 330 whereas experiment yields 14200. At higher temperatures Eq. (4) gives values of $1/T$ that get rapidly smaller, approaching zero, whereas the experimental curve in Fig. 6 shows a minimum value for $1/T$ of about 7000 at 100°C and an almost linear increase for $1/T$ at higher temperatures.

This lack of agreement between theory and experiment leads us to seek an equation fitting the actual conditions of the experiment more closely than does that of Milne. There are certain obvious differences between the conditions assumed in Milne's development and those actually present in these tests. One of these can readily be disposed of as not materially affecting the quantity in question, $1/T$. The use of a cylindrical enclosure for the vapor instead of an infinite slab affects, for the most part, the functions which are coefficients of the exponential terms in the exact solution of the problem. A simple calculation shows that, for a cylindrical boundary the exponential constant is given by an expression the same as Eq. (4) except that instead of π^2 entering, we have approximately the value 14. This slight difference is unimportant.

Milne's equation does not take into account the gaseous diffusion of excited atoms under the concentration gradient which exists in the slab

[11] Malinowski, Ann. d. Physik. **44**, 935 (1914).
[12] Orthmann, Ann. d. Physik. **78**, 601 (1925).

during the steady state, and the effect of dissipative impacts (impacts of the second kind). This can be done in a manner indicated by Milne in a footnote in his paper, by replacing $\partial n_2/\partial t$ of his paper, which represents the rate at which excited atoms are being formed in a unit volume due to imprisonment, by $\partial n_2/\partial t - g\partial^2 n_2/\partial x^2 + kn_2$ where $g\partial^2 n_2/\partial x^2$ represents the rate at which excited atoms are forming due to gaseous diffusion, and kn_2 represents the rate at which excited atoms are disappearing through impacts of the second kind. From the kinetic theory of gases we have $g = c/3(2)^{1/2}\pi s^2 N$, where c is the root mean square velocity, s the distance between centers at impact, and N the number of atoms per cc; and $k = (2)^{1/2}\pi b s^2 c N$, where b is the probability that an impact between a normal mercury atom and an excited one is of the second kind.

The outstanding discrepancy between Milne's theory and the conditions actually present in this experiment, however, cannot be handled so easily, i.e. the effect of the absorption and imprisonment of frequencies larger and smaller than the heart of the 2536.7 line. There is no doubt that such absorption occurs, for it is known that the breadth of the absorption line at the temperatures studied is much larger than can be explained on the basis of the Doppler effect. The process of the diffusion of these frequencies comprising a broad absorption line must be very complicated, for we cannot consider that the imprisonment processes (repeated absorptions and re-emissions) of all the frequencies are independent of one another. Instead, we must take into account the fact that an atom that picks up a frequency corresponding to one part of the absorption line can re-emit a frequency corresponding to another part. Because of our ignorance of these changes of frequency we are not in a position to treat the effect of the broad absorption line rigorously, but since we are led to believe that the radiation composing the whole absorption line diffuses as a whole through the vapor, we may make the plausible assumption that the total radiation included in the broad absorption line obeys the same law of diffusion as that given by Eq. (2), except that, instead of α standing for an atomic constant (the atomic absorption coefficient), it represents a "mean or equivalent absorption coefficient" which is a function of the line breadth. Denoting by β the equivalent absorption coefficient and taking account of gaseous diffusion of excited atoms and impacts of the second kind between excited and normal atoms, we obtain the differential equation

$$\partial n_2/\partial t + kn_2 = (1/4\beta^2 N^2 \tau + g)\partial^2 n_2/\partial x^2$$

The solution of this equation gives the result that the radiation emerging from the far face of the slab of vapor after the exciting light incident on the front face is cut off, falls off exponentially with an exponential constant, $1/T$, given by

$$\frac{1}{T} = \frac{\pi^2}{4\tau l^2 \beta^2 N^2} + \frac{\pi c}{3(2)^{1/2} l^2 s^2 N} + (2)^{1/2}\pi b s^2 c N \qquad (5)$$

The three terms of the right-hand member represent, in order, the effect of the imprisonment of the whole absorption line, the effect of gaseous diffusion, and the effect of impacts of the second kind.

The second term may be neglected completely, for numerical substitution shows it to be very small for the whole range of values of N. In the parts of the curves in Fig. 6 for which N is small, the third term may also be neglected. Comparison between experiment and the first term of Eq. (5) then, would serve only to determine the value of β as a function of N. Since the meaning of β in terms of physical constants of the vapor is not clear, the actual values of β are of no interest. It may be interesting, however to point out that if $1/\beta$ is taken as a linear function of N, good agreement is obtained between the form of the curves in Fig. 6 and the theoretical curves.

For large values of N the third term is of importance. This term, expressing the effect of impacts of the second kind, represents a linear relation between the exponential constant and N. Since the right-hand parts of the experimental curves in Fig. 6 show a distinct linear rise, we may regard this as strong indication that such impacts exist at these high vapor densities. There is abundant evidence for the existence of such collisions in *mixtures* of mercury vapor and inert gases, and the experiments of Wood and Kimura,[13] and Goos and Meyer[14] indicate that they are present also in pure mercury vapor. The experiments of Franck[15] and his students indicate that the probability of such impacts between normal and excited mercury atoms is small, but do not yield a numerical estimate of this probability.

The results of this experiment can be used to calculate this probability, if we make the assumption that the rise of the exponential constant for large values of N is due solely to impacts of the second kind. For Eq. (5) gives as the slope of the straight line representing this rise $(2)^{1/2}\pi b s^2 c$ and Fig. 6 gives for this slope the value 3×10^{-13} from which b, the probability of an impact of the second kind between a normal and an excited mercury atom, can be calculated in terms of s the distance between centers at impact and c the root mean square velocity of the atoms. With s equal to 6.0×10^{-8} cm, and c equal to 2.2×10^{4} cm/sec, b is found to be approximately 9×10^{-4}. That is, about one out of every thousand collisions between an excited mercury atom and a normal one is of the second kind. This does not contradict the result of Cario that *every* collision between an excited mercury atom and an air molecule is of the second kind, for, if an excited mercury atom pass on its excitation to a molecule of a foreign gas, the excited state of the mercury atom is destroyed; whereas if an excited mercury atom pass on its excitation to a normal mercury atom, there is merely a change in rôle and there still remains an excited mercury atom. Consequently, one would not expect every collision between an excited and a normal mercury atom to be dissipative. Cario's result shows clearly what effect we should expect a small amount of air to have in this experiment. Since the probability of

[13] R. W. Wood and Kimura, Phil. Mag. **32**, 329 (1916).

[14] Goos and Meyer, Zeits. f. Phys. **35**, 803 (1926).

[15] J. Franck, "Anregung von Quantensprüngen durch Stösse," p. 225.

a dissipative impact between an air molecule and an excited mercury atom is one thousand times the probability of such an impact in pure mercury vapor, air, at a pressure of .001 mm should have the same effect as mercury at a pressure of 1 mm. Consequently if there were air, at a pressure of .001 mm present in the cell at 100°C, instead of an exponential constant of 7000 we should expect a value of about 20000. This is approximately the value obtained by Miss Hayner for this temperature, and consequently it is suggested that the presence of a small quantity of air as an impurity liberated from the walls of the quartz absorption cell is a possible explanation of Miss Hayner's results. The failure of Miss Hayner to obtain persistent resonance radiation in a sealed-off absorption cell can be explained on the supposition that the cell was improperly evacuated and sealed off, so that, upon heating, the air pressure rose quickly to a value sufficient to increase the exponential constant to an unmeasureable value.

Further evidence that collisions of the second kind play an important rôle in the phenomenon of the diffusion of imprisoned resonance radiation is furnished by measurements of the opacity of the slab of mercury vapor. According to the simple theory of imprisonment neglecting impacts, the ratio of the incident to the transmitted light is

$$I_0/F_0 = 1 + l\alpha N$$

whereas, rough measurements show that the opacity of the slab for radiation from a cold resonance lamp increases much more rapidly with vapor density. Taking into account impacts of the second kind, the opacity is found to be

$$I_0/F_0 = \tfrac{1}{2}(\tau k)^{-1/2}\sinh 2l\alpha N(\tau k)^{1/2} + \cosh 2l\alpha N(\tau k)^{1/2}$$

which gives results in fair agreement with experiment.

In conclusion, I wish to express my indebtedness to Professor H. W. Webb, at whose suggestion and under whose guidance this work was done; and to Mr. L. J. Buttolph of the Cooper Hewitt Electric Company, I extend my sincere thanks for his kindness in placing at my disposal the mercury arc necessary for this work.

PHOENIX PHYSICAL LABORATORIES,
COLUMBIA UNIVERSITY,
December, 1926.

ON THE SURFACE HEAT OF CHARGING

By Lewi Tonks and Irving Langmuir

Abstract

Calculation of the surface heat of charging for pure metals, for oxide coated metals and for monatomic films.—Two methods are pointed out for calculating the theoretically necessary reversible heat development or absorption accompanying the charging of the surface of a conductor. One method depends on a new relation $\eta_{s1}-\eta_{s2}=kT\ln(A_1/A_2)+\epsilon P_{21}$ between the surface heats, η_s, of the two surfaces, the A's of electron emission equations of the type $i=AT^2\epsilon^{-b/T}$ and the Peltier heat at the interface between the conductors. The other method consists of a comparison of the cooling effect of electron emission and the latent heat calculated from the temperature variation of emission. Experimental evidence points to $\eta_s=0$ (nearly), $A=60.2$ amps/cm^2 deg^2 (nearly) for all pure metals. Oxide coated filaments present a difficulty. For monatomic films the first method gives appreciable values of η_s and experimental data for use in the second method is lacking.

Stopping potentials of Na, K and Li yield further evidence that η_s is very small for all pure metals. The relation between surface heat of charging and certain assumptions fundamental to electron emission theory is discussed.

I. Existence of a Surface Heat of Charging

THERE have long been grounds for believing that charging the surface of a conductor with electricity involves a reversible development of heat. By thermodynamical reasoning the quantity of heat may be estimated as of the order of the contact difference of potential times surface charge. Although by its smallness it has eluded experimental observation, such a surface heat of charging is required theoretically. By thermodynamical reasoning Kelvin showed that

$$dV_{21}/d\ln T=P_{21}' \tag{1}$$

where V_{21} is the contact difference of potential between two conductors, 1 and 2, T is the absolute temperature of the system, and P_{21}' is the heat absorbed by a unit of electricity in passing from the surface of 2 through the conductors and across the interface to the surface of 1. V_{21} is positive when the potential just outside of 1 is higher than that just outside of 2. P_{21}' has frequently been identified with the Peltier heat, P_{21}. With that interpretation, Eq. (1) fails experimentally even in order of magnitude.[1] Kelvin, himself, postulated a surface heat of charging to eliminate the discrepancy. Thus, denoting the heat absorbed when the surface of 1 is given an elementary positive charge by η_{s1}, Kelvin's relation becomes[1]

$$dV_{21}/d\ln T=P_{21}+(\eta_{s2}-\eta_{s1})/\epsilon \tag{2}$$

where $\epsilon=-4.77\times10^{-10}$ e.s.u.

[1] Bridgman, Phys. Rev. **14**, 306 (1919).

II. Calculation of the Heat of Charging for Pure Metal Surfaces

From Boltzmann's equation and the perfect gas laws Richardson first showed that

$$\epsilon V_{21} = kT \ln (i_2/i_1) \tag{3}$$

where k is the Boltzmann constant and i_2 and i_1 are the respective current densities of the emission from the surfaces of 2 and 1 under equilibrium conditions, that is, when all the electrons return to the surface. It seems most unlikely, however, that drawing off the whole emission current should appreciably affect the emission if we accept the electric image force point of view regarding the work function.[2] Eq. (3) gives an easy method for measuring the contact difference of potential, the direct measurement of which is difficult. This value of V_{21} may now be substituted in Eq. (2) giving

$$\frac{P_{21}}{T} + \frac{\eta_{s_2} - \eta_{s_1}}{\epsilon T} = \frac{k}{\epsilon} \frac{d}{dT}\left[T \ln \left(\frac{i_2}{i_1}\right)\right] \tag{4}$$

In many cases the electron emission data from a surface 1, can be accurately expressed by a law of the form

$$i_1 = A_1' T^{\alpha_1} \varepsilon^{-b_1/T} \tag{5}$$

where A_1' and b_1 are constants determined by the data after the constant α_1 has been chosen. But there is quite a range in the values of this constant which fit the data well. Substituting Eq. (5) and a similar one for surface 2 in Eq. (4) we find

$$\frac{P_{21}}{T} + \frac{\eta_{s_2} - \eta_{s_1}}{\epsilon T} = \frac{k}{\epsilon}\left[\ln \frac{A_2'}{A_1'} + (\alpha_2 - \alpha_1)(1 + \ln T)\right] \tag{6}$$

The form of Eq. (4) shows that any law of the type of Eq. (5) which reproduces the value of i and its first derivative at any temperatures gives the correct value to the left member of Eq. (6) at those temperatures.

Now, since the choice of α_1 and α_2 is not critical in accurately representing the data over wide temperature ranges, and since in most cases a value of 2 for these constants fits the experimental results well and has some theoretical basis, we may take them each equal to 2 and thus get

$$\eta_{s_1} - \eta_{s_2} = kT \ln (A_1/A_2) + \epsilon P_{21} \tag{7}$$

where A_1 and A_2 are written for the case $\alpha_1 = \alpha_2 = 2$. To estimate the difference between the surface heats for two surfaces, the terms of the right member must be calculated roughly. We can do this for some pure metal surfaces. P_{21} can be found from thermoelectric data, but unfortunately such data are lacking for the well-known metallic emitters. There is, however, no reason to think that the Peltier heat is materially different from that for platinum against iridium for which data are available. Roughly extrapolating their thermoelectric power,[3] dE/dT, to 2500°K, it is found that $dE/dT = P/T$

[2] W. Schottky, Jahrb. der Radioaktivität u. Elektronik, **12**, 204 (1915).

[3] Smithsonian Physical Tables, 6th Edit., Table 300.

$=3\times10^{-5}$ volts/deg. giving P_{21} a value of 0.075 volt. The values of A for the pure surfaces of the metals tungsten, molybdenum, tantalum[4] and thorium[5] are known to within 15 to 50 percent and A_0 (60.2 amps/cm^2 deg^2) is a possible value for each. Hence, for these metals, and perhaps for pure metals in general, we may put $1/1.5<A_1/A_2<1.5$ so that $(kT/\epsilon)\ln\ (A_1/A_2)<(2500/11{,}600)\times0.4=0.086$ volt in absolute value. It follows then that the absolute value of $\eta_{s1}-\eta_{s2}$ is less than 0.16 volt at 2500°K. It thus appears that the surface heats of charging of all pure metals do not differ from each other by more than a few percent of their work functions.

There is another method for evaluating η_s. Bridgman[1] has pointed out that three latent heats are involved in electron emission. First there is the latent heat of vaporization, η, which is absorbed when an electron evaporates from an isolated body into an electron atmosphere maintained at constant pressure. The body is left with the corresponding elementary positive charge. This quantity appears in the Clapeyron Equation (see below) applied to electron emission. Second, if everything is the same as above except that an electron flows into the body through a conductor when an electron evaporates, so that the surface charge remains constant during the process, then the latent heat of vaporization is denoted by η_ρ. This is the case in all electron emission experiments and η_ρ can be determined from the cooling effect of the electron emission. Third, if the body be simply given an elementary positive charge, the latent surface heat of charging, η_s, is absorbed from the surroundings.

It is easily seen that the second and third processes performed in succession are equivalent to the first, so that

$$\eta=\eta_\rho+\eta_s \tag{8}$$

and η_s can be found as the difference of η and η_ρ.

Since η_ρ applies to the evaporation of electrons under reversible conditions, and the cooling effect is always measured under irreversible conditions, these quantities are not identical. A simple analysis shows how they are related.

When an electron evaporates reversibly into an electron atmosphere maintained at constant pressure, there are three modes of heat absorption. First, there is the energy to free the electron at the temperature of the experiment which may be called $\eta_{\rho T}$. Second $3kT/2$ (on the average) is required to give the electron the proper kinetic energy and third kT is absorbed by a layer of the electron gas located roughly at the distance of the mean free path length from the emitting surface. This is the heat that is converted into the potential energy pdv of expansion.

Under experimental conditions, however, the electrons do not evaporate reversibly, so the energy absorptions may be different. First, the smallness of the Schottky effect shows that $\eta_{\rho T}$ is not changed appreciably when small

[4] Dushman, Rowe, Ewald and Kidner, Phys. Rev. **25**, 338 (1925).
[5] C. Zwikker, Proc. Roy. Acad. Sci. Amst. **29**, 792, (1926).

fields are used. Second, the kinetic energy carried away by each electron is $2kT$ (on the average). This is also true, of course, under reversible conditions, but then the faster electrons return to the surface more quickly leaving the average energy of those which remain in the space $3kT/2$. Third, the electrons evaporate into a space devoid of pressure so that no heat is absorbed in increasing the electron gas volume.

Thus it appears that the measured cooling effect is

$$\eta_c = \eta_{pT} + 2kT + 0$$

whereas the reversible cooling effect is

$$\eta_p = \eta_{pT} + 3kT/2 + kT$$

leading to

$$\eta_p = \eta_c + kT/2 \tag{9}$$

Then η can be found from the temperature variation of the electron emission. The relation is deducible directly from fundamental principles. Clapeyron's Equation applied to electron evaporation gives

$$\eta/kT^2 = d \ln p/dT$$

where p is the pressure of the electron gas. From kinetic theory $p/T^{1/2}\, i$ is a constant independent of T. Making the indicated substitution and noting that $dT/T^2 = -d(1/T)$ we have, in terms of measurable quantities

$$\eta = -k \frac{d \ln (iT^{1/2})}{d(1/T)} .$$

Since, however, emission data are usually plotted in the form $\ln(i/T^2)$ against $1/T$ it is worth while to subtract the identity

$$(5/2)\, kT = -k\, d \ln T^{5/2}/d\,(1/T)$$

from this equation, obtaining[6]

$$\eta - (5/2kT) = -k\, d \ln (i/T^2)/d(1/T) \tag{10}$$

The derivative in the right member is recognized as the "constant" $-b$ of Eq. (5) where $\alpha = 2$. It is to be emphasized, however, that the present derivation puts no requirement on that derivative. This derivation is independent of any assumption regarding the peculiar emitting properties of the surface and is valid whether or not Eq. (5) is valid. For convenience, and at the same time to distinguish between the derivative in Eq. (10) and b, we shall denote the derivative by $-b'$, so that

$$\eta = kb' + (5kT/2) \tag{11}$$

Now, combining Eqs. (9) and (11) in accordance with Eq. (10) we find

$$\eta_s = kb' - \eta_c + 2kT \tag{12}$$

[6] The simplest procedure is to plot $\ln i$ against $1/T$; then Eq. (12) becomes $\eta_s = kb'' - \eta_c$ where b'' is the slope of that curve.

Davisson and Germer[7] have measured both kb'/ϵ and η_c/ϵ for the same tungsten wire. They found the former to be -4.48 v. and the latter -4.91 v. For $T=2270°K$ $2kT/\epsilon=-0.391$ v., so that $-\eta_s/\epsilon=4.48-4.91+0.39=-0.04$ v. This value is less than the probable error of the measurements. Thus the surface heat of charging of tungsten is at most very small. We have already given the evidence that the surface heats for pure metals differ by amounts small compared to the work functions. It follows, therefore, that the surface heat of charging for all pure metals is probably but a small fraction of the work function.

III. The Heat of Charging of Other Surfaces

All the theoretical results obtained so far are directly applicable to surfaces bearing thin films of thorium, caesium, other alkali metals, etc., with the simplification that the Peltier heat can be eliminated if the junction of two metals be avoided by using the pure surface of the metal opposite the film-bearing surface. No measurements on the cooling effect of the evaporation of electrons from such a film are available so that only the difference of two surface heats can be calculated using Eq. (7). But in accordance with our conclusion regarding the magnitude of the surface heat of charging for pure metals we shall assume that for tungsten it is zero. Then, for a film, F, on tungsten Eq. (7) reduces to

$$\eta_{sF}/\epsilon=(k/\epsilon)T\ln(A_F/A_0) \tag{13}$$

This may be immediately applied to the following thermionic emission constants for the complete surface films listed with the results given in the

Type of surface	Mean temp. of observations	A	b	$-\eta_s/\epsilon$
Th on W[8]	1500°K	3	30,500°	−0.39 v.
Cc on 0 on W[9]	650°K	0.001	8,300°	−0.62 v.
0 on W[9]	1600°K	5×10^{11}	107,000°	+2.92 v.

last column. This contains the calculated surface heat in volts at the temperature given in column 2. The signs show that charging the surface positive is attended by the evolution of heat in the case of Th on W, for example, and by the absorption of heat in the case of O on W. The values for the surface heats calculated here are large enough to insure decisive results from cooling effect experiments performed on emitters of these types.

Another class of surfaces to be considered are those of the coated type. Here the coating is more than a surface, it constitutes a layer many molecules deep. Accordingly the cooling effect includes a Peltier heat, so that

$$\eta_c=\eta_{\rho T}+2kT+\epsilon P_{Pt\,C} \tag{14}$$

[7] Davisson and Germer, Phys. Rev. **20**, 300 (1922). For comparison with their notation $kb'=\phi_0$.

[8] From data to be published shortly by S. Dushman. Values of A and b now published[9] are 7 and 31,200 respectively, giving -0.28 v. for $-\eta_s/\epsilon$.

[9] K. H. Kingdon, Phys. Rev. **24**, 510 (1924).

Now

$$\eta_p = \eta_{pT} + (5kT/2)$$

as before, whence

$$\eta_p = \eta_c + (kT/2) - \epsilon P_{PtC}$$

giving

$$\eta_s = \eta - \eta_p = kb' - \eta_c + 2kT + \epsilon P_{PtC} \tag{15}$$

by use of Eq. (11). Experiments by Davisson and Germer[10] show that $kb' - \eta_C + 2kT = 0$. Apparently, then, for the oxide coating

$$\eta_{sC} = \epsilon P_{PtC} \tag{16}$$

This result leads to the expectation that $A_C = A_0$ within 3.7-fold where A_C is the A for the coated surface. For, taking surface 2 in Eq. (7) as pure tungsten and surface 1 as the oxide coating we have

$$\eta_{sC} - \eta_{sW} = kT \ln (A_C/A_W) + \epsilon(P_{WPt} + P_{PtC})$$

which, using Eq. (16), reduces to

$$kT \ln (A_C/A_W) = -\epsilon P_{WPt} - \eta_{sW} \tag{17}$$

From the Pt−Ir data again, dE/dT is 2×10^{-5} v./deg. at 1064°K, one of the standard temperatures used by Davisson and Germer. The Peltier term may therefore amount to $1064\times2\times10^{-5} = 0.02$ volt. Assuming η_{sW} to be proportional to temperature and to involve a possible error of 100 percent, it may still have a value of 0.04 volt at 1064°K. The result of the coated filament experiment expressed by Eq. (16) is probably good to 0.04 volt. Adding these possible discrepancies, multiplying by $\epsilon/kT = 11{,}600/1064$, taking the antilogarithm, and adding 25 percent to allow for the uncertainty in $A_W = A_0$ we obtain the factor 3.7 as noted above.

Estimating further that the error in determining A_C may amount to 70 percent we find finally, that

$$A_C \text{ (meas.)} = A_0 \text{ within a factor of 6.3.} \tag{18}$$

Calculation from the experimental data readily gives A_C (meas.) = 0.8. Even 6.3 times this is 12 times to small. Here is a direct contradiction.

But an escape lies perhaps in supposing that only a small fraction of the filament surface is active. On the point of view that the coating is of porous structure and that the emission comes from patches where metal atoms predominate in the surface layer, that hypothesis is not unreasonable though not without difficulties. It would seem, however, that the active patches must be of such a size, that they are separated by distances greater than about 10^{-6} cm, the thickness of the region in which the electric image force is active in determining the escape of electrons. If the separation were less than this, thermodynamics would not recognize the surface as dis-

[10] Davisson and Germer, Phys. Rev. **24**, 666 (1924).

continuous, and the A calculated from the data would have to stand. This limitation fixes a lower limit to the average number of atoms in each patch.

The above difficulty leads to the question whether similar conclusions may have to be drawn for the monatomic surface films first discussed. It is known, however, that these films, when "complete", contain the proper number of atoms to cover the surface one deep. In these cases, then, such an explanation would be untenable and the difficulty if it should arise would be a serious one, indeed.

IV. Stopping Potentials and the Heat of Charging

Further light is thrown on the value of A for pure metals, and therefore on surface heats of charging by some stopping potential experiments of Millikan.[11] He cites the equation

$$-\epsilon V_{21}=h(\nu_{02}-\nu_{01})-V_1+V_2$$

where ν_0 is the threshold frequency for the emission of photoelectrons, V a stopping potential, and h Planck's constant. Experimentally he has found that the stopping potentials for clean surfaces of Na, K and Li in vacuum are identical. For these metals, then,

$$-\epsilon V_{21}=h(\nu_{02}-\nu_{01}) \tag{19}$$

Now assuming emission equations of the type $i=AT^2e^{-b/T}$ for substitution in Eq. (3), we have

$$\epsilon V_{21}=kT\ln(A_2/A_1)+k(b_1-b_2)\ ; \tag{20}$$

It is reasonable to identify $h\nu_0$ with η_0, η_0 being the value of η at 0°K. In accordance with conclusions 1 and 2 below, $\eta_0=kb$. Substituting this and comparing with Eq. (19) we find

$$kT\ln(A_2/A_1)=0$$

and

$$A_{Na}=A_K=A_{Li}$$

which is in accordance with the idea that $A=A_0$, nearly, for all pure metals, and that η_s is small.

V. The Heat of Charging and Fundamental Assumptions

The theoretical result expressed in Eq. (7) is quite in accord with certain conclusions of Bridgman[12] regarding, particularly, the significance of the value of A in the electron emission equation.

$$i=AT^2e^{-b/T}.$$

He denotes the specific heat of neutral atoms in the emitting surface which are associated with a single emitted electron by C_{pm} and the specific heat of the positively charged atoms left when the electron evaporates by C_{pp}. Summarizing his conclusions and writing ΔC for $C_{pm}-C_{pp}$, we have:

[11] Millikan, Phys. Rev. **18**, 236 (1921).
[12] Bridgman, Phys. Rev. **27**, 173 (1926).

(1) $A = A_0 = 60.2$ amps./cm^2 deg^2, Dushman's[13] value, and $b = \eta_0/k$ if (a) the entropy of the positively charged atoms left when an electron evaporates is zero at 0°K and (b) $\Delta C = 0$.

(2) $A = A' \neq A_0$ and $b = \eta_0/k$ if (a) the entropy of the charged atoms is not zero at 0°K and (b) $\Delta C = 0$.

(3) A is a function of T and $b \neq \eta_0/k$ if $\Delta C \neq 0$.

(4) None of these possibilities is incompatible with the existence of a surface heat of charging since it is only necessary that

$$\Delta C = -\epsilon\sigma - Td(\eta_s/T)/dT \tag{21}$$

where σ is the specific heat of electricity in the metal. Let us confine ourselves to *first order effects* and consider the following practical cases (a) $A_1 = A_0$, the case of pure metal surfaces. We have shown in this case that $\eta_s = 0$ [Eq. (7) and conclusions from data on pure tungsten] so that $\Delta C = 0$ by Eq.(21). This case thus approximates to conclusion 1.

(b) $A_1 = A' \neq A_0$ but is constant, the case of surface films. Eq. (7) shows that η_s/T is a constant so that again $\Delta C = 0$. This case thus approximates to conclusion 2, but in addition our results show that a constant A which is not equal to A_0, a charged surface entropy different from zero at 0°K, and a surface heat proportional to temperature are three aspects of one phenomenon.

It is noteworthy, perhaps, that so far as the writers are aware all surface films which maintain a constant structure have a constant value for A. On this basis we must exclude from consideration all experiments in which the emission is not reproducible or in which the surface film is subject to a rapidly established equilibrium which is variable with temperature. This happens, for instance, with adsorbed films of alkali metals on tungsten unless special precautions are taken.

RESEARCH LABORATORY
GENERAL ELECTRIC COMPANY.
JANUARY 3, 1927.

[13] Dushman, Phys. Rev. **21**, 623 (1923).

PIEZOELECTRICITY OF CRYSTAL QUARTZ

By L. H. Dawson

Abstract

Piezoelectricity of crystal quartz at constant temperature.—Experimental measurements with the quadrant electrometer of the distribution of the piezoelectric charge over the surface of a quartz crystal in a plane normal to the optic axis were found to vary in such a manner as to produce six regions of charge, three positive areas alternating with three negative. The areas had definite geometrical relations to the electric axes and therefore these facts yielded a new and accurate method of determining the directions of the electric axes in crystal quartz. In planes containing the optic axis there was a region of positive charge separated by a line in the direction of the optic axis from a region of negative charge.

Variation with temperature of the piezoelectric effect in quartz.—The piezoelectric effect increased by 20 percent from room temperature to 60°C and decreased thereafter, reaching zero at about 573°C. Cooling curves showed a lag.

Variability of the piezoelectric effect.—The piezoelectric charge produced on different specimens or on different areas of the same specimen, all specimens being optically perfect, varied from large positive values of charge to large negative values. In general, the surface of the crystal quartz produced piezoelectric charges of the same sign, but of varying magnitudes. The charge measured over the entire surface of a crystal appeared to be the average of the effects of the elementary areas. The specimens in the present experiments varied on the negative side of the crystal from 5.8×10^{-8} to 7.1×10^{-8} e.s.u./cm$^2\times$dyne, while on the positive side the variation was from 4.9×10^{-8} to 6.4×10^{-8} e.s.u./cm$^2\times$dyne. These numbers are not far from the accepted value of 6.3×10^{-8} e.s.u./cm$^2\times$dyne, of the "piezoelectric constant" of P. and J. Curie. Such variations are in keeping with recent x-ray investigations on the imperfections of crystals which indicate that crystals are mosaics of an elementary perfect struture.

Introduction

An investigation perhaps more extensive than has been hitherto attempted of the piezoelectric effect in crystalline quartz is described in the following pages. The experiments have been greatly facilitated by exceptional opportunities existing in this laboratory for the selection and cutting of samples of quartz. The general laws of piezoelectric action, already well established, have been corroborated in full but in addition many new and unsuspected facts have been discovered. The theory of the piezoelectric effect available at present, although adequate for a description of the more general laws, is apparently incapable of coping successfully with the new phenomena. It appears that the formulation of a complete theory must await a more comprehensive understanding of the molecular structure of quartz. Further, the piezoelectric effect at various temperatures has been measured.

At the outset we may call to mind that a crystal of quartz is in the form of a hexagonal ~~cylinder~~ prism surmounted by a hexagonal pyramid; the faces of

the crystal, which may vary in length and breadth, lie at definite angles with each other. In Fig. 1, *JEGK*, *GDLK*, *DLMF*, *MNHF*, *HNIC* and *CIJE* are the sides of the hexagonal cylinder, the angle between any two adjacent sides is 120°. The faces of the hexagonal pyramid *JKLMNIA* lie at an angle of 38°13′ to the faces of the cylinder. The quartz crystal, a section of which is shown in Fig. 1, has four axes of symmetry namely, *AB*, *CD*, *EF* and *GH*. *AB* is called, in crystallographic terms, the trigonal axis, as there exists three symmetrical positions of the crystal as it is rotated about this axis. *AB* is also called the optic axis, because along this direction the crystal has unique optical properties. *CD*, *EF* and *GH* are digonal exes of symmetry, for there are only two positions of symmetry as the crystal is rotated around each of these axes. *CD*, *EF* and *GH* are known as the electric axes, since a pressure applied to the crystal parallel to these directions produces piezoelectric polarization in the same direction.

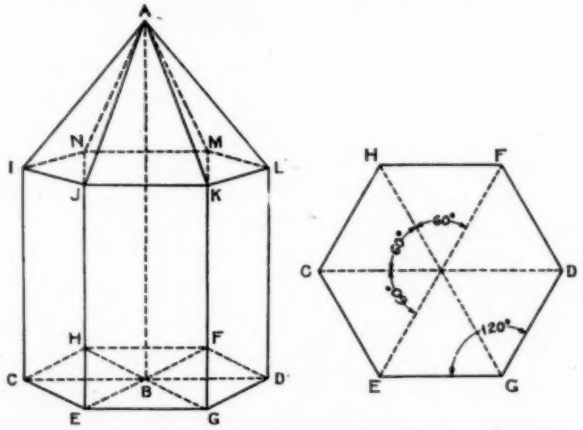

Fig. 1. A section of a quartz crystal showing the direction of the optic and electric axes.

No complete historical summary of the many researches on the piezoelectric phenomenon will be attempted here, but some of the more important papers may be mentioned. We pass over the early qualitative experiments of W. C. Roentgen[1] and direct attention to the more quantitative investigations of P. and J. Curie[2] in which were first brought out the laws governing the piezoelectric effect in quartz. Their studies made on a rectangular parallelopiped of quartz cut in such a manner that one of the electric axes was perpendicular to one of the faces, led them to conclude that a force applied along the electric axis produced a charge on the faces perpendicular to this axis that was directly proportional to the force, a positive charge accumulating on one of the faces and an equal negative charge on the opposite face. A reversal of the sign of the force produced a reversal of the charges. The magnitude K of the charge, was found to be 6.32×10^{-8} esu/dyne cm². This has been the accepted value. The present investigation shows that this

[1] Roentgen, Ann. d. Physik und Chemie, NF19–20, 513 (1883).
[2] P. and J. Curie, Comptes rendus 91, 294 (1880).

value is not a constant for all quartz but varies very materially for different specimens of optically perfect quartz. This is in keeping with the general ideas of crystal imperfections as discussed later.

W. Voigt[3] has developed theoretical formulas for the piezoelectric charges in terms of the piezoelectric and elastic constants of the quartz. His formulas agreed with the experimental results of P. and J. Curies and from their piezoelectric constant he was able to deduce the various piezo-electric constants of the equations for quartz.

Recently W. Bragg[4] and R. E. Gibbs[5], from their x-ray studies of the molecular structure of crystal quartz have explained the piezo-electric effect as a distortion of the uniaxial nature of the crystal; while the production of pyroelectricity is due to the change of structure towards or away from hexagonal symmetry.

Experimental Details

The apparatus shown in Fig. 2 consisted of a Compton electrometer *A* with a sensitivity of about 0.004 V/mm suitably shielded by an earthed brass cylinder *B*. The quartz *C*, under investigation, was placed upon the circular platform *D*. This platform was fixed in a horizontal position in such a manner that it could be rotated about the vertical axis *G* and the

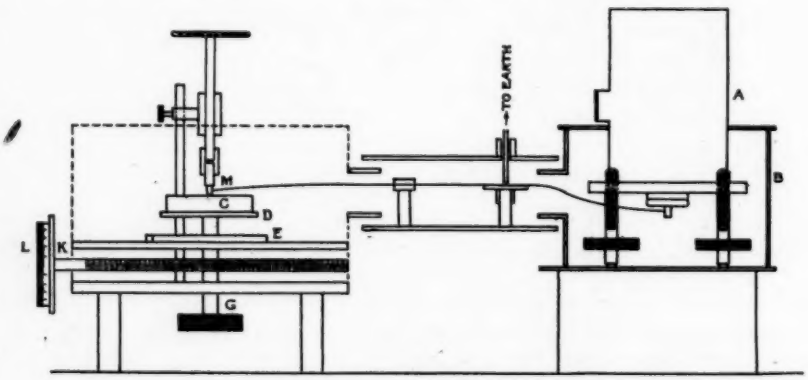

Fig. 2. Apparatus for the investigation of the piezoelectricity of quartz.

amount of rotation measured by the circular scale *E*. A longitudinal motion could be given the platform *D* by the screw *K* and measured by the divided head *L*. Thus any point of the quartz could be brought under the copper contact point *M*. The contact point was connected to the electrometer and insulated throughout by fused quartz. The apparatus was thoroughly shielded electrically and properly insulated switches were placed in the system. In some of the experiments, it was found desirable to apply or release the pressure on the quartz in a direction parallel to the plane of the

[3] Voigt, Ann. d. Physik u. Chemie, NF55, 701 (1895).
[4] Bragg and Gibbs, Proc. of Roy. Soc. **A109**, 405 (1926).
[5] Gibbs, Proc. of Roy. Soc. **A110**, 443 (1926).

platform *D*. To accomplish this an instrument was designed in which a quick application or release of pressure to the contact point could be made by a suitably actuated cam.

In order to raise the quartz to any desired temperature an electric resistance furnace with a metal core was constructed which could be placed over the quartz and the core earthed, thus shielding effectually the quartz and contact point. To measure the temperature a calibrated chromel-nichrome thermocouple was inserted in the furnace with the quartz.

The capacity of the system which varied during the investigation from 34 m.m.f. to 41 m.m.f. was compared with the capacity of a standard condenser by the heterodyne beat method, the measurements being reliable to less than one percent.

Piezoelectric Effects in the Direction of Pressure

Experiments were undertaken to determine the character of the distribution of charge over the surface upon which the pressure was applied. Specimens of optically perfect quartz were selected and cut in such a manner that the electric axis was normal to the large face of a parallelopiped $25 \times 28 \times 1$ mm. Each crystal was placed on table *D*, Fig. 2, and explored over the largest faces by releasing 1000 grams pressure from the contact point which had an area of about 0.1 mm^2.

In general one side of the crystal would give positive deflections while the opposite side gave negative deflections. Small areas of negative charge were often found on the faces which gave positive deflections over most of the face; and corresponding areas of positive deflection were found on the negative face. Large deflections might occur at the center of the quartz or at the edge and the deflection for one crystal was often twice that of another crystal. There seemed to be no uniformity of results.

The question arose whether such a distribution was of permanent character. To answer this a crystal was subjected to a force of about 25 kilograms for 20 seconds and the surface explored and no change in the distribution could be observed. The same crystal was then raised to a temperature of approximately 600°C, thus transforming it to the Beta-quartz. After allowing it to return to the alpha-quartz state, the surface was again explored. Again no change was observed. Thus the distribution seems to be permanent.

To substantiate further the above results, a piece of quartz cut in the above manner and about $150 \times 100 \times 3$ mm was subjected to the exploring test and again the charge was found to vary over the surface. The piece was then cut into three parts and each part explored, but no change could be observed in the character of the distribution of the original charge. Each part was examined optically and observed to be free from twinning and other defects.

These variations in the piezoelectric charge are naturally to be attributed to imperfections in the quartz crystal, although these imperfections may be so minute as to escape detection by the usual examination with polarized

light. All that can be said is that the imperfections might be in the nature of small crystal fragments variously oriented in perhaps a random manner with respect to the large parent crystal, and that these little fragments are small in size, say less than 0.1 mm in their largest dimension. It may be pointed out further than these imperfections may be very small, indeed such as would result from a displacement of a small group of molecules. Recent developments in x-ray analysis of crystals lead to the idea that crystals are not perfectly formed as hitherto supposed[6,7,8], but are constituted of a mosaic of more elementary perfect structures, and that the axes of the more perfect crystals are not oriented in the same direction but may vary from a mean position. This explanation may account for the peculiar variation of the piezoelectric charge over the surface of quartz, although surface or volume strains may be contributing factors.

Distributions of Charge Around the Cylindrical Surface of a Circular Piece of Quartz Cut Perpendicular to the Electric Axis

A cylindrical specimen of quartz 60 mm in diameter and 30 mm thick was cut from a rough piece of quartz free from flaws and twinning, in such a

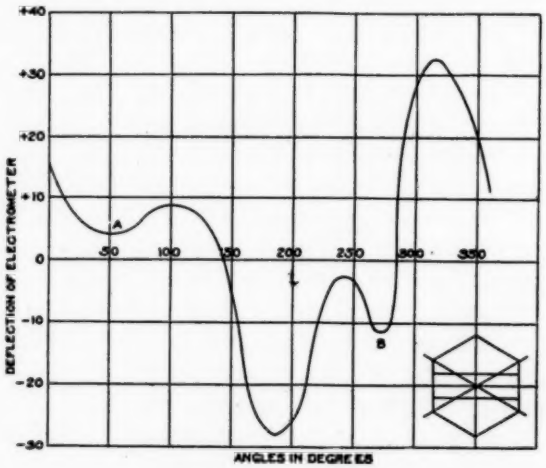

Fig. 3. Distribution of piezoelectric charge over the cylindrical surface of a crystal of quartz in which the plane containing the optic axis and the line perpendicular to one of the hexagonal sides of the crystal is parallel to the ends of the cylinder.

manner that an electric axis was normal to the ends of the cylinder and the optic axis parallel to the plane of the ends, the other electric axes being as shown in Fig. 3. An exploration of the distribution of the charge over the cylindrical surface was carried out by the application of a weight of 1000 gms directly to the exploring point which was placed perpendicular to the surface of the quartz. Care was taken to fasten the quartz cylinder concentrically on

[6] W. L. Bragg, Darwin and James, Phil. Mag. 1, 897 (1926).
[7] A. Muller, Nature, 121 (May 22, 1926).
[8] Burgess, Nature, 116 (July 24, 1926).

table D, Fig. 2 and to have points of reference marked on it in such a manner that the data could always be referred back to the original sepcimen. The character of the distribution is shown in Fig. 3 where the abscissas are the angles of rotation of the quartz which were read every degree and the ordinates are electrometer deflections.

There appears to be one well defined region of positive charge and another of negative charge, the magnitude of the deflections of each being about equal, but the area of the positive region is larger than that of the negative.

One peculiarity which seems to be characteristic of the curve is the decrease of the curve to a minimum at *A* and then a rise to a maximum and finally a decrease to zero in the positive area and a similar phenomenon taking place in the region of point *B* in the negative area. It may be mentioned that the general characteristics of the curve always remained the same regardless of the method of holding the specimen to the plate.

Distribution of Charge Around the Surface of a Cylindrical Piece of Quartz in Which Two Electric Axes Lie at 60° to the End Faces

Next a cylindrical crystal of the same dimensions but cut as indicated in Fig. 4 was placed concentrically on table D. The results of a procedure

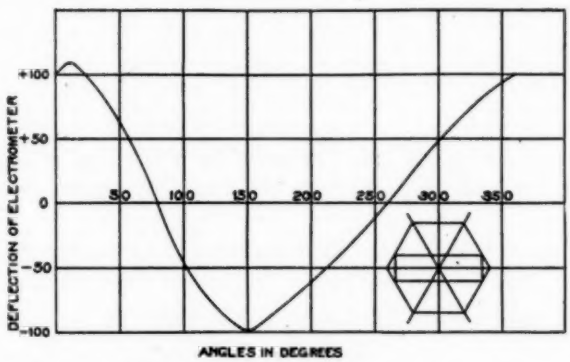

Fig. 4. Distribution of piexoelectric charge over the cylindrical surface of a crystal of quartz in which the plane containing the optic and an electric axis is parallel to the ends of the cylinder.

similar to the previous case is shown in Fig. 4 and it can be seen that there are two well defined regions, one of the positive charge and the other negative. The maximum deflections in both the positive and negative regions are of the same magnitude, but appear to occur about 150° apart and not 180°. The direction of the line dividing these areas lies more or less in the direction of the optic axis.

Distribution of Charge Over the Cylindrical Surface of a Crystal in which the Optic Axis is Perpendicular to the Ends of the Cylinder

Finally, a crystal of the same dimensions as in the two previous cases was cut from a rough crystal in such a manner that the optic axis was normal to

the ends of the cylinder. The exploration of the cylindrical surface was carried out in a manner similar to the two preceeding cases, and the character of distribution of the charge is shown in Fig. 5. There are three positive maxima and three negative and they occur accurately 60° apart and are the same magnitude and alternate in sign. There are six points where the charge becomes zero and they lie 60° apart.

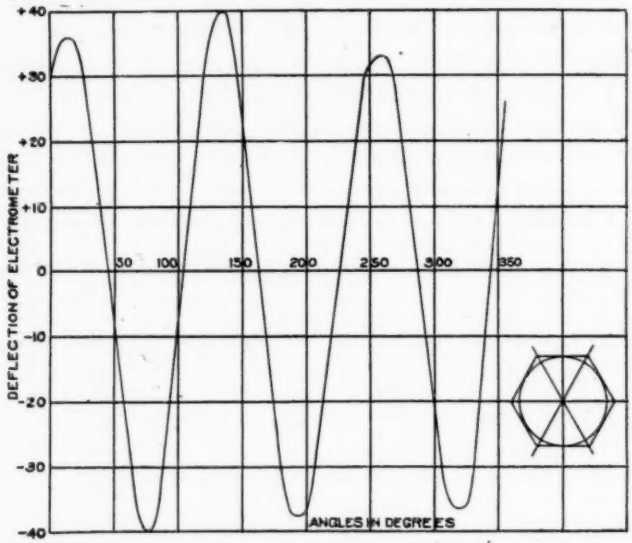

Fig. 5. Distribution of piezoelectric charge over the cylindrical surface of a quartz crystal in which the ends of the cylinder are parallel to the plane of the electric axes.

A Method for Determining the Electric Axes of a Slab of Quartz Cut in Such a Manner that the Optic Axis is Perpendicular to Its Plane

The above experiment serves as a new and precise method for determining the direction of the electric axes of a piece of quartz cut normal to the optic axis and in which there are no indications of the crystal form. The rough piece of quartz must first be examined for the optic axis and then cut into slabs of the desired thickness in which the optic axis is normal to the plane of the slab. The slab in which the directions of the electric axes are to be determined is placed on table *D* Fig. 2 and an exploration of a cylindrical surface, more or less parallel to the optic axis, is carried out and the points of either maximum or minimum deflection observed. In most cases the latter is preferable as being more accurately determined. In case two diametrically opposite points can be determined, it is only necessary to draw a line joining them, but in case of the absence of the opposite point the lines must be drawn in the direction of pressure. Now it must be remembered that the direction of production of zero charge lies normal to the electric axis of the piece; therefore it is only necessary to draw lines perpendicular to the observed lines to locate the electric axis.

In many cases that may arise it is impossible to find a surface on the quartz which will be nearly normal to the direction of pressure; then it is possible to produce such a surface by grinding a semi-cylindrical notch in the side of the quartz in such a manner that the generator of the semi-cylindrical surface is parallel to the optic axis. Thus placing the quartz on the table D in such a manner that the center of the notch coincides with the center of rotation of the table the exploring point can be brought in normal contact with this surface.

Many trials were made with this procedure both on samples of quartz in which faces were present and others in which faces were absent. In either case the electric axis could easily be determined within 2°.

Measurement of the Magnitude of the Piezoelectric Effect

Samples of quartz 28×25×2 mm and 28×25×1 mm were cut with an electric axis normal to the 28×25 side and the two faces in contact with the electrodes parallel to each other within .025 mm. Forces of 50, 100, 200, 500, 1000 and 2000 grams were applied to each in the direction of the electric axis and in such a manner as to be equally distributed over the entire surface of the crystal. It was found after a few experiments that more consistent results could be obtained by sputtering the surfaces of the quartz in contact with the electrodes with platinum. Four samples of the results obtained are given in Table I and are representative of the results obtained in many trials on different crystals.

Table I

Crystal Number	Dimension in mm of surface in contact with electrodes	Charge (esu/cm² dyne) ×10⁸	Date	Temp. °C
1 (a)	27×25	(−6.27 ± .23)	June 10	19.5
(b)	27×11.5	(−6.37 ± .11)	" 24	24
(c)	16×12	(−7.18 ± .16)	" 28	24
(d)	11×8.5	(−6.89 ± .10)	" 28	24
(e)	12×12	(−7.11 ± .16)	July 1	21
(f)	11.5×12.5	(−6.43 ± .18)	" 1	21
2 (a)	27×25	(−6.05 ± .15)	June 11	19.5
(b)	27×25	(−5.88 ± .12)	" 16	21
(c)	27×25	(−6.16 ± .16)	" 17	19.5
(d)	27×25	(−6.42 ± .30)	" 17	19.5
(e)	27×25	(+4.94 ± .40)	" 17	19.2
(f)	27×25	(+5.38 ± .04)	" 19	19.0
(g)	27×25	(+5.47 ± .26)	" 21	19.0
3	27×25	(+4.99 ± .04)	June 28	24
4	27×25	(+6.41 ± .05)	June 28	24

Crystal number 1 was first explored by the point method and it was found that while each surface produced charges of like character there appeared to be a variation of 250 percent in the magnitude of the piezo-

electric charge. No regularity of distribution could be detected on any of the crystals.

The crystal was then subjected to test for the production of piezoelectric charge over the entire surface. The resulting charge is given in Table I, crystal I (a). The crystal was next cut into three pieces of unequal size and the piezoelectric charge of each measured with the resulting charge as given in (b), (c), (d), Table I. The largest of these three pieces was cut into two pieces and the charge determined (e) and (f), Table I. It can be seen that the charge produced varies very markedly among the separate pieces and that the charge for the whole piece is smaller than that for any one. No explanation of this peculiarity is available. To explain this phenomenon satisfactorily it will be necessary to investigate more samples of quartz; further work on this is in progress.

In order to show the accuracy with which the measurements could be repeated, crystal number 2 was measured on different days and under as nearly identical conditions as possible. Both the positive and negative faces were tested with the result that the charge on the positive face appeared to be uniformly smaller than that on the negative as is shown in crystal 2(*a*), (*b*), (*c*), (*d*), (*e*), (*f*), (*g*) of Table I. The results taken for the different days on the negative side of the quartz agree with each other within the limit of error that one would expect in this type of experiment, and the same may be said of the positive side.

As an example of the difference of charge produced on different samples of quartz, 3 and 4 of Table I are crystals cut from optically perfect material in as nearly the same manner as possible. They were subjected to test within a very few minutes of each other thus insuring as nearly identical conditions as possible, and it is seen from the table that they differ in charge by a large amount. This appears to be typical of the behaviour of quartz and is perhaps to be explained by the imperfections in crystal structure mentioned in an earlier paragraph.

Temperature Coefficient of the Piezoelectric Effect of Quartz

In the experiment on the variation of the piezoelectric effect with temperature, the specimen was placed on table *D*, Fig. 2 and the electric furnace placed over it. The apparatus was suitably shielded electrically and the temperature measured by a chromel-nichrome thermocouple. The charge was produced by lifting a 500 gm weight from the quartz. The temperature was varied by convenient intervals to a point well above 573°C, thus passing the transformation point of α-quartz to β-quartz. The apparatus was brought to the desired temperature and allowed to stand until temperature equilibrium conditions and been reached. Six readings were taken and the mean of the six was used as the recorded result. Two crystals from the different pieces of quartz were used.

The curves in Fig. 6 exhibit the results, where the abscissas are the temperatures of the quartz and the ordinates are electrometer deflections. The upper curves were taken with ascending and the lower with descending

temperatures. It is seen that the curves for both crytsals are of the same character, starting from approximately the same value at room temperature and rising to a maximum at about 60°C. From the maximum the curves descend slowly until a temperature of about 300°C is attianed. Beyond this point they descend rapidly, reaching low values in one case at a temperature of 440°C and in the other case at 480°C. Beyond these points the piezoelectric effect is extremely small and in the neighborhood of 550°C has practically disappeared.

Upon cooling no deflection of the electrometer could be detected until the apparatus had cooled down to 280°C, and then there appeared a very rapid rise to a maximum value at 60°C and from here to room temperature a decreasing charge was observed. The maximum reached on cooling was

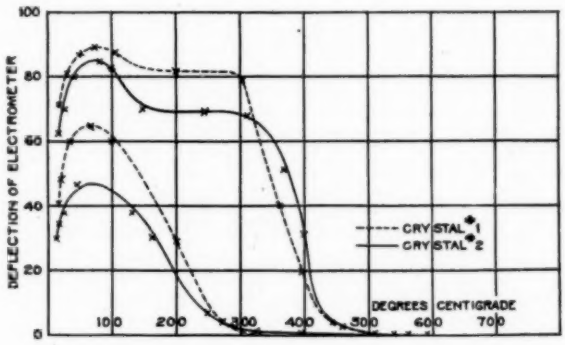

Fig. 6. Curves showing the effect of temperature on the piezoelectric effect in quartz.

approximately one half in one case and two thirds in the other of the maximum reached on heating, and the resulting piezoelectric effect at room temperature after cooling was about one half of the value of that before subjecting the crystal to heating. It was found that after the apparatus had remained untouched for 24 hours that both crystals had returned to their previous piezoelectric condition.

It was thought that the peculiarities of the curve might be due to the oxidation of the copper electrode, although this was very slight, but on substituting an aluminum rod for copper the same results were obtained.

The maximum in the curve has no evident explanation and was not expected. The lag in the piezoelectric effect however, is a phenomenon to perhaps be expected, since other effects of similar nature, for example in the moduli of elasticity, have been observed in the transformation of β-quartz to α-quartz.

I wish to express my thanks to Dr. E. O. Hulburt for suggesting the problem and for his keen interest and help in the work.

HEAT AND LIGHT DIVISION,
NAVAL RESEARCH LABORATORY,
September 10, 1926.

THE TRANSFORMATION PERIOD OF THE INITIAL POSITIVE AIR ION

By Leila M. Valasek

Abstract

Time constant of transformation from initial to final positive ion. Erikson has shown that when first formed in air at atmospheric pressure the positive ion has a mobility of 1.87 cm/sec. per volt/cm, but that it quickly changes over into an ion having a mobility of 1.36. By a method essentially the same as that used by Erikson, a quantitative study was made of the rate of transformation. It was found to be dependent on the humidity of the air. At a relative humidity of 32 percent, the half-value period was found to be 0.0132 sec.; at a relative humidity of 80 percent, it is 0.0354 sec.

IT HAS been shown that in the case of air and certain other gases the products of ionization consist of a negative ion, which retains its identity for a considerable time, and an "initial" positive ion, which is quickly transformed into a less mobile structure, the "final" positive ion.[1,2] Rough estimates of the value of the time rate of the transformation of the initial positive ion have been given by Grummann[2] and by Tyndall and Grindley.[3] The present research was undertaken for the purpose of making a more exact evaluation of this transformation constant.

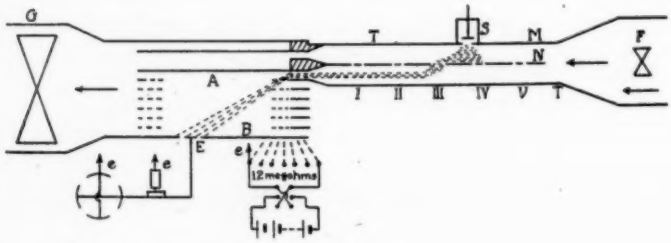

Fig. 1. Diagram of apparatus.

Measurements were made by means of an apparatus similar to that employed by Erikson.[1,2] The ionic spectrum was obtained by passing a narrow stream of ionized air into the moving air between two plates, A and B, Fig. 1, between which was maintained a difference of potential. In the lower plate was a narrow insulated strip, E, connected to an electrometer. The ions, moving with the air stream in a horizontal direction and being deflected vertically by the electric field, were made to fall on E by proper adjustment of wind velocity and voltage. A curve showing the ionic mobility spectrum was obtained by plotting electrometer readings

[1] Erikson, Phys. Rev. **20**, 117 (1922); **24**, 622 (1924); **26**, 465; **26**, 625; **26**, 629 (1925).
[2] Erikson, Phys. Rev. **24**, 502 (1924).
[3] Tyndall and Grindley, Proc. Roy. Soc. **A110**, 358 (1926).

against the voltage at constant wind velocity (See Fig. 2). The ions were formed in the upper half of the double tube T, Fig. 1, by alpha-rays from a polonium plate in the chamber S. Five windows were cut in the partition N dividing this tube, and S was placed so that ions entered the lower half of T through one of these windows, the others being, of course, closed. Between M and N a potential difference of 180 volts was maintained, to draw the positive ions vertically downward. Before obtaining the curves presented in this paper, a set of readings was taken at the air velocity used in this experiment, with a constant potential difference between A and B, in which the position of S was varied with respect to one of the windows. Then, in obtaining the curves of Fig. 2, the position of S with reference to a window was chosen to give the maximum possible current. It was found that with this arrangement about 97 percent of all the ions entering the lower half of the tube T were positive in charge. Hence, no correction was made for the loss of positive ions by recombination with negative ions in in their passage into the measuring apparatus. Moreover, since the times

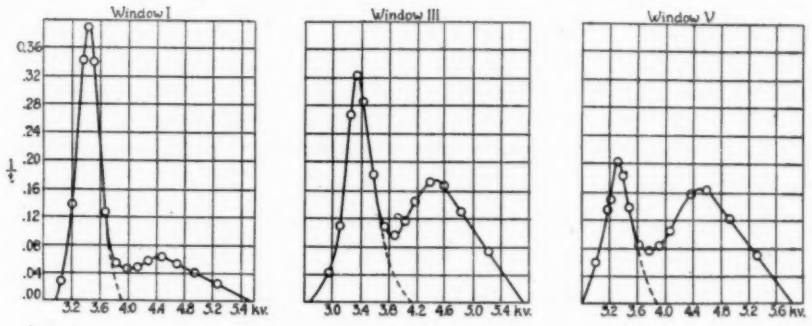

Fig. 2. Spectra of positive air ions of different ages.

here involved were very short, the number of positive ions lost by diffusion to the walls was considered negligible. To measure the current due to ions of different ages, a set of curves was obtained by placing S, successively, at each of the five windows. The relative ages of the ions from these windows were calculated from the wind velocity in T. To measure the latter, a small fan anemometer was placed at F, Fig. 1, and the velocity in T was deduced from its readings by a comparison of the cross-sectional areas of the two parts of the tube. The calibration of the anemometer was checked at the U. S. Bureau of Standards.

One may define λ, the time constant of the transformation, by the equation

$$dn/dt = -\lambda n. \tag{1}$$

Its integral is

$$n/n_0 = \exp(-\lambda t). \tag{2}$$

Here n_0 is the number of initial positive ions formed per second by the ionizing agent, and n is the number of these ions still unchanged after the

passage of a time t. Now, in Fig. 2 the ordinates are proportional to the number of ions reaching E per second. The area under the entire curve is accordingly proportional to the total number of positive ions entering the lower part of the tube T per second. Thus, the ratio n/n_0 can be taken as the ratio of the area under the first maximum of the curve to that under the entire curve. These areas were measured for all the curves with a planimeter.

In Fig. 3 are plotted as ordinates the values of $\log_{10} n/n_0$ obtained from the curves of Fig. 2. The relative "age" of the ions, plotted as abscissa in each case, is the time of passage of the ions from the window in question

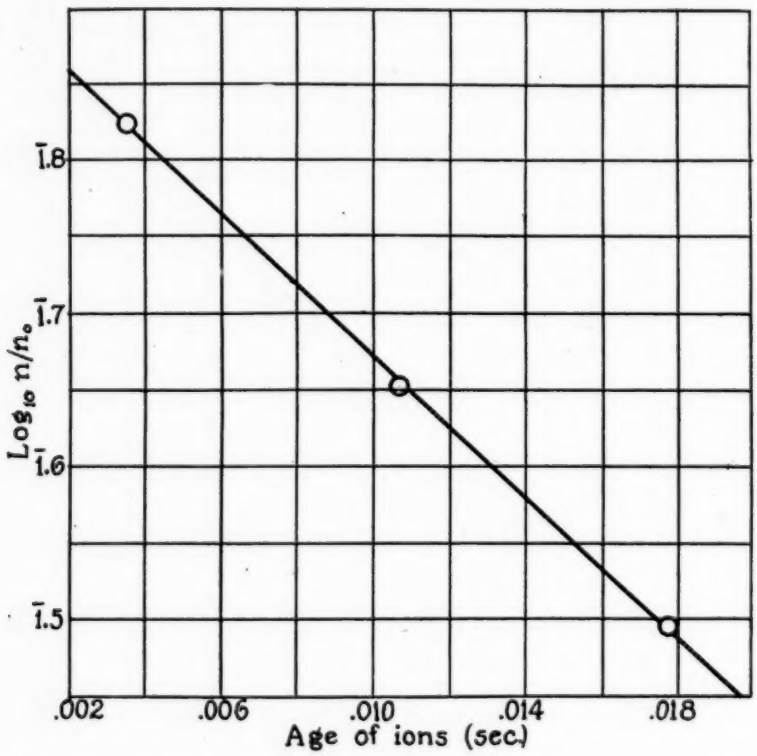

Fig. 3. Dependence of the logarithm of the relative number of initial positive ions on the age of the ions.

to a point 5 cm in front of window I. The actual time of passage to electrode E was not computed, since only the difference in times from the various windows is needed in determining λ.

In accordance with Eq. (2), λ is the product of $\log_e 10$ and the slope of the straight line of Fig. 3. The result of this calculation is

$$\lambda = 52.6\,(\text{sec.})^{-1}$$

The half-value period is, accordingly,

$$\log_e 2/\lambda = 0.0132 \text{ sec.}$$

These curves were obtained at a humidity of about 32 percent.

It was found, however, that the value of λ is considerably affected by humidity conditions.[3] At a relative humidity of 80 percent, for example, $\lambda = 19.6$ (sec.)$^{-1}$, giving, as half-value period, 0.0354 sec. The values of the humidity here cited are those recorded at the U. S. Weather Bureau on the days on which the work was done. The windows of the room were kept open enough to assure that the humidity of the room was nearly the same as that outside. In the course of a set of readings, the humidity did not vary by more than 25 percent.

In seeking a conception of the mechanism of the humidity effect on the rate of transformation, it would seem natural to assume that the final ion has a greater tendency to load up with the water molecules than has the initial ion. For, if the curves were not carried to voltages high enough to include these heavy ions, the ratio n/n_0 would obviously be abnormally large. But this explanation can hardly be the correct one, for the results of this experiment do not in any way point to a successive decrease in the value of n_0 at the different windows. The data are, however, too meagre at present to point the way to a clear-cut picture of the action of the water molecules on those of the air.

The writer is indebted to Professor H. A. Erikson for his guidance in the course of this research. It was at his suggestion that the problem was undertaken.

PHYSICAL LABORATORY,
UNIVERSITY OF MINNESOTA,
November, 1926.

passage of a time t. Now, in Fig. 2 the ordinates are proportional to the number of ions reaching E per second. The area under the entire curve is accordingly proportional to the total number of positive ions entering the lower part of the tube T per second. Thus, the ratio n/n_0 can be taken as the ratio of the area under the first maximum of the curve to that under the entire curve. These areas were measured for all the curves with a planimeter.

In Fig. 3 are plotted as ordinates the values of $\log_{10} n/n_0$ obtained from the curves of Fig. 2. The relative "age" of the ions, plotted as abscissa in each case, is the time of passage of the ions from the window in question

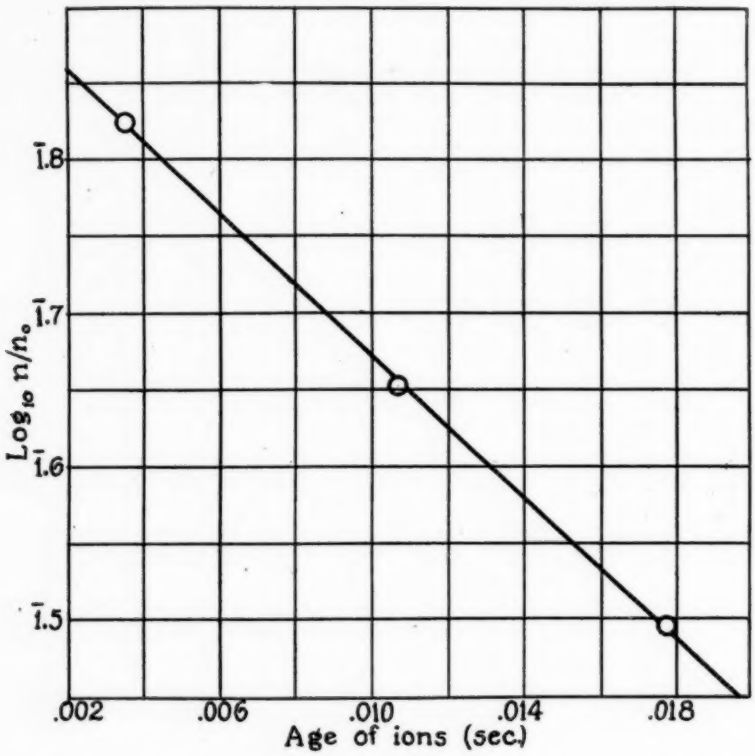

Fig. 3. Dependence of the logarithm of the relative number of initial positive ions on the age of the ions.

to a point 5 cm in front of window I. The actual time of passage to electrode E was not computed, since only the difference in times from the various windows is needed in determining λ.

In accordance with Eq. (2), λ is the product of $\log_e 10$ and the slope of the straight line of Fig. 3. The result of this calculation is

$$\lambda = 52.6\,(\text{sec.})^{-1}$$

The half-value period is, accordingly,

$$\log_e 2/\lambda = 0.0132 \text{ sec.}$$

These curves were obtained at a humidity of about 32 percent.

It was found, however, that the value of λ is considerably affected by humidity conditions.[3] At a relative humidity of 80 percent, for example, $\lambda = 19.6$ (sec.)$^{-1}$, giving, as half-value period, 0.0354 sec. The values of the humidity here cited are those recorded at the U. S. Weather Bureau on the days on which the work was done. The windows of the room were kept open enough to assure that the humidity of the room was nearly the same as that outside. In the course of a set of readings, the humidity did not vary by more than 25 percent.

In seeking a conception of the mechanism of the humidity effect on the rate of transformation, it would seem natural to assume that the final ion has a greater tendency to load up with the water molecules than has the initial ion. For, if the curves were not carried to voltages high enough to include these heavy ions, the ratio n/n_0 would obviously be abnormally large. But this explanation can hardly be the correct one, for the results of this experiment do not in any way point to a successive decrease in the value of n_0 at the different windows. The data are, however, too meagre at present to point the way to a clear-cut picture of the action of the water molecules on those of the air.

The writer is indebted to Professor H. A. Erikson for his guidance in the course of this research. It was at his suggestion that the problem was undertaken.

PHYSICAL LABORATORY,
UNIVERSITY OF MINNESOTA,
November, 1926.

RESONANCE IN ALTERNATING CURRENTS CONTAINING A SINGLE HARMONIC

By Frederic H. Miller

Abstract

Current-frequency relations in alternating current circuits as affected by harmonics.—*Series circuit.* The form of a current-frequency curve depends only upon the ratio $K = R^2C/L$ (herein designated as the "resonance factor"), and the ratio a of the harmonic to the fundamental e.m.f. amplitude. Special cases are considered, particular attention being given to the third harmonic, and a method for plotting generalized current-frequency curves is outlined. As K increases, the value of a, below which the I-f curve can have only one maximum, increases from zero to unity; for eacn harmonic n, there is a definite value of K given by $K_E = (n-1)^2(n^2+4n+1)/n(n^2+1)$, above which there can be only one peak to the curve no matter what the value of a. *Parallel circuit.* The current-frequency curve has only one minimum, regardless of the number of harmonics, but the position of the minimum point is dependent upon the number and amplitude of any harmonics present. A simple method of plotting generalized current-frequency curves is given, and the inductive and condensive currents briefly discussed. For each circuit, utilizing the relations obtained analytically, there is given an experimental method for determining the amplitudes of fundamental and harmonic in an e.m.f. wave.

THE phenomenon of resonance in a circuit having impressed upon it a sinusoidal e.m.f. is a familiar one, and full discussions of it have been presented by many writers. But the current-frequency relations as affected by the presence of harmonics in the voltage wave, although often met with in practice, are not so well known. It is the purpose of this paper to investigate some of these relations for the case in which one harmonic, of order n, is present in the applied e.m.f. Methods of analysis are here merely outlined, and the conclusions arrived at, stated.[1]

The assumption is made that as the frequency varies, the ratio of the amplitudes of the two e.m.f. components remains a constant. The term "resonance" will be used in a broad sense, to denote the condition which obtains whenever the current becomes a maximum for the series circuit, or a minimum for the parallel circuit.

I. Series Circuit

When a resistance R, a self-inductance L, and a capacitance C are connected in series, and an e.m.f. made up of the two components E_1 and E_n is impressed upon the circuit, the current is given by

$$I^2 = \frac{E_1^2}{R^2+(L\omega-1/C\omega)^2} + \frac{E_n^2}{R^2+(nL\omega-1/nC\omega)^2}, \qquad (1)$$

[1] A complete formulation may be found in the writer's thesis having the same title, in the Cornell University Library.

where ω is the angular velocity, equal to 2π times the frequency f. Now when E_n is sufficiently large, the current-frequency curve will ordinarily have two maxima and one minimum, and will be similar in form to the upper curve ($a=1$) of Fig. 1. Hence by equating $dI/d\omega$ to zero, the angular velocities corresponding to the three points of zero slope will be represented by roots of the resulting equation. By taking the derivative in this manner, and employing the substitutions

$$K=R^2C/L, \qquad x=nLC\omega^2, \qquad a=E_n/E_1,$$

there will be obtained the relation

$$\begin{aligned} &n^2(n^2+a^2)x^6+2n^3(K-2)(1+a^2)x^5+[n^2(K^2-4K-n^4+6)\\ &\quad+(n^4K^2-4n^4K+6n^4-1)a^2]x^4-2n(n^4-1)(K-2)(1-a^2)x^3\\ &\quad-[(n^4K^2-4n^4K+6n^4-1)+n^2(K^2-4K-n^4+6)a^2]x^2\\ &\quad-2n^3(K-2)(1+a^2)x-n^2(1+n^2a^2)=0. \end{aligned} \tag{2}$$

From this it is evident that the form of a current-frequency curve is dependent not only upon the relative amplitude of the harmonic e.m.f., but also upon the ratio $K=R^2C/L$, which may therefore be designated as the "resonance factor". However, no change is produced in the curve when any of the three circuit constants are varied, provided this ratio K is preserved.

Physical considerations show that there may be no more than three positive roots of Eq. (2), and, depending upon the coefficients, there may be only one, two equal ones and a greater one, or three distinct positive roots. As a increases from zero to unity, these three conditions will successively prevail. When the value of a is such that two equal positive roots are obtained, K being given, then the $I-f$ curve will have a horizontal inflection point and one peak; this may be called the transition case.

From the symmetrical form of the above equation, it is seen that if $1/a$ be substituted for a, and $1/x$ for x, the equation will remain unchanged. It therefore follows that there are two values of a, one the reciprocal of the other, for each of K such that the current-frequency curve shall have a horizontal inflection point. In the ordinary case, when $a<1$, the inflection point occurs to the left of the maximum, whereas if the reciprocal value $1/a$ be taken, the amplitude of the nth harmonic e.m.f. will exceed that of the fundamental, and the inflection point occurs to the right of the crest. The former case, a being less than unity, is the one usually met with in practice, and therefore of greater importance; this reciprocal relation has been indicated principally because of its value to the subsequent analysis.

Although it has not been found possible to express algebraically the function connecting K and a in the transition case, critical values of a for various values of K may be found by empirical methods, and, in addition, special cases falling under Eq. (2) may be treated by analytical methods.

By making the same substitutions in Eq. (1) as were employed in the development of (2), there is obtained

$$\frac{LI^2}{CE_1^2} = \frac{1}{x/n+K-2+n/x} + \frac{a^2}{nx+K-2+1/nx} . \tag{3}$$

This mode of expression allows for simpler calculation and plotting; furthermore, the current-frequency curves so drawn for various values of n and K will be perfectly general and may therefore by used in practice for all cases, no matter what the constants of the circuit may be. Such graphing consists in plotting $(I/E_1)(L/C)^{1/2}$ against $x^{1/2}=2\pi f(nLC)^{1/2}$. Fig. 1 shows a typical current-frequency curve of this generalized form, n having been taken equal to 3, K to unity, and a taken as zero, lower critical value, and unity.

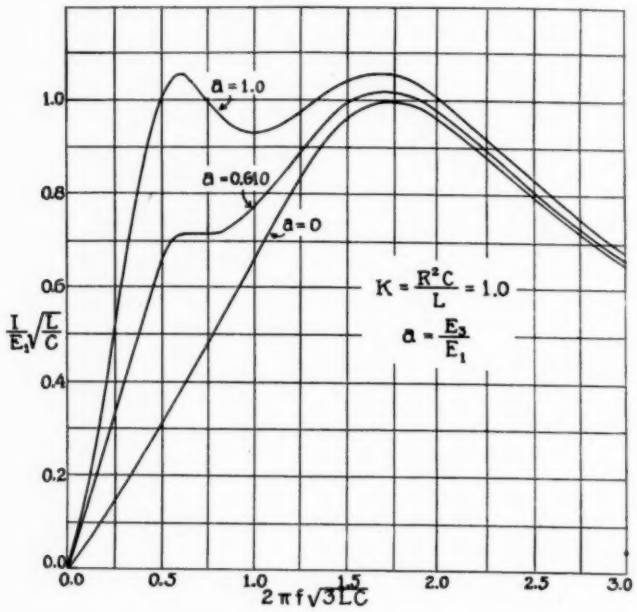

Fig. 1. Generalized current-frequency curves for the series circuit in which K is unity.

For the case of the third harmonic, curves have been drawn for a number of values of the resonance factor; these indicate several important characteristics. The depth of the trough obtained when $a=1$ becomes less pronounced, and the three points of zero slope approach each other, as K is increased. The curves for the transition cases lie between the other two throughout the frequency range, and recede from the curve of $a=0$ and approach that of $a=1$ as the resonance factor becomes larger. Finally, a for the transition cases grows larger and larger as K increases.

In view of the latter statement, we should expect that since the reciprocal relation for a holds in the transition case, there would be a maximum value of the ratio R^2C/L beyond which there could be only one peak to the current-frequency curve regardless of the relative amplitude of E_n. That this is so is evidenced by the nest of $K-a$ curves shown in Fig. 2. For each value

of K up to the cusp-point of any particular curve considered, there are two reciprocal values of a; and when the resonance factor is greater than that represented by the cusp-point, there can be no value of a yielding the transition case. Furthermore, if the values of K and a in any given case are such that the point having these values as coordinates lies within the area bounded by the proper curve and the a axis, there will be two maxima to the $I-f$ curve; if this point lies without that area, there will be but one maximum.

Turning now to a consideration of special cases, it will be at once noticed that when $K=2$, Eq. (2) reduces to a cubic in x^2, and by applying the condition for equal roots as given in the theory of equations to the resulting relation, the transition value of a is readily obtained. In particular, when

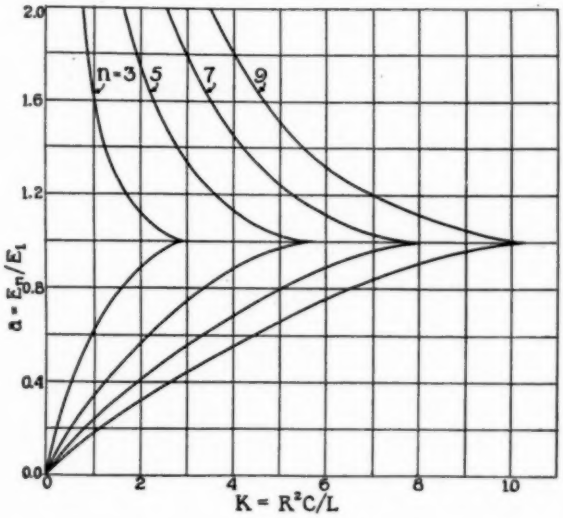

Fig. 2. Relation between K and a in transition cases for the series circuit. n = order of harmonic.

$n=3$, the most common case arising in practice, we find for a the value 0.8893, or the reciprocal, 1.1245. Again, it is plain that when the resonance factor is zero, which occurs when there is no resistance, a must be zero (or infinite).

Thirdly, and most important of all, the exact limiting value of the resonance factor may also be determined. By putting $a=1$ in Eq. (2), we get

$$n^2(n^2+1)x^6+4n^3(K-2)x^5+(n^2+1)(n^2K^2-4n^2K-n^4+7n^2-1)x^4$$
$$-(n^2+1)(n^2K^2-4n^2K-n^4+7n^2-1)x^2-4n^3(K-2)x-n^2(n^2+1)=0. \quad (4)$$

This equation has the roots ± 1; dividing through, therefore, by (x^2-1), there is obtained after reduction a symmetrical fourth degree equation. Now since $a=1/a$ in this case, we must have the double root $x=1/x$; that is, x is unity. Hence substituting $x=1$ in the fourth degree equation, it will be found that

$$K_E=(n-1)^2(n^2+4n+1)/n(n^2+1). \quad (5)$$

Thus, for all values of n, the resonance factor has a real and rational value when $a=1$ in the transition case. Fig. 3 shows the graph of Eq. (5); it is seen that there is approximately a linear relation between K and n, the resemblance to strict proportionality increasing as n becomes larger. It is particularly significant that the value of the resonance factor below which there may be two maxima to the $I-f$ curve increases as the order of the harmonic present increases.

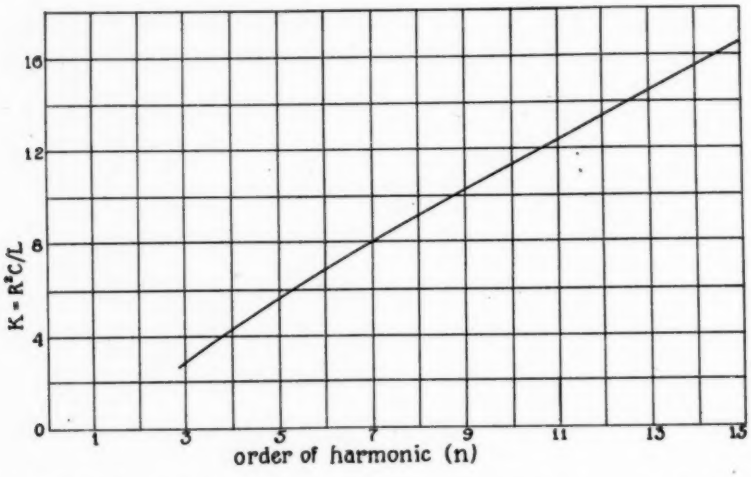

Fig. 3. Relation between K and n in transition cases for the series circuit. $K_E=(n-1)^2\,(n^2+4n+1)/n(n^2+1)$.

By applying the test for turning points to Eq. (3), it will be found that when $a=1$ and K is less than the value given by (5), the current-frequency curve will always have its minimum at the frequency

$$f=1/2\pi(nLC)^{1/2}. \tag{6}$$

The above relations are of theoretical interest alone, but in certain cases they may also be used in an experimental determination of the e.m.f. component amplitudes of a wave made up of the fundamental and the nth harmonic. Thus, if the variation in current as the frequency increases from a little below $f=1/2\pi n(LC)^{1/2}$ to a little above $f=1/2\pi(LC)^{1/2}$ is noted for a circuit whose resonance factor is small, and this process rpeated for various values of K until the transition point is obtained, the magnitude of a may then be found from the proper $K-a$ curve; hence, if E is the measured voltage, the components will be given by $E_1=E/(1+a^2)^{1/2}$, and $E_n=aE_1$. Even when additional harmonics are present, provided they are small compared to the nth harmonic, the latter may be approximately determined by this method.

II. Parallel Circuit

The line current in a parallel circuit consisting of the the three branches R, L, and C, is in general given by[2]

$$I^2 = E^2[g^2 + (\sigma/L\omega)^2 + (\delta C\omega)^2 - 2C/L], \tag{7}$$

where g is conductance, $1/R$; and σ and δ are the distortion factors

$$\sigma = \left(\frac{E_1^2 + (E_3/3)^2 + \cdots + (E_n/n)^2}{E_1^2 + E_3^2 + \cdots + E_n^2}\right)^{1/2}; \quad \delta = \left(\frac{E_1^2 + (3E_3)^2 + \cdots + (nE_n)^2}{E_1^2 + E_3^2 + \cdots + E_n^2}\right)^{1/2}.$$

Differentiating this equation with respect to ω, and setting the derivative equal to zero as before, there is found

$$\omega^2 = \sigma/\delta LC. \tag{8}$$

Thus, no matter what the number of harmonics, there will be only one minimum point to the current-frequency curve, but the resonant frequency

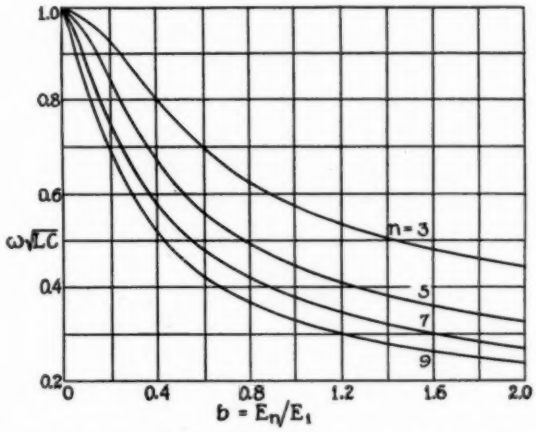

Fig. 4. Relation between b and $\omega(LC)^{1/2}$ for minimum current in the parallel circuit. n = order of harmonic.

depends upon both the orders of the existing harmonics and their voltage amplitudes. Now when only E_1 and E_n are present in the e.m.f. wave, (8) reduces to

$$\omega^2 = \frac{1}{nLC}\left(\frac{n^2 + b^2}{1 + n^2b^2}\right), \tag{8'}$$

where $b = E_n/E_1$. Fig. 4 shows the relation between b and $\omega(LC)^{1/2}$ for various values of n. It is seen that for a given harmonic, the frequency at which minimum current is obtained becomes less as the ratio b of the ampli-

[2] For the derivation of this equation, see F. M. Mizushi, "An Analytical and Graphical Solution for Non-Sinusoidal Alternating Currents," Proceedings, A.I.E.E., June, 1915, pp. 1075–1086.

tudes increases. In addition, this frequency is less when n increases, b having some particular value.

Inserting the reduced distortion factors into Eq. (7), there is obtained for the current

$$I^2 = E^2\left[g^2 + \frac{n^2+b^2}{n^2(1+b^2)L^2\omega^2} + \frac{(1+n^2b^2)C^2\omega^2}{1+b^2} - 2C/L\right]. \tag{9}$$

Now the differential equations for the series and multiple circuits are of the same form, the only differences lying in the interchange of e and i, L and C, and R and g. Hence, substitutions similar to those employed for the series circuit may be made here; thus, when the expressions

$$K' = g^2L/C, \quad y = LC\omega^2, \quad \text{and} \quad b = E_n/E_1$$

are put into (9), the following simpler form is obtained:

$$LI^2/CE_1^2 = (K'-2)(1+b^2) + (n^2+b^2)/n^2y + (1+n^2b^2)y. \tag{9'}$$

It will be noticed that the compound constant K' is the reciprocal of the resonance factor K used for the series circuit.

Typical generalized current-frequency curves have been plotted from equation (9'), n having been taken as 3, K' as unity, and b equal to both zero and unity. These indicate that the presence of a third harmonic of large amplitude produces a greater effect as the frequency increases beyond the minimum point. Equation (9') also shows that the current at any given frequency becomes greater as K' increases.

The values of current flowing into the inductive and capacitive branches are given by

$$I_L = E\sigma/L\omega; \qquad I_C = E\delta C\omega \tag{10}$$

respectively. When only the nth harmonic in addition to the fundamental is present, Eq. (10) may be expressed as

$$LI_L^2/CE_1^2 = (n^2+b^2)/n^2y; \qquad LI_C^2/CE_1^2 = (1+n^2b^2)y. \tag{11}$$

These two quantities constitute two of the terms of equation (9'); hence a comparison between each of the branch currents and the line current may be readily made.

In all cases, σ and δ being constant, the inductance current varies inversely, and the condenser current directly, as the frequency. If, therefore, these two currents be plotted against frequency, the resulting curves will be rectangular hyperbolas and straight lines respectively. The slope of the straight lines increases as the number or order of the harmonics increases, so that the current at a given frequency is greater in magnitude. But there is very little difference in the graphs for the inductance current for various

wave forms; for example, if in Eq. (11) we take $b=0$ in the one case, and $n=3$ and $b=1$ in another, the curves will have as equations

$$(I_L/E_1)(L/C)^{1/2}=1/2\pi f(LC)^{1/2}\,; \qquad (I_L/E_1)(L/C)^{1/2}=1.054/2\pi f(LC)^{1/2}$$

By the use of curves similar to Fig. 4, the amplitudes of the fundamental and any harmonic may be determined experimentally, just as for the series circuit. Since there is in all cases only one minimum to the current-frequency curve for the parallel circuit, the method is here somewhat more readily applied; but on the other hand, the presence of a number of harmonics is not made so evident.

DEPARTMENT OF PHYSICS,
CORNELL UNIVERSITY,
January 20, 1927.

THERMO-ELECTRIC EFFECT IN SINGLE CRYSTAL ZINC

By Ernest G. Linder

Abstract

Thermal e.m.f., thermo-electric power, Peltier heat of single crystal Zn against Cu as functions of crystal orientation.—In continuation of previous work data are presented on the thermal e.m.f. against copper of six single crystal wires of zinc, of which the orientations of the main crystallographic (hexagonal) axis with respect to the wire axis, range from 11.4° to 90°. (The average deviation from the mean for these observations is 0.8°.) The temperature interval is from −182° to 475°C. The apparatus designed to enable measurements to be made above the melting point is described in detail.

Thermo-electric power, Peltier heat, and difference of Thomson coefficients for $Zn_\perp$ against $Zn_\parallel$.—From the data are calculated the thermo-electric power, Peltier coefficient, and difference of the Thomson coefficients for $Zn_\perp$ against $Zn_\parallel$. The data also provide a test for the Voigt-Thomson law for the variation of the thermo-electric power with crystal orientation. The law seems to be verified within the limits of experimental error for the low temperatures, but the deviations at the high temperatures (300°–400°) are greater than the experimental errors are thought to be.

Thermal e.m.f. of liquid Zn against single crystal and polycrystalline Zn.—Further, the thermo-electric powers of liquid Zn against solid single crystal Zn of different orientations, and against polycrystalline Zn are given. The value -7.89μv. per deg. for $e_l - e_s$ for Zn (polycrystalline) having been found. A theoretical discussion of the thermo-electric effect in polycrystalline substances having different properties along only two of the crystallographic axes, leads to the formula $\bar{e} = (1/3)(2e_\perp + e_\parallel)$, and indicates that such a polycrystalline metal wire should behave the same as a single crystal wire of orientation 54.5°, the experimental value found being between 65° and 70°. It appears from this formula that polycrystalline Zn may be considered as an alloy of two parts $Zn_\perp$ and one part $Zn_\parallel$.

Introduction

In 1925 the author published a preliminary account[1] of measurements which he was then making of the thermo-electric properties of single crystal zinc. Since that time papers have appeared by P. W. Bridgman[2] who investigated the thermo-electric properties of Sn, Bi, Cd, Sb, Te, and Zn, from 20 to 100°C for various ranges of orientations, and by Grüneisen and Goens,[3] who made similar measurements on Zn and Cd from −253 to 100°C. The work which is described in this paper is a continuation of that previously reported. It consists of measurements with an improved apparatus of the thermo-electric properties of six Zn crystals, over an increased range of both orientation and temperature.

[1] E. G. Linder, Phys. Rev. **26**, 486 (1925).

[2] P. W. Bridgman, Nat. Acad. Sci. Proc. **11**, 608 (1925); Proc. Amer. Acad. Sci. **61**, 101 (1926).

[3] Grüneisen and Goens, Zeits. f. Physik. **37**, 378 (1926).

General Method and Apparatus

Only in a few details was the general method of investigation different from that usually employed in thermo-electric research. The Zn crystals were prepared by a method similar to that devised by Czochralski,[4] the apparatus shown in Fig. 1 being used. The electric furnace, *F*, contained the crucible of molten Zn from which the crystal was drawn. The square brass bar, *B*, ran vertically through the two guides, *C*, and was raised at the desired rate by a weight motor which wound up a steel wire, *K*, running over a pulley and fastened to the lower end of *B*. Another steel wire, *L*, ran to a counterbalance. The entire mechanism was mounted on a heavy wooden

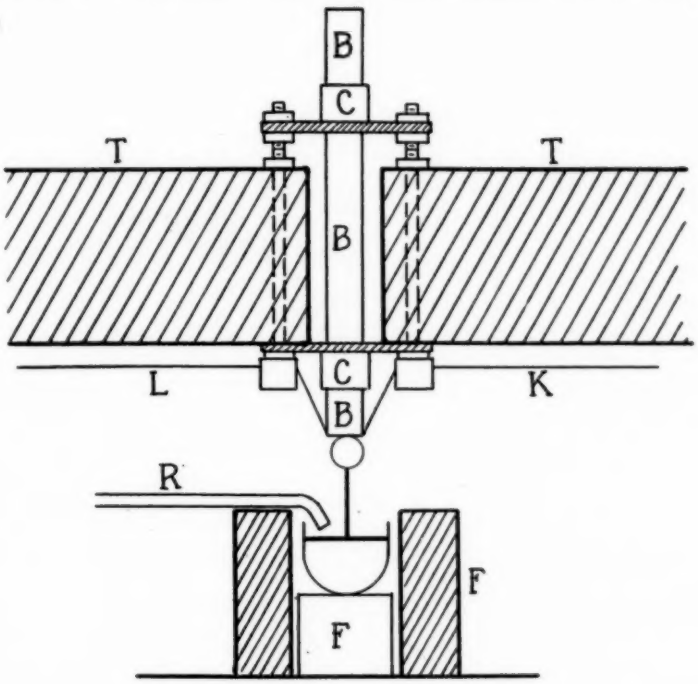

Fig. 1. Apparatus for production of crystals.

support, *T*. In order to regulate the rate of cooling of the crystal, an air current was directed against it through the tube *R*.

The thermal e.m.f. against Cu was measured for various temperature differences by keeping one junction at 0°C and varying the temperature of the other. The essential parts of the apparatus employed for this are shown diagrammatically in Fig. 2. The Zn single crystal, *Z*, was held in a vertical position, its lower end, the hot junction, being at *H*, and the upper end, or cold junction, at *C*. The entire crystal was snugly surrounded by a glass tube, the purpose of which was to protect the crystal and to support it after the temperature at *H* rose above the melting point. *H* was actually a hemispherical Cu block, which closed the lower end of the tube and into

[4] Czochralski, Zeits. f. Phys. Chem. 92, 219 (1918).

which were fused three wires leading to the binding posts A, B and C. No solder was used to make the hot junction, the crystal being fused directly to the copper by pressing it against H while H was heated and a zinc chloride flux applied. It was found that the crystal structure was not thus destroyed, but maintained up to the surface of contact with the copper. Obviously solder would contaminate the junction, especially above its melting point, and further, this contamination would cause serious errors since the temperature gradient at H was usually very steep. This entire junction was surrounded by fire clay held in a crucible and heated by a bunsen burner. For temperatures lower than that of the room the crucible was removed and the junction immersed in, or placed at suitable heights above, the

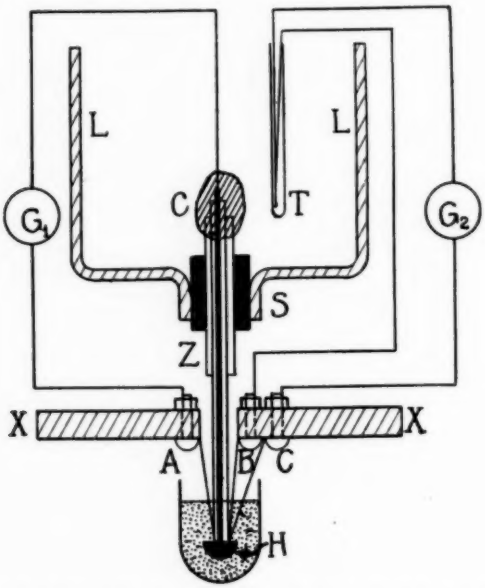

Fig. 2. Apparatus for measuring thermo-electric e.m.f.

surface of liquid oxygen. The wire leading to A was of Cu, and constituted the second element of the thermo-electric circuit, AG_1CZH. G_1, a sensitive galvanometer in series with a high resistance, was calibrated in microvolts. The wires leading to B and C constituted elements of the Cu-Advance, temperature-measuring circuit, BTG_2CH. The asbestos board, X, served both as a support for H and as a shield between the flame and the ice container L. The crystal in its glass tube, passing into L through a second, larger tube in a rubber stopper, S, was soft soldered to the copper wire at C, and this junction, together with the ends of the two glass tubes surrounded with a wad of sealing wax.

This apparatus is different from that employed in the previous work, modifications being necessary in order to measure the e.m.f. above the melting point, and also because it was thought that possibly the previous method of sealing in the crystal had introduced some error.

Results

1. *Thermo-electromotive force, thermo-electric power and Peltier heat as functions of crystal orientation.* The observed values of the thermal e.m.f. against Cu for each of the six single crystals are given in Table I, the e.m.f. being considered positive when it is directed from the hot to the cold junction through the Zn. The data are partially represented in the graphs of Fig. 3

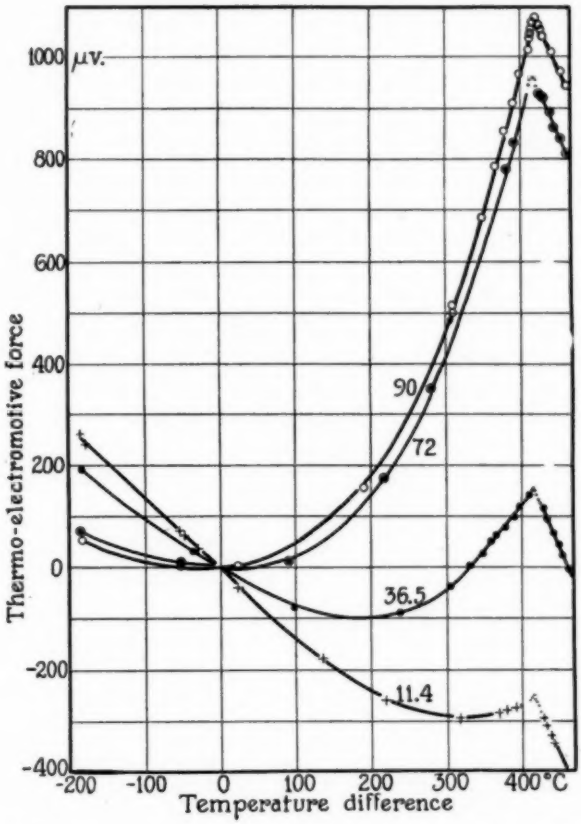

Fig. 3. E.m.f. vs temperature-difference for various orientations. Each curve is labeled with its orientation angle.

orientations 70° and 74° being omitted since their curves are very nearly coincident with that for 72°. The curves of Fig. 3 may be well represented between 0°C and the melting point by empirical equations of the type: $E=At+Bt^2+Ct^3$, where E is the thermal e.m.f., t the temperature difference of the junctions, and A, B, C, constants characteristic of the individual curves. Bridgman[2] found that second degree equations represented his results for zinc, but this may be due to his more limited temperature range. Over the same range the writer's results can also be represented by second degree equations. Differentiation of such an equation with respect to t yields the thermo-electric power e.

TABLE I

Observed thermal e.m.f. of single crystal Zn against Cu.

8, $\theta=11.4°$		10, $\theta=36.5°$		7, $\theta=70°$		11, $\theta=72°$		5, $\theta=74°$		9, $\theta=90°$	
t°C	$E\mu V$	t°C	$E\mu V$	t°C	$E\mu V$	t°C	$E\mu V$	t°C	$E\mu V$	t°C	$E\mu V$
−181	263	−180	192	−182	82	−182	73	−182	75	−181	53
−174	242	− 33	34	−179	76	− 81	22	− 77	20	− 52	3
− 52	74	99	− 76	− 68	20	− 50	11	20	− 1	24	2
− 45	64	238	− 88	− 64	18	90	13	73	9	191	157
− 28	39	304	− 38	− 42	10	217	179	80	12	307	515
25	− 34	331	3	− 32	7	280	354	191	126	348	686
136	−178	348	27	− 26	5	381	780	292	403	307	504
219	−258	358	50	21	− 3	389	830	332	565	367	788
317	−292	368	63	56	− 1	411	939	361	700	378	856
368	−284	378	79	103	16	413	950	392	925	389	910
378	−278	389	96	194	120	415	956	394	930	398	965
389	−274	398	118	262	287	417	960	413	1060	409	1015
398	−267	409	140	317	480	419	954	418	1020	411	1035
409	−257	411	144	368	720	422	945	419	1020	413	1045
411	−255	413	148	378	725	425	930	422	1025	415	1055
413	−253	415	149	389	808	428	925	425	1013	417	1070
415	−257	417	148	409	910	430	920	428	1013	419	1075
417	−264	419	140	411	920	437	890	431	993	422	1070
419	−270	422	132	413	930	444	860			423	1065
422	−280	423	125	415	944	452	840			425	1055
423	−284	428	114	417	955	459	810			430	1045
425	−294	433	94	419	965	465	800			441	1010
430	−308	441	67	423	982	470	775			452	970
435	−327	448	44	425	990	474	760			459	945
441	−343	455	21	430	972					470	910
455	−400	465	− 5	432	970					474	890
465	−436	474	− 39	441	935						
470	−455			452	885						
474	−461			465	845						
				474	808						

The only theory so far proposed to explain the thermo-electric properties of crystals is the thermodynamical one of Voigt[5] and Thomson,[6] according to which

$$e=e_{\parallel}\cos^2\theta+e_{\perp}\sin^2\theta=e_{\perp}+(e_{\parallel}-e_{\perp})\cos^2\theta \qquad (1)$$

where θ is the angle between the hexagonal axis and the axis of the wire, $e_{\parallel}$ and $e_{\perp}$ are the thermo-electric powers parallel and perpendicular to the hexagonal axis, respectively.

The treatment of Voigt leads specifically to Eq. (1) above. Bridgman[7] considers that Voigt's and Thomson's analyses have taken no account of either the internal or surface Peltier heat and that therefore Eq. (1), as derived by Voigt, cannot be expected to apply to an actual thermocouple. leaving aside the theoretical considerations underlying the derivation of the equation it is interesting to test it experimentally, considering it, for the moment, as purely empirical. Bridgman has made such a test for zinc and other metal crystals and arrives at the conclusion that the equation is not generally valid for the representation of the experimental facts. The

[5] Voigt, Lehrbuch der Kristallphysik.

[6] W. Thomson, Math. and Phys. Papers I, p. 232.

[7] Reference 2, p. 128.

chief deviation is found in the case of the Peltier heat. This conclusion is based on the non-linear relation between specific resistance and a constant a', which is shown to be proportional to the Peltier heat at 0°C.

The writer's own results have been applied to test the validity of Eq. (1) in a somewhat different fashion. It is evident from the equation that e plotted against $\cos^2\theta$ should give a straight line. Such curves for various temperature differences are given in Fig. 4, (points plotted as circles) and, as is evident, the law appears to hold for the lower temperatures, but there seems to be a deviation for the 300° and 400° curves. That is deviation actually exists and is not due to experimental error is further indicated by the fact that the author's previous data[1] show the same type of variation. (e was not calculated in the previous paper but may be obtained from the

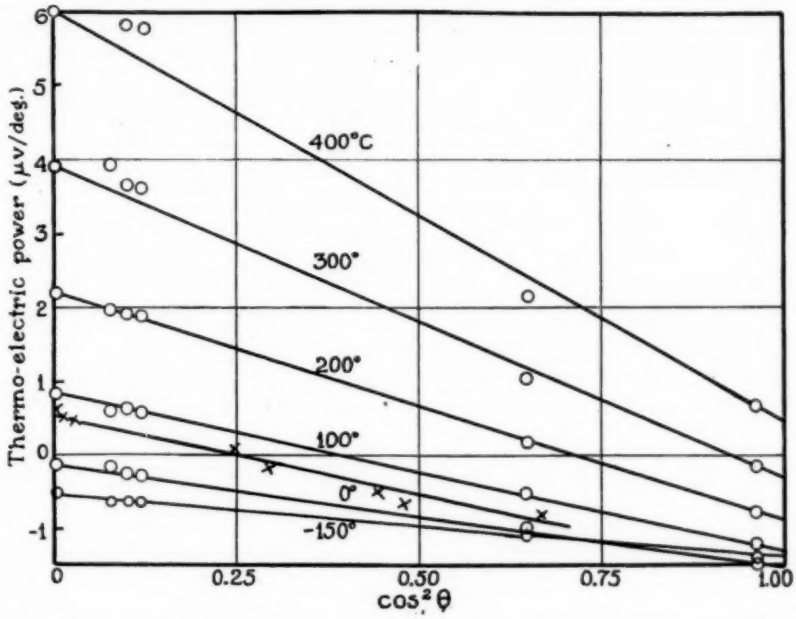

Fig. 4. Thermo-electric power against copper vs $\cos^2\theta$ for various temperature differences. Linder, O; Bridgman, X.

curves there given.) Neither can this be due to the variation of θ with the temperature since a simple calculation based on thermal expansion coefficients found by Grüneisen and Goens[3] shows this to be considerably too small.

It should further be pointed out that if the usual thermodynamical relation for the Peltier heat, $\Pi = T\,dE/dt$, is assumed, then the curves of Fig. 4 also show how far Eq. (1) is valid to express the nature of the variation of Peltier heat with the orientation angle. Returning now to Bridgman's data, they may be reduced in a similar fashion. dE/dt is, in his notation, given by $a'+2bt$, and expressions are given for calculating a' and b from the

[3] Grüneisen and Goens, Zeits. f. Physik. **29**, 141 (1924).

points plotted in his Fig. 4.[9] The thermo-electric power thus computed for $t=60°$ is plotted as crosses ($\times$) in Fig. 4 against $\cos^2\theta$. As is evident, a fairly good straight line results; what deviations exist are not systematic and may well be due to experimental error. In fact Bridgman's 46.5° curve[10] is of doubtful validity since it differs considerably from its neighbors and resembles very much curves which the author has obtained from specimens which were not single crystals but consisted of two or three single crystals together. The same criticism may be made of his 80° or 83° curve. The other curves for the Peltier effect, which Bridgman gives are all nearly straight lines with the exception of the one for tin. Here, however, the experimental points are so scattered that it is uncertain whether the curve is straight. In view of the above it seems that the Voigt-Thomson symmetry relation is obeyed to a much closer degree than was concluded by Bridgman.

II. *Relative Thermo-electric Properties of $Zn_\perp$ and $Zn_\parallel$.* Grüneisen and Goens[3] have pointed out the desirability of obtaining the thermo-electric properties of a single metal. To do this they have expressed the various thermo-electric constants of one principal orientation, $Zn_\perp$(i.e., $\theta=90°$) against the other, $Zn_\parallel$(i.e., $\theta=0°$). The results described under Section I above may be presented in a similar fashion.

From the Voigt-Thomson law, Eq. (1), we get, by integration,

$$E=E_\parallel \cos^2\theta+E_\perp \sin^2\theta, \tag{2}$$

where E is the e.m.f., providing that θ is independent of the temperature difference, t, of the junctions. As has been mentioned above, this is very

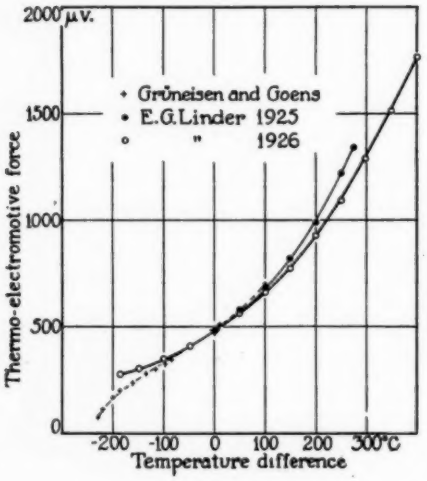

Fig. 5. Thermal e.m.f. for $Zn_\perp$ against $Zn_\parallel$.

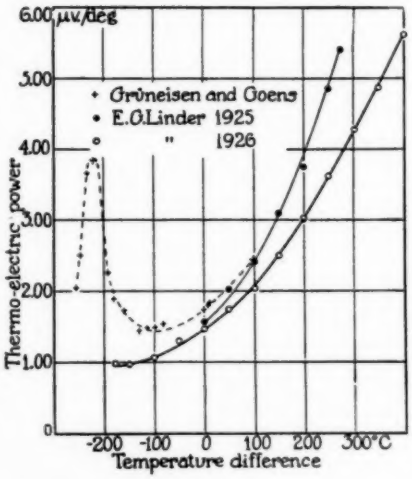

Fig. 6. Thermo-electric power for $Zn_\perp$ against $Zn_\parallel$.

[9] Reference 2. There is an error in Bridgman's Fig. 4, p. 116, since he has not plotted the angles between the crystal axis and the length of the rod as abscissas but their complements. He also has the sign of his Δ wrong according to its definition on p. 114.

[10] Reference 2, Fig. 3, p. 115.

nearly true and will be assumed so. Hence, by introducing into Eq. (2) the observed values of $E_\perp$ and E for 11.4°, the values of $E_\parallel$ may be calculated. For the purpose of comparison we now introduce the value $E(0°, -253°) = 483.6\mu v$. (i.e., the e.m.f. with one junction at 0° and the other at −253°C) taken from the work of Grüneisen and Goens, and by use of the law of intermediate metals, get

$$E(t, -253°) = E(0°, -253°) + E(t, 0°)$$

where all of the E's are for $Zn_\perp$ against $Zn_\parallel$. The values obtained in this manner together with those of Grüneisen and Goens are represented graphically in Fig. 5, and are tabulated in Table II. In this figure, and also in

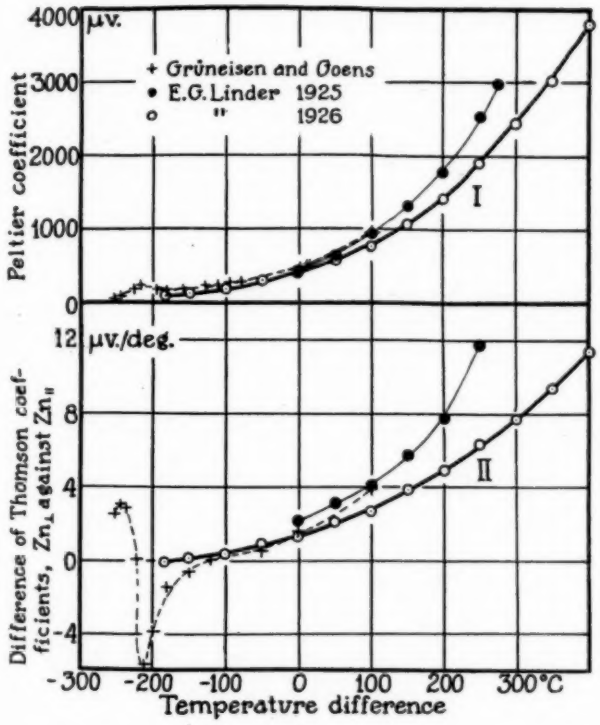

Fig. 7. I Peltier coefficient for $Zn_\perp$ against $Zn_\parallel$. II differences of the Thomson coefficients for $Zn_\perp$ against $Zn_\parallel$.

Figs. 6 and 7, are displayed the writer's earlier results, reduced in the same fashion, together with those of Grüneisen and Goens.

The thermo-electric power, $e = dE/dt$, can be obtained by measuring the slope of the tangents to the curve of Fig. 5. It is to be noted that dE/dt is independent of the additive constant, $E(0°, -253°)$. The values of the thermo-electric power thus obtained are listed in Table II and graphed in Fig. 6.

According to Kelvin's thermodynamical theory, the Peltier coefficient is given by

$$\Pi = Te,$$

where T is the absolute temperature of the junction. The values calculated according to this formula are given in Table II and curve I, of Fig. 7.

The difference of the Thomson coefficients, which, from the same theory, is given by

$$\sigma_{\perp}-\sigma_{\parallel}=T(de/dt),$$

TABLE II

Thermal e.m.f., thermo-electric power, Peltier heat and difference between Thomson coefficients for $Zn_{\perp}$ against $Zn_{\parallel}$.

T	$E(t,-253°)$	e	Π	$\sigma_{\perp}-\sigma_{\parallel}$
−182°C	275 μv	.99 μv/deg.	90 μv	−.11μv/deg.
−150	304	.96	118	.10
−100	355	1.07	185	.37
− 50	414	1.32	295	.92
0	484	1.47	402	1.39
50	564	1.77	572	2.18
100	661	2.05	765	2.69
150	771	2.53	1075	3.87
200	921	3.00	1420	4.87
250	1087	3.63	1900	6.33
300	1285	4.28	2450	7.67
350	1511	4.85	3025	9.45
400	1770	5.65	3800	11.40

can also be calculated by using values of de/dt obtained by measuring the slope of the tangents to the curve of Fig. 5. The data so obtained are given in Table II and curve II of Fig. 7.

III. *Behavior at the melting point.* Observers disagree as to whether there is a break in the thermo-electric power curve at the melting point. For zinc Darling and Grace[11] and also H. Pélabon[12] write that they observed no

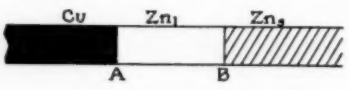

Fig. 8. Diagram of zinc crystal—copper junction above the melting point of zinc.

change, while, on the other hand, J. Koenigsberger[13] observed one, and gives the experimental value $e_e-e_s=-10\mu$v./degree, where e_e is the thermo-electric power of liquid Zn and e_s that of solid Zn. He also gives the theoretical values, -5.6μv./deg. from Bernoulli's formula[13] and -6.0μv./deg. from Lorentz's formula.[13] As may be seen from Fig. 3, the author found a distinct break at the melting point. The crystal structure—at least insofar as it determines the thermo-electromotive force—breaks down suddenly and not gradually as the temperature passes that point. Further, those parts of the curves above 419°C are approximately parallel, which is precisely what we should expect, for after the Zn crystal has melted we have the situation depicted in Fig. 8. The junction A, between the solid Cu and liquid

[11] Darling and Grace, Proc. Lond. Phys. Soc. **30, 14** (1917).
[12] H. Pélabon, Ann. d. physique, **13,** 169 (1920).
[13] J. Koenigsberger, Ann. d. Physik. **47,** 563 (1915).

(homogeneous) Zn may vary in temperature from 419°C up, and the e.m.f., E_A, due to it, is the same for all crystals; on the other hand, the junction B, between liquid Zn and crystalline Zn, is always at the same temperature, i.e., 419°C, but the e.m.f. due to it, E_B, is different for crystals having different orientations. Thus E_B acts as an additive constant, and the total e.m.f., $E=E_A+E_B$, represents a family of parallel lines. The values of e_l-e_s for different orientations, and values for two specimens of polycrystalline Zn are arranged in Table III. The average value, -7.98 μv./deg.,

TABLE III

Thermo-electric power of solid and liquid zinc at the melting point.

θ	e_s μv/deg.	e_l μv/deg.	e_l-e_s μv/deg.
11.4	1.13	−3.61	−4.75
36.5	2.00	−3.20	−5.20
72	4.87	−3.58	−8.45
90	5.30	−3.23	−8.55
P.C.1	4.25	−3.64	−7.89
P.C.2	4.88	−3.18	−8.06

which the author obtained for Zn_{poly}, is in better agreement with the theoretical values than those of Koenigsberger mentioned above.

The principal sources of error in the measurements presented in the above three sections probably are: (1) the determination of the orientation[1]; (2) the measurement of the temperature of the hot junction (a different copper-advance thermocouple and block, H, Fig. 2, were used in order to prevent contamination of the block due to diffusion into it by the liquid Zn, each being made, however, with wires from the same spools and in an identical manner); (3) impurity of the zinc. Merck "highly pure" zinc was employed.

IV. *Effect in polycrystalline substances.* As is well known, many so-called isotropic substances are, in reality, quasi-isotropic, i.e., random aggregates

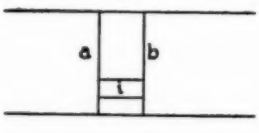

Fig. 9.

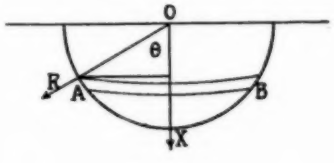

Fig. 10.

of small crystal particles. Since this is the case, it should be possible to express the properties of the aggregate in terms of the properties of its component single crystal parts. An attempt to do this in the case of the thermo-electric properties of polycrystalline metals has met with a fair degree of success.

Consider an arbitrary, cross-sectional element, ab, Fig. 9, of a polycrystalline conductor constituting one of the elements of a thermo-electric circuit. The two plane boundaries of ab, we shall assume to be equipotential surfaces. Let V be the potential difference between them. Let I_i, r_i and E_i be the

current, resistance and thermal e.m.f. of any one crystal in this element Then, assuming that each crystal extends from a to b, we have, from Kirchoff's second law

$$V = I_i r_i + E_i.$$

Further, the total current I is given by

$$I = \sum_i p_i I_i = \sum_i p_i \, V - E_i)/r_i, \tag{3}$$

where p_i is the concentration of crystals having the orientation θ_i. This may be found as follows: In Fig. 10 let OX represent the axis of the Zn wire, and OR the hexagonal axis of any crystal. It is evident that the probability of the hexagonal axis making an angle between θ_i and $\theta_i + d\theta$ with the wire axis is (area of strip AB_i)$/2\pi r^2$ or $p_i = \sin\theta_i d\theta$. Now Eq. (3) holds for any value of I, hence put $I = 0$, then,

$$V \sum_i p_i/\sigma_i = \sum_i p_i E_i/\sigma_i,$$

where σ_i is the specific resistance of any Zn crystal of orientation θ_i, and is given by

$$\sigma_i = \sigma_\parallel \cos^2\theta_i + \sigma_\perp \sin^2\theta_i.^{5}$$

Introducing the similar expression for E, Eq. (2), we have

$$V = \frac{\displaystyle\int_0^{\pi/2} \frac{E_\parallel \cos^2\theta + E_\perp \sin^2\theta}{\sigma_\parallel \cos^2\theta + \sigma_\perp \sin^2\theta} \sin\theta d\theta}{\displaystyle\int_0^{\pi/2} \frac{\sin\theta}{\sigma_\parallel \cos^2\theta + \sigma_\perp \sin^2\theta} d\theta}$$

$$= E_\perp + (E_\parallel - E_\perp)/(4 - r)$$

where $r = \sigma_\parallel/\sigma_\perp$. Assuming that $r = 1$, we have

$$V = \overline{E} = E_\perp + (1/3)(E_\parallel - E_\perp) \tag{4}$$

and by comparison with Eq. (2) it follows that $\cos^2\bar{\theta} = 1/3$; whence $\bar{\theta} = 54.5°$. In other words, a polycrystalline wire should give the same thermal e.m.f. as a single crystal wire having an orientation of 54.5°. The author found the experimental value of 65 − 70° for Zn. The agreement is not good, but in view of the assumptions we could not expect it to be better.

Unfortunately, as far as the author is aware, there are no other data suitable for checking this result. The variation among the different available measurements on polycrystalline metals is so great that it appears that a reliable check can be obtained only when the polycrystalline and single crystal measurements are made by *identical* methods and on the *same* samples of metal. For this reason it seems that Bridgman's conclusion, based on experimental data, that the thermo-electric properties of the aggregate cannot be found by averaging the properties of the single crystals, is scarcely justified.

By differentiating Eq. (4) with respect to t, and rearranging, we have,

$$\bar{e}=(1/3)(2e_{\perp}+e_{\parallel}),$$

and this is identical with a type of formula which has been found to give the thermo-electric properties of alloys of mechanically mixed crystals of different metals,[14] therefore it appears as if polycrystalline metal, might be considered as an alloy of three components having properties corresponding to the three crystallographic axes, respectively, (two parts $Zn_{\perp}$ and one part $Zn_{\parallel}$ in the present case).

It should be pointed out that we obtain the same result, if, instead of taking a cross-sectional element, we consider a long strip parallel to the axis of the wire. In this case, instead of assuming the electrical conductivities equal, we assume the thermal conductivities so, and hence the temperature difference across each crystal will, on the average, be the same, so that we get,

$$E=\sum_i p_i E_i,$$

which leads to Eq. (4).

It may also be worthwhile to mention that expressions for the thermal and electrical conductivities of polycrystalline metals can be obtained by similar methods and that these formulas are identical with those which have been found to hold for alloys of mechanically mixed crystals.[15]

Conclusion

Obviously the present electron theories of thermo-electricity are inadequate for the explanation of this effect in crystals, since electron gas pressure or electron concentration, as ordinarily understood, are not vector quantities, i.e., their magnitude is not a function of direction in the crystal. If, however, we take into consideration the fact that the spacing of the atoms in the lattice is different for different directions, and that, therefore, the mean free path of the free electrons would vary with direction and in consequence the electron gas pressure, we have a possible explanation.

The author wishes to express his thanks to Professor E. P. T. Tyndall for his valuable suggestions and criticism.

Physical Laboratory,
University of Iowa,
November, 1926.

[14] A. L. Bernoulli, Jahrb. d. Radioakt. **9**, 270 (1912).
[15] W. Guertler, Jahrb. d. Radioakt. **5**, 17 (1908).

MAGNETIC PERMEABILITY OF IRON AND MAGNETITE IN HIGH FREQUENCY ALTERNATING FIELDS

By G. R. Wait

Abstract

Relative values of the permeability of cast-iron filings, iron wires, and iron powder in high frequency magnetic fields.—Wwedensky and Theodortschik have found the magnetic permeability of iron, steel, and nickel in alternating fields to be abnormally large in certain frequency bands (at about 100 meters for iron) and nearly normal in other regions. The general appearance of the phenomenon suggested the existence, in the material, of resonators corresponding to these frequencies. The phenomenon has been observed also by Kralovec. Two experimental methods have been followed in the present investigation, one the resonance method and the other the heterodyne method. Both utilized, in principle, the measurement of the change in inductance of a coil due to the introduction of the sample of material into it. The wave-length ranges covered were from 80 to 1700 meters by the heterodyne method and from 50 to 160 by the resonance method. The heterodyne method was used in an improved form which eliminated drifts. The results are in disagreement with those of Wwedensky and Theordortschik and with those of Kralovec. No anomalous change in permeability was found at any frequency. The following errors, which may have misled previous investigators, were found in the course of the present work: (a) anomalous behavior of capacities in series when these are connected in tube circuits, an effect the nature of which is unknown but which is related in some way to the length of the connecting wires; (b) a general variation in the apparent permeability as measured by one coil, presumably due to effects of distributed capacity; (c) apparent anomalies when a number of coils are used without comparing the results at the same wave-length; (d) an apparent anomaly in the permeability, at a critical frequency, arising from the presence of a metal shield inside the coil; (e) an effect of drift in the heterodyne method.

The absolute value of the permeability of powdered magnetite.—The permeability of magnetite in powdered form has been measured by two fairly independent methods. The values decrease from about 1.532 at 132.2 meters to 1.401 at 85.8 meters. After due allowance is made for density of packing, these values compare favorably with the results obtained by a static method by Welo and Baudisch.

THE magnetic permeability of iron in oscillating magnetic fields of wave-lengths greater than 1000 meters, has been found to be approximately constant[1] and similar to that in stationary fields. For shorter wave-lengths, Wwedensky and Theodortschik,[2] using soft iron wires, determined the permeability between wave-lengths 54 and 705 meters and, using steel and nickel wires, between 50 and 500 meters. Their curve for iron wires, where μ, the permeability, is plotted against λ, the wave-length in meters, is shown in Fig. 1. This shows a sharp maximum of the permeability at about 100 meters, between two sharp minima. This apparently anomalous behavior of the

[1] R. Brown, J. Frank. Inst. **183**, 41 (1917).

[2] B. Wwedensky and K. Theodortschik, Ann. d. Physik. **68**, 463 (1922), and Phys. Zeits. **24**, 216 (1923).

permeability, at about 100 meters, was explained by the above workers as being due to the resonance of elementary magnets of which the iron is supposed to be composed, their frequency of oscillation being approximately 3×10^6 per second. J. Kralovec, making measurements on cast-iron filings,

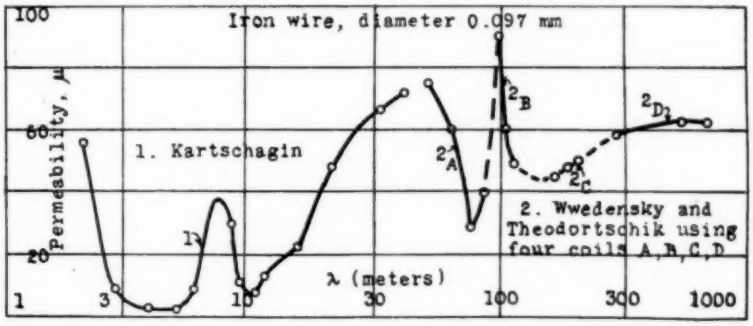

Fig. 1. Results by Kartschagin and by Wwedensky and Theodortshcik.

found anomalies between 80 and 90 meters and again between 100 and 110 meters. Observations on magnetite failed to show similar critical changes in permeability. The fundamental importance of obtaining definite proof as to the existence of such oscillators has led to the present investigation.

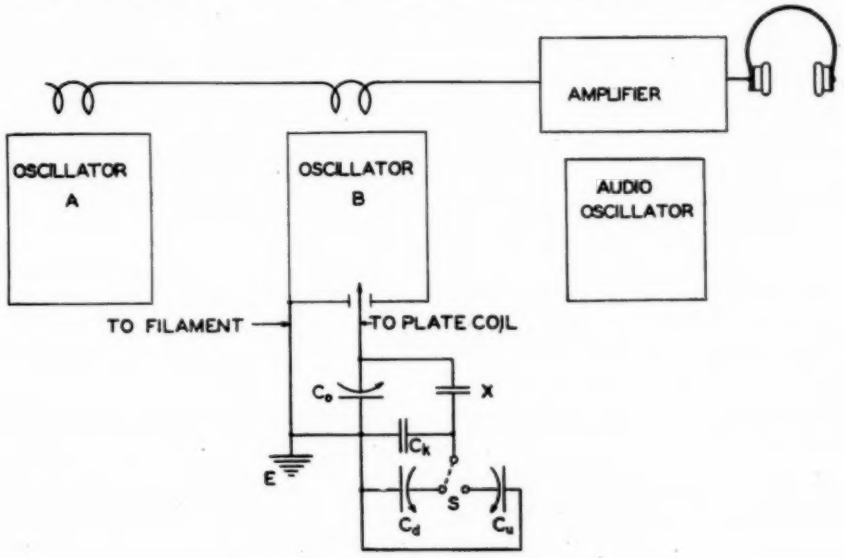

Fig. 2. Diagrammatic sketch of apparatus.

Apparatus and Experimental Methods

Two of the four methods used by Wwedensky and Theodortschik were used in a modified form in the present investigation. In method I, two electron-tube oscillators, *A* and *B*, of Fig. 2 were tuned so as to give a small number of beats which were detected by means of an audio-frequency

amplifier. The two oscillators were coupled loosely; the coupling coils were connected to the "input" of a three-tube amplifying unit and the phones to the "output." The sample, upon being introduced into the coils of set B, changed the tuning of the two sets by changing the inductance of the coil. The sets were returned to the original pitch by compensating for the changed inductance by a corresponding change in the capacity C of the system of condensers shown. This change was affected by altering the setting of C_o, a variable air condenser in series with the coil. The capacity of the air condenser X, was kept constant at about 219 mmf. C_k is a mica condenser of about 5500 mmf. C_u and C_d are variable air condensers, each with a range of about 30 mmf to 900 mmf. S is a mercury switch which automatically substitutes C_d for C_u when the sample is introduced quickly into the coil by a lever system. A rigid iron structure provides for exact centering of the sample in the coil and prevents movement of the sample in any direction after introduction. Sets A and B are shielded electrically by brass boxes. The amplifying unit and also all "A" and "B" storage batteries are in wooden boxes covered with sheet iron. All exterior electrical connections are properly shielded. In some of the work a tin-foil shield was introduced into coil "B" to shield the sample. A set of six pairs of oscillating coils of properly selected inductances, wound on bakelite tubing, gave considerable overlapping of wave-lengths. The total range of wave-lengths extended from about 80 meters to 1,700 meters. Table 1 gives particulars regarding each coil.

TABLE I

Particulars of coils used.

Coil No.	1	2	3′	3	4	5
Length (cm)	5.0	5.0	5.0	5.0	5.0	7.5
Diameter (cm)	8.8	8.8	8.8	8.8	8.8	8.8
No. of turns	7	10	14	26	51	76
Obs. inductance (micro-henries)	5.1	9.5	16.4	58	208	373

To measure the wave-lengths used, an auxiliary oscillator was set at resonance with sets A and B so as to leave unaltered the tuning that had been obtained between them. Then by means of a calibrated wave-meter the frequencies of the auxiliary oscillator were determined.

The selection and arrangement of capacities shown in Fig. 2 as X, C_k, and C_u (or C_d) acted as an extremely fine adjustment of capacity of condenser C_o. The curve connecting ΔC_d and ΔC is almost a straight line, and a change of nearly 900 mmf is required in ΔC_d to produce a change of 1 mmf in ΔC.

In practice, the sample was removed from the coil, sets A and B were tuned to a convenient pitch, and the audio-frequency amplifier was tuned to a pitch giving a very small number of beats. Upon introducing the sample into the oscillating coil of set B, retuning was effected by condenser C_d. Some drift was frequently present when it was necessary to remove and reintroduce the sample several times and to make appropriate readjustments of C_d for each determination of ΔC_d. The drift was kept to a minimum by

frequent charging of the storage batteries and replacing from time to time of the oscillating tubes (*UV* 199).

In method II, a resonating circuit was set at resonance with an oscillator. Upon introducing a sample into the coil of the resonating set, resonance could again be obtained by compensating for the changed inductance by a corresponding change in the capacity of the circuit. Detection was made by a thermocouple and galvanometer, a low and a high sensitivity galvanometer being used for magnetic fields of high and low intensity respectively.

Belz[3] showed that for a substance with cross-sectional area A' and length l', volume $V'=A'l'$, with sufficiently small susceptibility k, introduced into an oscillating coil of cross-sectional area A and length l, volume $V=Al$, if the inductance, L, of the coil is altered by an amount ΔL, then, neglecting effects arising from eddy-currents, demagnetization, end effects of the sample, and an alteration in the magnitude of the field due to the presence of the interior shield,

$$(V/V')(\Delta C/C)=(V/V')(\Delta L/L)=4\pi k$$

where C is the capacity of the system and ΔC the change in capacity necessary to compensate for the change in inductance. Wwedensky and Theodortschik applied this formulae to their results to get a quantity termed "apparent permeability." In their case, since their sample was longer than their coil, the ratio V/V' reduced to the corresponding ratio of areas. In the present paper, to make proper comparison with their results easier, the quantity $\Delta C_d/(C_o+K_n)$ has been plotted against λ, the wave-length in meters, where the expression (C_0+K_n) represents the total capacity and ΔC_d that necessary to compensate for the change in inductance of the coil due to the introduction of the sample. This procedure is sufficient to show any apparent changes in the relative values of permeability.

Results by the Beat Method

Iron filings as a sample. In preliminary work an apparently anomalous behavior for iron filings was obtained for particular settings of condenser C_o, in general similar for the various oscillating coils used. Tests showed that this could not be attributed to a faulty calibration of C_o, nor to the resonance of portions of the circuit having long lead-in wires with the main part of the circuit. The magnitude of the anomaly did not appear to depend upon the amount of iron used as a sample, and consequently could not be a permeability effect. Tests with experimental shields showed the cause of the anomaly was connected with eddy-currents set up in the shield altering the inductance of the oscillating set over the band of frequencies where the anomaly appeared.

In the definitive experiments the region of wave-lengths from about 99 to 1700 meters was covered, using iron filings as a sample. The same sample was not used throughout this range, as was the case later with the iron powder in insulating wax, consequently the results have not been given in

[3] M. H. Belz. Proc. Cambridge Phil. Soc. **21**, 52 (1922); Phil. Mag. **44**, 479 (1922).

graphs. However, in all the tests with these samples, after remedying the difficulty produced by the interior shield, no change in permeability at apparently critical frequency occurred.

Iron powder as a sample. For iron powder embedded in insulating wax, and formed into a sphere, relative premeability curves are shown in Fig. 3 for wave-lengths 84 to 1300 meters. Aside from small irregularities, the curves are smooth. In the region of 85 to 95 meters, there are irregularities amounting to about three percent of the value of ordinate. This is greater than can be ascribed to experimental error. This variation always occurred to some extent in the preliminary work, and was always of the same form regardless of the sample used. Various tests applied definitely proved that this was not due to eddy-currents set up in the sample nor to a change in its permeability.

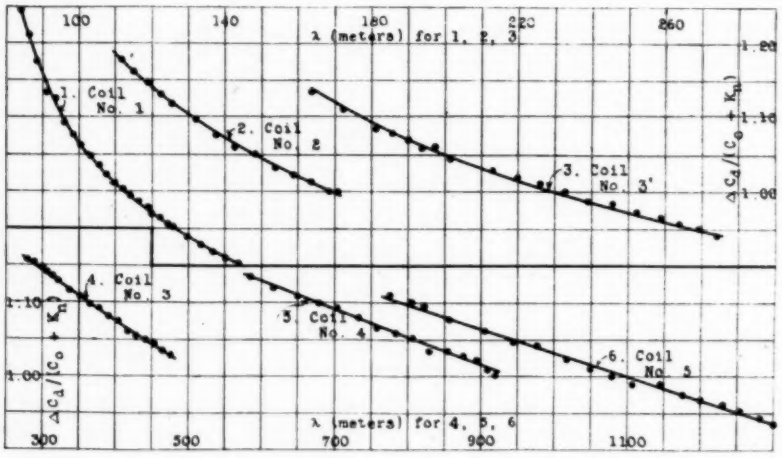

Fig. 3. Results for iron powder embedded in insulating wax, made into spherical form, for wave-lengths 84 to 1300 meters.

In Fig. 4 are presented curves for iron powder and iron wires showing the usual depression at 91.3 meters. When, however, the inductance in series with condenser C_d is increased, the depression gives way to a small maximum. When the inductance is added both to condensers C_u and C_d, the irregularity at this point disappears. This together with considerable additional evidence (a fuller discussion of which is prohibited on account of the lack of space) indicate that this irregularity is due to resonance between certain parts of the circuit.

A regular run with iron powder as a sample, made after shortening the connections between condensers X and C_x gives a curve (curve 6, Fig. 4) that is free from any resonance phenomenon, and is approximately horizontal. Data for curve 5 of Fig. 4 were obtained after replacing the connections as before. It will be seen that the resonance phenomenon has reappeared. It may be well to point out that the value of condenser C_k was different for these two curves from that for all previous curves; this has altered the

absolute values involved in these curves. All the above evidence points to the fact that the phenomenon shown between 85 and 95 meters is due to the resonance of one part of the circuit with another, and has nothing to do with

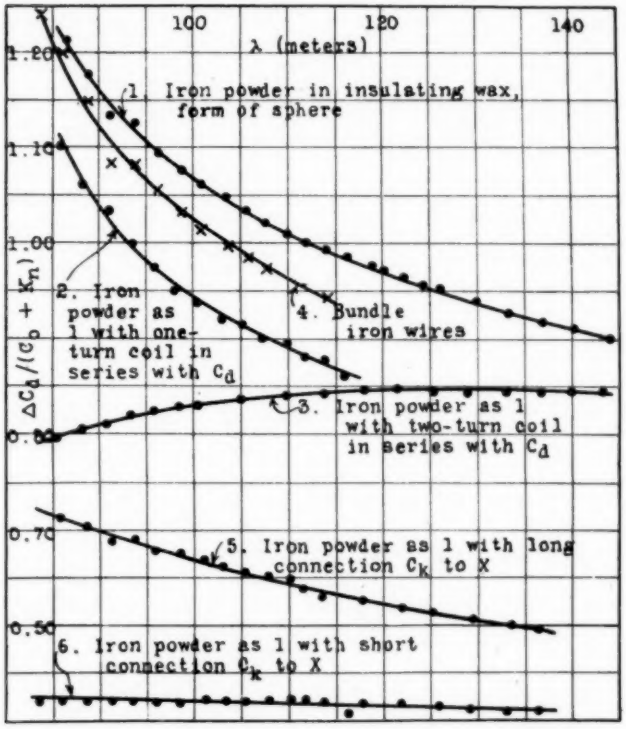
100
120
140
λ (meters)
1.20
1.10
1.00
0.90
0.70
0.50
1. Iron powder in insulating wax, form of sphere
2. Iron powder as 1 with one-turn coil in series with C_d
3. Iron powder as 1 with two-turn coil in series with C_d
4. Bundle iron wires
5. Iron powder as 1 with long connection C_k to X
6. Iron powder as 1 with short connection C_k to X
$\Delta C_d/(C_0 + K_n)$

Fig. 4. Tests on iron powder and wires showing apparent irregularities due to particular circuit connections.

the resonance of the elementary magnets of the sample. A sample set of observations and computations is shown in Table 2.

TABLE II

Sample set of observations and computed values of approximate permeability μ, for a bundle of 24 iron wires 24 cm long, 0.0127 cm in diameter each, using oscillating coil No. 1.

$C = X^2 C_d/(C_u + C_k + X)(C_d + C_k + X)$; $C_k = 5501$ mmf; $X = 219$ mmf; $\mu = A\Delta C/A'C + 1$

A, cross-sectional area of oscillating coil, $= 60.85$ cm²

A', cross-sectionl area of sample, $= 0.0121$ cm²

Div	C_0 mmf	Div	C_d mmf	ΔC_d mmf	C_u mmf	ΔC mmf	μ	λ meters
5	44.5	93.3	510.1	508.7	1018.8	0.580	8.47	83.7
10	65.5	91.8	501.9	516.6	1018.5	0.590	8.21	85.8
15	91.2	89.8	491.0	527.1	1018.1	0.603	7.92	88.5
20	117.2	89.7	490.5	527.2	1017.7	0.603	7.53	91.2
25	142.8	84.8	464.4	552.9	1017.3	0.636	7.52	93.7
30	168.5	82.0	449.6	567.4	1017.0	0.654	7.36	96.2
35	194.5	79.1	434.1	582.4	1016.5	0.673	7.24	98.5
40	220.0	76.2	418.4	597.8	1016.2	0.692	7.13	100.7
45	246.0	73.0	401.2	614.6	1015.8	0.714	7.04	103.3
50	272.0	70.0	385.0	630.4	1015.4	0.734	6.99	105.5
55	298.0	67.0	369.4	645.6	1015.0	0.747	6.81	107.5
70	376.0	57.0	312.2	696.6	1008.8	0.821	6.68	114.0

Magnetite in a powdered condition in insulating wax. Results for powdered magnetite in insulating wax formed into a sphere, are shown by curve 1 in Fig. 5. It will be seen that the slope of the curve is large, the difference between the maximum and minimum values of ordinate amounting to about 27 percent of the smallest value. Now, using the same data to compute the permeability (designated as method A), by means of the equation $\mu=(V/V')(\Delta C/C)+1$, curve 7 of Fig. 5 is obtained. The slope of the latter curve is very small compared with that of the former. The difference between the maximum and minimum values of ordinate in this case is less than 5 percent

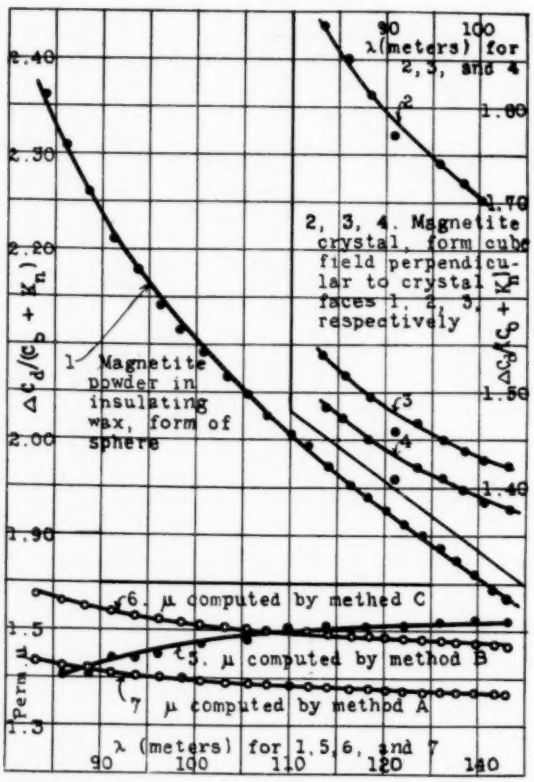

Fig. 5. Results for magnetite powder and magnetite crystal.

of the smallest value. Similarly, if the premeability (obtained as for curve 7, Fig. 5) had been used as the ordinate in curves of Fig. 3 their slopes would have been somewhat smaller. The difference in ordinates at overlapping wave-lengths for any two curves would under these circumstances have been less; however, each curve would still require an appreciable correction-factor in order to produce superposition throughout the overlap. It is probable that the failure of Wwedensky and Theodortschik to consider this possibility has led to an error in their results. This is particularly evident

in the region (see Fig. 1 for wave-lengths between 90 and 100 meters) where the greatest change in permeability appears to have occurred, and which was explained by them on the basis of resonance of elementary magnets.

A crystal of magnetite was sawed perpendicular to its crystal axes so as to form a cube, 0.8 cm on a side. The results using this as a sample are shown in curves 2, 3, and 4 of Fig. 5. It will be seen that the value of the former quantity depends upon the direction of magnetization with respect to the axes of the crystal. The value of the ordinates for curve 2 are about 22 percent greater than those for curve 3, whereas those for curve 4 are about 3 percent less than those for curve 3. Calculating the permeabilities by means of the equation $\mu=(V/V')\ (\Delta C/C)+1$ (which is permissible for relative values only) one finds that the permeability perpendicular to face 2 is less than that perpendicular to face 1 by 1.8 percent and greater than that perpendicular to face 3 by 0.26 percent. As a check, the relative permeabilities along the three different axes of the cube were determined by a static method at the Bureau of Standards by Mr. R. L. Sanford and his staff to whom thanks are due for this as well as for other courtesies extended. The permeability perpendicular to face 1 was found at field strengths 20 and 50 gauss, respectively, to be 2.2 and 3.4 percent greater than that perpendicular to face 2. No difference in permeability perpendicular to faces 2 and 3 could be detected by this method. The results by the two methods are thus in very good agreement, particularly so since the field strengths in the interior of the oscillating coil (calculated from a knowledge of the current flowing through the coil and the number of turns per centimeter) was always smaller than 20 gauss.

Curves 2, 3, and 4 of Fig. 5, show the usual depression of about 1.5 per cent at about 91 meters, which becomes less than 0.15 percent using the equation $\mu=(V/V')\ (\Delta C/C)+1$. This then is a very small variation but, small as it is, its presence has been successfully explained on the basis of the resonance of one part of the circuit with another. This again brings out the extreme sensitiveness of the method used in these measurements, and indicates how small any variation in permeability must be if it has escaped detection.

Absolute value of permeability of magnetite in a powdered condition. A magnetite crystal was powdered and the powder then worked into soft insulating wax. Observations were made with this as a sample, first in the form of a sphere and then as a flat sheet perpendicular to the magnetic field. In case of a sphere, for static conditions, the demagnetizing field is equal to $4\pi I_1/3$, consequently, $H_1=H'-4\pi I_1/3$, where I_1 is the intensity of magnetization, H' is the magnetizing field with the sample absent, and H_1 the actual field inside the sample. Substituting I_1/k for the value of H_1, and μ for $(1+4\pi k)$ in the above equation and solving for I_1, then $I_1=3kH'/(2+\mu)$, where k is the susceptibility of the material in question. In the case of a sheet perpendicular to the field, $H_2=H'-4\pi I_2$, and one obtains in a similar way, $I_2=kH'/\mu$. If the ratio $I_1/I_2=r$, then $\mu=2r/(3-r)$. Now r may be taken as being equal to the ratio of ΔC_d for sphere and sheet, which

can be obtained for various wave-lengths. This then, gives a method (designated B) of determining the absolute value of permeability in which the demagnetizating effect of the sample has been eliminated. In Fig. 5, curve 5 shows the value of the permeability obtained by this method for wave-lengths 85.8 to 132.2 meters. It will be seen that the values decrease from about 1.532 for the greatest wave-length to about 1.401 for the shortest wave-length.

The following circumstances all tend to make the observed value of the permeability lower than its true value (some of the effects are the most pronounced at shorter wave-lengths and possibly may account for the observed decrease with wave-length):

1. Because the eddy-current effect is larger in the sphere than in the slab, the ratio of ΔC for the sphere and slab is reduced. The reductions are relatively greater for the shorter wave-lengths since the eddy-current effect increases with frequency.

2. The mean field strength for the slab is greater than for the sphere since the periphery of the slab is nearer the coil than is the surface of the sphere.

3. The decrease in the field strength of the coil with decreasing wave-length will cause the observed values of the permeability to fall off at the shorter wave-lengths.

4. Because of the finite thickness of the slab, the values of ΔC obtained for this case are too large for all values of the wave-length.

Welo and Baudisch[4] recently determined, by a static method, the permeability of chemically prepared powdered magnetite. Since the permeability of a powder depends upon its density of packing,[5] a direct comparison between the results of their work and the present can be made only after each has been reduced to conditions of similar packing. Each of the results may be reduced to a permeability of the material in solid form by means of formulas developed in the paper[5] by Dr. Breit. The final results, however, will depend upon the assumptions made regarding conditions and state of the powder. For instance, Dr. Breit has treated the following cases: (a) a space lattice of spheres; (b) a space lattice of spherical holes; (c) laminary structure of powder the direction of the laminae being distributed statistically.

For an approximate determination of permeability under condition (a) the equation $(\mu-1)/(\mu+2)=q[(\mu_o-1)/(\mu_o+2)]$ may be used, where μ is the permeability of powdered form, μ_o is the true permeability in solid form and q is the ratio of volume occupied by the solid material to the volume occupied by solid material and holes. From the results of Welo and Baudisch, μ is taken as equal to 2.1 (which is only approximate, since it was not measused for such low field strengths as was used in the present case). The value of q is taken as equal to 0.254 (which also is only approximate since the density of packing, where it varied from 1.32 grams per cm^3, was reduced to

[4] L. A. Welo and O. Baudisch, Phil. Mag., **50**, 399 (1925).
[5] G. Breit, Amsterdam Proc. Akad. Wet. **25**, 293 (1922).

results for this density by a method only approximately correct, and since the density of the solid material is assumed to be equal to 5.2 grams per cm³). The value of μ_o comes out negative for this case, which indicates that the conditions specified under (*a*) cannot be true here. Turning now to the results of the present investigation, the value of μ is taken equal to 1.521 and q by assuming that the density of the solid is equal to 5.2 grams per cm³, equal to 0.229, from which we get μ_o equal to 6.5. For the case of (*b*) the equation as given, may be rewritten into a more convenient form for use, for instance,

$$\mu_0=(1/4)\{1+(\mu-1)(2+3p/q)+([1+(\mu-1)(2+3p/q)]^2+8\mu)^{1/2}\}$$

where $p=(1-q)$. By means of this equation, from the results of Welo and Baudisch we get μ_o equal to 6.6 and from the present data it comes out equal to 3.9. For the case of (*c*), the equation as given may be rewritten in the form,

$$\mu_0=-3+(3p/q)(\mu-1)+\{9[1-p/q)(\mu-1)]^2+24(p/q)(\mu-1)+1\}^{1/2}$$

Calculating μ_o from the results of Welo and Baudisch, we find it equal to 7.0 and from the present results equal to 4.0. In view of the fact that the sample used by Welo and Baudisch had the greater density of packing, it would seem that cases (*b*) and (*c*) might more appropriately be applied to their results than to the present ones, and that case (*a*) might more appropriately be applied to the latter. One can see from these comparisons that μ_o obtained by the static method and that obtained for an oscillating magnetic field are in approximate agreement, perhaps as closely as the difference in conditions and the uncertainty of assumptions should warrant one to expect.

A second method (designated *C*) of determining the absolute value of permeability, while retaining certain defects that have been eliminated by the previous method, may also be considered. This method makes use of a simple calculation for the change in the inductance of a solenoid of finite length due to the introduction into its center of a sphere of permeability μ. It neglects the effect of eddy-currents and of the inhomogeneity of the field.

By definition, the change in the inductance of a coil brought about by the introduction of the sphere is equal to the change in flux through the coil produced by the sphere, provided a unit current is flowing through the coil. The unit current causes a certain field H in the region into which the sphere is put. Under the influence of this field the sphere is magnetized so as to have a magnetic moment $r^3[(\mu-1)/(\mu+2)]H$. As long as the sphere is small, the field H is sufficiently homogeneous to cause a uniform magnetization of the sphere. Under these circumstances, it is equivalent to a doublet. The flux through the coil due to the doublet may, for convenience, be thought of as produced by a small turn of wire enclosing an area S, carrying a current J and placed in the same position as the sphere. The area S must be perpendicular to H and the product SJ must be equal to $r^3[(\mu-1)/(\mu+2)]H$ so

as to make the equivalent shell of S have the same moment as the sphere. The flux through S due to a unit current in the big coil is SH and, therefore, on account of the reciprocity of mutual induction the flux through the big coil due to a current J in the single turn is $SJ \cdot H$. This is the required change in induction $\Delta L = SJH = r^3[(\mu-1)/(\mu+2)]H^2$.

If the coil is a solenoid of length $2b$, radius a, with n turns per unit length, $H = 4\pi n\, b/(b^2+a^2)^{1/2}$. Also the inductance, with the sphere removed is $L_o = 8\pi^2 a^2 n^2 b \cdot K$, where K is Nagaoka's correction factor. Hence

$$\frac{\Delta L}{L_0} = \frac{[4\pi r^3/3][3(\mu-1)/(\mu+2)]\,[b^2/(b^2+a^2)]}{2\pi a^2 bK} = -\frac{\Delta C}{C}$$

(The development of this equation is due to Dr. G. Breit.)

The above equation may now be applied to the case of the sphere of wax containing the magnetite powder, where $r = 0.906$ cm. For the oscillating coil used, $a = 4.4$ cm, $b = 2.5$ cm, $K = 0.5562$, therefore $(\mu-1)/(\mu+2) = 602.9(-\Delta C/C)$. The values of μ computed by means of this formula have been plotted in curve 6 of Fig. 5. The values of the permeability obtained by means of the equation $\mu = (V/V')\,(\Delta C/C)+1$ have been plotted in curve 7 of Fig. 5. If due allowance be made, as explained before, for the various factors that tend to lower the value of the permeability of curve 5 at the shorter wave-lengths, there is fair agreement between the values given in curves 5 and 6. The values represented by curve 7 could hardly be expected to give a closer agreement with the other two curves since several factors are operating to effect both its slope and its absolute value.

Results by Resonance Method

Iron filings, iron powder, and iron wires as samples. Results by this method have been obtained on iron filings, coarse and fine, in and out of paraffin, iron powder, and iron wires. The bundle of wires used as a sample was packed into a glass tube having a diameter of 0.8 cm and 10.5 cm long, each wire being on the average about 0.002 cm in diameter. The other samples were packed into glass tubes having diameters between 1.2 and 1.3 cm and lengths between 10 and 11 cm. In the case of the fine and the coarse filings in paraffin, two different field strengths were used, namely, 0.05 and 0.6 gauss respectively, and for the other cases 0.6 gauss only. The strength of the field was kept constant by varying the coupling between the oscillating and the resonating circuits, thereby keeping the deflection of the detecting galvanometer constant.

In the early part of the work, considerable difficulty was experienced with apparent variations in permeability, which were not always reproducible. Later results, however, showed that this was only an apparent variation and was in reality due entirely to instrumental causes. The region where the apparently large variation in permeability appeared in the results of Wwedensky and Theodortschik[2] has been covered by this method, yet

there appeared to be no critical variation in permeability with frequency within this range.

Discussion of Results

Comparison of the present results with those obtained by previous investigators. The methods and results of Wwedensky and Theodortschik[2], hereafter referred to as W. and T., have been critically examined in an effort to find an explanation of discrepancies that exist between this work and theirs. It will be well to point out a few things, which in the opinion of the writer may have seriously affected the results of the previous investigations.

1. A serious drift occurred in the work of W. and T., which affected what they called their zero-reading (corresponding to the reading of C_u in the present investigation), amounting sometimes to as much as 13 percent of their total compensating capacity. This necessarily must have affected the accuracy of their results if the drift was not uniform, and if the time of reading the condenser with the sample in was not midway between the times of the two zero-readings. The methods in the present investigation greatly reduced, if they did not entirely eliminate, the possibility of drift. Two separate condensers were used, one when the sample was "out," and the other when it was "in," making it unnecessary to consume time in reading the compensating condenser until the sample was "out." A lever system permitted introduction of the sample in less than a second, and at the same time substitution of one condenser for the other. Thus adjustments with sample "in" and "out" were made within few seconds at most and any drift, was found negligibly small in actual practice.

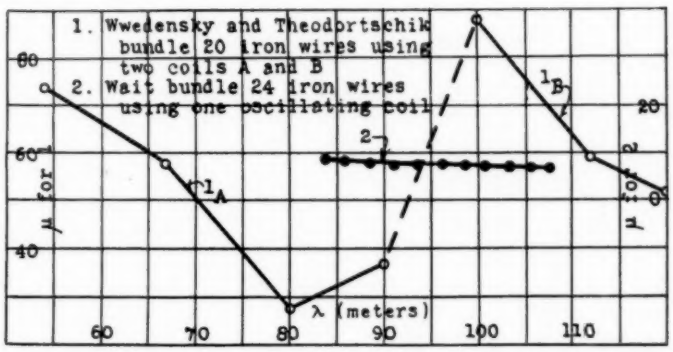

Fig. 6. Comparison of results on iron wires by Wwedensky and Theodortschik, and by Wait.

2. Fig. 6 gives the results of W. and T., the sample being a bundle of soft iron wires used in two different oscillating coils and shows the resonance band ascribed by W. and T. to the resonance of the elementary magnets of which the iron was supposed to consist. Fig. 6 gives also the results of the present investigation, the sample being a bundle of soft iron wires

of a similar diameter to those used by the other workers and like theirs having a length much greater than that of the coil, using, however, only one oscillating coil. W. and T. connected points, as shown by the dotted portion of their curve, obtained by different coils, a procedure which the writer's results show is not justified as correction-factors are required to refer data obtained with different coils to a standard coil.

The author wishes to express his indebtedness to the Director and staff of the Department of Terrestrial Magnetism, and particularly to Dr. G. Breit for valuable advice and assistance, to Mr. J. A. Fleming for continued interest, to Mr. C. Huff and assistants for help in designing and constructing apparatus, and to Mr. J. B. Goldsmith for assistance in the construction of graphs.

CARNEGIE INSTITUTION OF WASHINGTON,
DEPARTMENT TERRESTRIAL MAGNETISM,
October, 1926.

PHENOMENA DEPENDING ON THE CHANGE OF ELASTIC FREQUENCIES IN SOLID BODIES WITH PRESSURE

By F. Zwicky*

Abstract

Shift with pressure of the residual rays of a crystal.—Born's theory of the constituent forces in heteropolar crystals is adopted. As a new conclusion of this theory a formula for the shift of frequencies of residual rays with pressure is deduced. The shift corresponding to a pressure of 10,000 atm. amounts approximately to 7μ in the case of NaCl (residual rays at 50μ).

Effect of pressure on the electrical conductivity of metals.—Qualitative conclusions are drawn with respect to the dependence of elastic frequencies on pressure in any crystal. This leads to a rational explanation (suggested at first by Grüneisen) for the effect of pressure on the specific electric conductivity of metals, this conductivity being in general increased by pressure. The relation of our results to those obtained by Grüneisen and Bridgman previously in a quite different way, is discussed.

1. Introduction

THIS investigation was at first concerned with the problem of determining the shift of frequency of residual rays with pressure. It dealt naturally with heteropolar substances only, as only crystals built up by ions show selective frequencies in the far infra-red. From the results, however, it could be seen that it is possible to draw some important conclusions with regard to the conductivity of metals.

We first give the derivation for the change of frequency ν of residual rays with pressure P. The actual computation will be carried through only for the simple case of a cubic lattice of the type NaCl. The extension of the calculations to more complicated types of crystals would not involve any particular difficulties. Cases in which different tensions are applied in different directions of the crystal could also be calculated in the same way as described in this paper.

From the work of Born, Kossel and others it is known, that the cohesive forces in heteropolar chemical compounds are mainly of electrostatic origin, resulting from the electric field produced by the different ions. This theory has proved to possess a considerable range of validity, as lattice constants, compressibilities, elastic constants, frequencies of residual rays and heats of sublimation can be calculated from it. The results of such computations are in good agreement with the experimental data. The only very serious discrepancy between the theory and the facts seemed to appear between the calculated values of the breaking stress and the observed ones. The theoretical breaking stress, as deduced by the author,[1] was 400 times greater than

* Research Fellow in Physics, International Education Board.

the measured values known at that time. But also in this case the theory was proven to be right by the careful investigations of A. Joffé and his school.[2] Joffé showed that in all the previous experiments much too low values for the breaking stress had been found because of imperfect surfaces of the crystals used (tiny cracks). Eliminating this source of error Joffé found values for the breaking stress approaching very nearly those predicted by the calculations.

Born's theory was extended by different investigators,[3] who have taken into account the deformability of the ions in an electric field. In addition to this the repulsion forces were taken more exactly into consideration. These are necessary to secure the stability of the lattices. No real explanation has yet been found as to their true origin. A satisfactory treatment, however, of all the phenomena mentioned above could be given by assuming these forces to be inversely proportional to some high power of the mutual distance r_{ik} of two ions i and k. The two particles then, carrying charges e_i and e_k respectively, possess the mutual potential energy

$$\epsilon_{ik}=e_ie_k/r_{ik}+A_{ik}/r_{ik}^{p_{ik}} \tag{1}$$

The constants A_{ik} and p_{ik} are to be determined. Three points of view have been adopted with regard to these constants. At first, attempts were made by Born and Landé to deduce the exact values for them in a rational way, with the help of atomic models. But no consistent results could be obtained because of lack of knowledge of the fundamental quantum laws governing the mutual interaction of two atomic systems.

The second procedure consists in the deduction of A and p from the behaviour of gas atoms similar to the ions in question. From viscosity measurements in argon, for instance, the repelling force acting between two argon atoms can be determined.[4] A slight extrapolation permits one to apply the same law of force for the interaction of two Cl^- ions or of two K^+ ions, because of the fact that these ions have very similar electronic structure to the neutral A-atom. In this way the different properties of the alkali-halide crystals could be deduced.

The third method was originally applied by Born,[5] who used the experimental data of the lattice constant and of the compressibility to determine A_{ik} and p_{ik} in every special case. The other properties of the crystals may then be calculated with the help of the A and p thus obtained. We choose this simple point of view as our starting point.

[1] F. Zwicky, Physik. Zeits. **24,** 131 (1923).

[2] A. Joffé and M. Lewitzki, Zeits. f. Physik, **35,** 442 (1926).

[3] See for instance M. Born, Die Atomtheorie des festen Zustandes, Enzyklopaedie der math. Wissenschaften, Vol. V_3, Heft 4. All references made in our paper to previous work on heteropolar crystals may be found summarized in this book.

[4] J. E. Lennard-Jones, Proc. Royal Soc. London, **109,** 584 (1925).
J. E. Lennard-Jones and P. A. Taylor, Proc. Royal Soc., **109,** 476 (1925).

[5] Ref. 3, p. 733.

Assuming for the mutual potential energy of two ions the expression (1) we get for the energy contained in a crystal of the type NaCl the amount (per ion).[6]

$$\epsilon = \sum_k \epsilon_{ik} = -13.9e^2/a^4 + \alpha' A/a^p \tag{2}$$

a = lattice constant, α' = some function of p.[6] The sum has to be taken over all the particles surrounding the ion i. For numerical computations see Ref. 3.

The condition necessary for the equilibrium of the crystal is

$$(\partial\epsilon/\partial a)_{a=a_0} = 0 \tag{3}$$

or

$$1.74e^2 - \alpha A/a_0^{p-1} = 0 \tag{4}$$

which means a relation between A and p, provided that the lattice constant a_0 is taken from the experiments.

Deducing on the same basis a formula for the compressibility and comparing it with the observed data, Born was able to determine A and p seperately. It is found that p is approximately equal to 8 or 9. For different crystals one finds slightly different values varying from 7.5 to 9.5. Numerical computations then give α for different values of p as in the following table.

TABLE I

p	7.5	8	8.5	9
α	4850	7200	10380	15200

2. Residual Rays

It has been shown by previous authors[7] that the origin of the selective absorption and reflection of radiation in the far infra-red by heteropolar crystals is connected with the oscillations which the positively charged part of the lattice is able to perform relative to the negatively charged part. These oscillations will indeed be excited by incoming electromagnetic radiation, as the electromagnetic field connected with this radiation will force the charges of different sign in opposite directions. Resonance occurs when the incoming and the elastic oscillations have approximately the same frequency. It is easy to show that crystals of the NaCl type possess only one characteristic oscillation of the kind mentioned. Our task is to calculate its frequency in the case of uniformly applied external pressure. For this purpose we have to determine the force which is necessary to hold the positive and the negative partial lattices in relative displacement $\xi^+ - \xi^- = \xi$ (see Fig. 1.). We will obtain this force by deriving first the change in potential energy $\Delta\epsilon$ of a particle due to the displacement ξ.

The effect of the displaced electric charges may be obtained by making use of the expression for the Lorentz force in a polarized isotropic medium.

[6] A_{ik} and p_{ik} in (1) are really dependent on the individual ions i and k. It has been shown however that the effect produced by their differences is a very small one and can be neglected in the first appoximation.

[7] Ref. 3, p. 740.

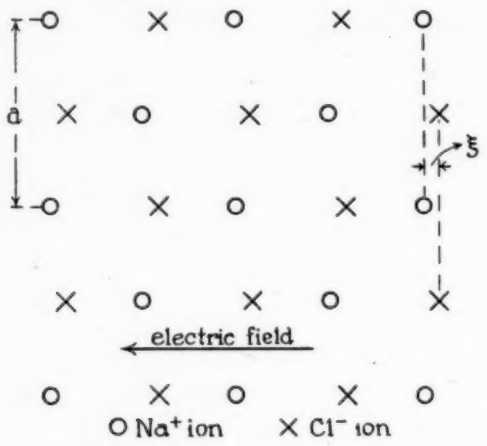

Fig. 1

The electric polarization or the moment per unit volume M being in our case equal to

$$M=\tfrac{1}{2}Ne\xi \tag{5}$$

(N = number of ions per cm^3)

The force per ion, due to the polarization is

$$4\pi eM/3=2\pi Ne^2\xi/3 \tag{6}$$

For the work necessary to produce a displacement $\delta\xi$ we then get

$$\delta\epsilon^-=-2\pi Ne^2\xi\delta\xi/3 \tag{7}$$

By integration we obtain

$$\Delta\epsilon^-=-\pi Ne^2\xi^2/3 \tag{8}$$

$\Delta\epsilon^-$ is a negative quantity as can easily be seen. We transform our formula by making use of the fact that there are eight particles contained in the elementary volume a^3.

$$\Delta\epsilon^-=-\pi Na^3e^2\xi^2/3a^3=-8\pi e^2\xi^2/3a^3 \tag{9}$$

The member $\Delta\epsilon^+$ originating from the repelling forces is obtained by adding the contributions of all the single ions surrounding the one considered. As a result,

$$\Delta\epsilon^+=\beta A\xi^2/a^{p+2} \tag{10}$$

where

$$\beta=4p(p-1)\left[2^p+4(2/3^{1/2})^p/9+4(2/5^{1/2})^p/5+\cdots\right]$$

Numerical values of β for some values of p are reproduced in table II.

TABLE II

p	7.5	8	8.5	9	9.5
β	35600	57700	92800	148000	235000

The whole energy due to the displacement ξ of the lattices is therefore

$$\Delta\epsilon=\Delta\epsilon^{-}+\Delta\epsilon^{+}=(-8.4e^2/a^3+\beta A/a^{p+2})\xi^2 \tag{11}$$

From this we get the force K per ion by differentiation

$$K=\partial(\Delta\epsilon)/\partial\xi=2[-8.4e^2/a^3+\beta A/a^{p+2}]\xi=f\xi \tag{12}$$

Now the equations of motion for the two different ions are

$$\begin{aligned} m^{+}d^2\xi^{+}/dt^2&=f(\xi^{-}-\xi^{+})=-f\xi \\ m^{-}d^2\xi^{-}/dt^2&=f(\xi^{+}-\xi^{-})=f\xi \end{aligned} \tag{13}$$

Combining these equations we obtain

$$d^2\xi/dt^2=-f\xi(m^{+}+m^{-})/m^{+}m^{-} \tag{14}$$

The harmonic oscillations representing the solution of this equation are characterized by the frequency

$$\nu=[f(m^{+}+m^{-})/m^{+}m^{-}]^{1/2}/2\pi \tag{15}$$

Denoting this frequency by ν_0 in case no external pressure is applied we have

$$\nu_0=[(-8.4e^2/a_0^3+\beta A a_0^{p+2})(m^{+}+m^{-})/2m^{+}m^{-}]^{1/2}/\pi \tag{16}$$

Making use of the relation (4) this may be written as

$$\nu_0=[(-8.4+1.74\beta/\alpha)e^2(m^{+}+m^{-})/2m^{+}m^{-}a_0^3]^{1/2}/\pi \tag{17}$$

Application of external pressure changes the lattice constant from a_0 to $a_0+\delta$, where δ is to be considered as a small quantity in all practical cases. Developing to the first order in δ we obtain

$$\nu=\nu_0(1-\gamma\delta/a_0) \tag{18}$$

where

$$\gamma=[3\cdot 8.4-1.74\beta/\alpha(p+2)]/2(-8.4+1.74\beta/\alpha)$$

Evaluating γ numerically the following table can be established

TABLE III

p	7.5	8	8.5	9
γ	11.2	10.5	9.9	9.5

From this it may be concluded that the frequency changes relatively much more rapidly with pressure P than does the lattice constant. Expressing δ with the help of the volume-compressibility κ we get

$$\begin{aligned} \delta&=-\kappa a_0 P/3 \\ \nu&=\nu_0(1+\gamma\kappa P/3) \end{aligned} \tag{19}$$

As an application we shall give the actual figures in the case of rock salt. For NaCl the compressibility found in the experiment is (P measured in Kg per cm^2)

$$\kappa=4.14\cdot 10^{-6}$$

So to a pressure of 10000 atm. there would correspond the following frequency (for p the value 8 is used as given by Born's calculations)

$$\nu = \nu_0(1+0.145)$$

This means a displacement of the selective absorption line from $\lambda = 50\mu$ to $\lambda = 43.6\mu$. Pressures of this order can be realized experimentally either directly in some mechanical way (Bridgman) or by some indirect method, as for instance by electrolysis of the crystals. Joffé[8] has shown that extremely high pressures can be reached in this latter way because of the enormous forces the space charges in the lattice exert on each other. So the possibility exists of checking our formula experimentally. As I hear through the kindness of Professor Joffé, measurements of this kind are going on in the Polytechnical Institute at Leningrad. The results thus obtained will be of some importance for the theory of crystals because they supply a new means of getting more information about the nature of the repelling forces. These are not yet very well known.

3. Resistance of Metals Under Pressure

The specific electric resistance of metals in general decreases with pressure. This has been shown especially by Bridgman[9] in a long series of beautiful experiments. Now this fact presents considerable difficulty to the classical theories of metallic conduction. In fact we can deduce from these theories an approximate relation of the following type

$$1/\rho \propto N_e \Lambda$$

where $\rho = 1/\sigma$ is the specific resistance, N_e the number of free electrons per cm^3 and Λ the mean free path for these electrons. Now Λ, being inversely proportional to the number of atoms N_a per cm^3, ρ will be roughly independent of the pressure in case we assume that N_e increases in the same way as N_a. More rigorous calculations show that the resistance should increase under all circumstances with pressure, which is in strict contradiction with the facts. Now there has been advanced an explanation of this fact by Grüneisen.[10] The underlying idea is essentially this. The mean free path of electrons in the metal is not independent of temperature for the reason that the thermal oscillations of the atoms disturb their motion.[11] This may be thought to happen in the following way. In the space lattice of the metal the electrons of long path, moving approximately parallel to one of the lattice planes, contribute most to the conductivity. Now these electrons are more and more disturbed in their motion as the atoms are more and more displaced by the thermal agitation. The mean free path will then be approximately

$$\Lambda \propto 1/d^2$$

[8] My information is taken from Joffé's lectures at the Calif. Inst. of Technology, 1925.

[9] See for instance P. W. Bridgman, American Acad. of Arts and Sciences. Several papers in 1922–1925.

[10] E. Grüneisen, Verh. d. D. Phys. Ges. **15**, 186 (1913). I am indebted for this reference to the Editors of the Physical Review.

where d is now the mean amplitude of the atom in its thermal agitation. From this standpoint we have the possibility of accounting for the experimental variation of conductivity with temperature[12] without being in contradiction with the facts of specific heat and the pulling of electrons from cold wires (electric field currents).[13] Furthermore the increase of specific conductivity with pressure can easily be explained on this basis without making use of any artificial assumptions. Indeed the amplitudes of the atoms in their motion of thermal agitation are determined by the strength of the elastic force (f dynes per cm displacement are pulling the atoms back to their average positions). Now this elastic force can be compared with that mentioned above in the case of heteropolar crystals. We then make use of the results obtained in Section 2, and assume that they are approximately right for homopolar crystals also, i.e. that they have the same dependence on pressure as far as the magnitude is concerned. This could be justified indeed in a general way by merely making use of the fact that the repelling forces vanish much more rapidly with increasing distance of the particles under consideration than the attractive forces, which will be nearly always the case. If then d be the average maximum displacement of an atom we shall have for high temperatures this relation

$$fd^2=3kT \qquad (k=1.37\times10^{-16}\text{erg})$$

Denoting with f, d and f_0, d_0 the elastic constant and the amplitude of the atom in the compressed and in the natural state of the crystal respectively, then

$$d^2/d_0^2=f_0/f=\nu_0^2/\nu^2=(1-2\gamma\kappa P/3)$$

$$\sigma\propto\Lambda\propto 1/d^2\propto(1+2\gamma\kappa P/3)$$

$$\sigma=\sigma_0(1+2\gamma\kappa P/3) \tag{20}$$

Thus from this point of view the increase of specific electrical conductivity σ with pressure is explained as follows. Since the elastic bonds of the atoms in the crystal increase in strength very rapidly with pressure, it is seen that the areas covered by the atoms in their thermal agitation decrease with pressure much more rapidly than the whole volume under consideration. For this reason the free space between the atoms (counted per cm²) increases with pressure, so as to allow the conductivity electrons to move on longer mean free paths than before.

Experimentally it is found that

$$\sigma=\sigma_0(1+cP) \tag{21}$$

[11] This conception has been adopted by different theories of metallic conduction. See for instance R. Seeliger, Enzyklopaedie d. math. Wissenschaften, Teubner 1922, Vol. V_2, Heft 5, p. 870.

[12] Assuming Λ constant, the classical theory gave $\sigma\propto T^{-\frac{1}{2}}$ instead of $\sigma\propto T^{-1}$.

[13] R. A. Millikan and C. F. Eyring, Phys. Rev. **27**, 51 (1926).

So that for a lattice of the type NaCl, comparing (20 with 21) we should predict the following relation between the pressure coefficient c of electric conductivity and the compressibility κ

$$c = 2\gamma/3\kappa \sim 7\kappa \tag{22}$$

Now for metals we shall not have exactly the same molecular forces acting as in NaCl. Still our formula should give the right order of magnitude for the coefficient c, since its derivation is based essentially only on the fact that the repelling forces, compared with the attractive forces, decrease very rapidly with distance. Some experimental data obtained by Bridgman are collected just at random in Table IV, to show that our conclusion is right.[14]

TABLE IV

	Fe	Co	Rh	Pd	Ir	Pt	Au
$c\times10^7$	24.2	9.3	17.4	19.6	13.5	19.5	33.3
$\kappa\times10^7$	5.87	5.39	3.72	5.2	2.7	3.6	4.8
c/κ	4.1	1.7	4.65	3.75	5	5.4	6.9

There are also some metals, as for instance Bi, Sb, Ca, Li and Sr which behave abnormally. Their specific resistance increases with pressure. Evidently such a treatment as that suggested in this paper cannot be complete. It does not take into account such individual properties of the different metals as the dependence of number of free electrons on pressure, the forces acting on electrons in the interior of the crystals, etc.

In Grüneisen's original paper the change of elastic frequency with pressure has been computed in a quite different way from ours. He makes use of the quantum theory of equation of state of solid bodies (Debye, Grüneisen). Grüneisen's method is mainly a phenomenological one. This involves the necessity of making some general assumptions as to the behavior of solid bodies with temperature. It is, however, interesting to see that the results thus obtained check in the order of magnitude with those obtained in this paper in a more direct way. This is a justification of Grüneisen's assumptions.

Bridgman[15] in his gap theory of metallic conduction also deduces the effect of pressure on conductivity by making use of the fact that the elastic frequencies decrease with pressure. His final formula for the change of conductivity is essentially the same as we have used it. His underlying picture, however, is quite different from that given above insofar as the electrons do not move freely through the spaces between the atoms. They on the contrary do not meet any resistance in moving through the atoms. It appears, however, to the writer that this theory is based too much on an overestimation of the size of the atoms in a crystal. Bridgman indeed considers them in general to be in direct mutual contact at the absolute zero point. Now most of the known evidence seems to indicate that there are large free spacings between the atoms. Such evidence is for instance

[14] P. W. Bridgman, Proc. Amer. Acad. of Arts and Sciences, Vol. 59, No. 5, p. 114.
[15] P. W. Bridgman, Phys. Rev. **9**, 269 (1917); **17**, 161 (1921); **19**, 114 (1922).

furnished by the direct determination of atomic radii in crystals by investigation with x-rays. Scherrer and Debye[16] find for instance in the case of diamond that the diameter of a C-atom (volume actually covered by the revolving electrons) amounts only to one-fourth of the mutual distance of the atoms. A second method of determining the gaps consists in direct comparison of diameters known from the kinetic theory with measured lattice constants. This gives in the case of alkali-halides dimensions of the gaps comparable with the dimensions of the constituting ions. Very strong evidence in favor of large gaps seems furthermore to be indicated by the fact that large amounts of matter may be transported through crystals without disturbing the lattice (electrolysis through crystals). The fact that constituent atoms may be extracted from crystals (mica for instance)without destroying the crystals, points also in the same direction.

It would be of very great importance if some conclusive evidence could be found with regard to the question whether slow electrons pass through atoms in approximately straight lines or not. Many physicists seem to consider, for instance, Ramsauer's well known results on behavior of slow moving electrons in certain gases as such evidence.[17] The writer[18] has tried to show, however, that even from the standpoint of classical dynamics it is not necessary to draw this conclusion. It would be, however, of extreme interest for the modern development of the quantum theory if this question could be settled definitely by some new experiments.

As another phenomenon connected with the change of elastic frequencies with pressure we may mention the specific heat of solid bodies. It is obvious that from the point of view of the quantum theory this change will affect the characteristic temperature Θ (Debye). Increase of ν means a higher value for Θ. The abnormal behavior (drop of specific heat) should be found then at higher temperatures in case external pressure is applied.

NORMAN BRIDGE LABORATORY OF PHYSICS,
CALIFORNIA INSTITUTE OF TECHNOLOGY,
January 18, 1927.

[16] P. Scherrer and P. Debye, Physik. Zeits., Vol. 19, p. 474 (1918).

[17] C. Ramsauer, Ann. d. Physik. Vol. **64**, p. 513, 1921. "Slow" electrons means that their energy is less or about equal to the resonance energy of the deflecting atoms. The free electrons moving in the electric field in the metal will probably be such. Ramsauer's result is, that for several atoms as A, Kr, and Xe the effective area in their interaction with slow electrons is much smaller than the area given by the kinetic theory of gases. Electrons with their initial line of motion pointing towards the atom may in this case continue their path without being deflected appreciably by the atoms.

[18] F. Zwicky, Phys. Zeits. **24**, 171 (1923).

A DIRECT COMPARISON OF THE LOUDNESS OF PURE TONES

By B. A. Kingsbury

Abstract

The loudness of pure tones of frequencies 60 to 4000 cycles and for intensities from the threshold to 90 T.U. above the 700 cycle threshold.—The loudness of eleven pure tones was studied by adjusting the voltage applied to a telephone receiver to make these tones as loud as certain fixed levels of a 700 cycle tone. The average results of 22 observers, 11 men and 11 women, were arranged as contour lines of equal loudness through the normal auditory sensation area in terms of r.m.s. pressure in ear canal as a function of frequency. Frequencies from 60 to 4000 cycles were used and intensities from threshold of audibility to 90 T.U. above the 700 cycle threshold. It was found that if the amplitudes of pure tones are increased in equal ratios the loudness of low frequency tones increases much more rapidly than that of high frequency tones. For frequencies above 700 cycles the rate is nearly uniform.

A loudness unit.—As a loudness unit the least perceptible increment of loudness of a 1000 cycle tone was employed. In absolute magnitude this varies from level to level, but in the ordinary range of loudness it becomes constant. This unit takes into account the subjective character of loudness.

Sources of variation in data on loudness.—The variability of the data from which the averages were computed was separated into a factor expressing dissimilarity of ears and another expressing errors of observers' judgment. There was no level at which the variances were a minimum. Dissimilarity of ears causes more variation than errors of observers' judgment. The variances showed no significant sex difference.

THE purpose of this paper is to give data on the relative loudness of pure tones as judged by a group of eleven men and eleven women whose average threshold of audibility approximated former measurements. Since most ears probably can perceive nearly the same minimum amounts of sound energy and recognize about equal changes in pitch and intensity, measurements made by the above group should apply to the hypothetical average normal ear.

In Fig. 1 are shown the usual curves for the threshold of feeling and audition expressed in 20 times the common logarithm of the r.m.s. pressure on the ear drum (dynes per square centimeter) as a function of frequency. The pressure is that which would be produced in the ear canal if the walls and drums were rigid. The difference between any two ordinates is then the ratio of the pressures in transmission units (T.U.). This is the common unit for expressing amplitude ratios in telephony and at the same time takes into account the logarithmic relation between sensation and stimulus. The lower of the curves is the average threshold of audibility for the above group.

Let us imagine that the r.m.s. pressure of a test tone at the threshold of audibility is increased until it comes up to a level P. If one listens first to this tone and then to a tone of frequency f_1, he can tell which appears

the louder and by adjusting the level of the tone f_1, he can make the two appear equally loud. By comparing several tones with a test tone in this way a contour line of equal loudness through the region of audition may be determined. For instance, P_1, P_2, P_3, etc. are points which were experimentally determined for one of these contours. In the work to be described 700 cycles was made the test tone, while the frequencies compared with it were distributed at approximately equal logarithmic intervals through the more important range of audition. This seemed the best way to secure results applicable in general to pure tones with measurements at a minimum number of frequencies.

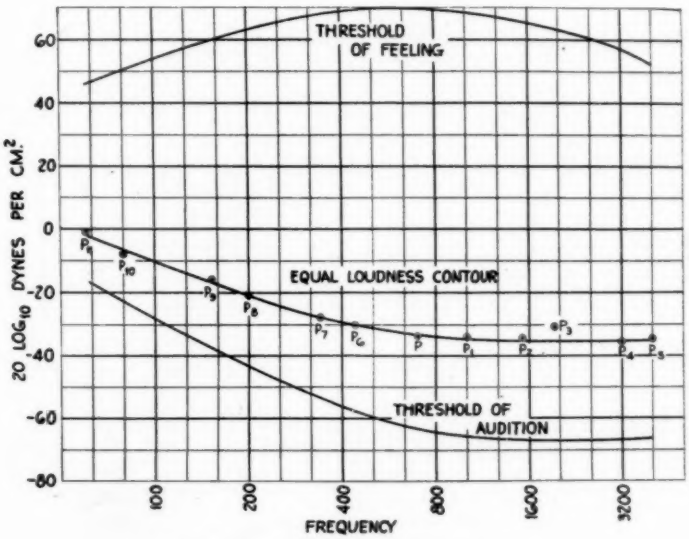

Fig. 1. Normal auditory sensation area.

In order to cover most of the intensities of ordinary sounds contours of equal loudness 10 T. U. apart at 700 cycles were selected up to levels somewhat above that of ordinary conversation. The 10 T. U. interval means that the amplitude of the sound wave for the 700 cycle tone at any contour was 3.16 times its value at the contour below this. There is no necessity for smaller intervals because a few fairly widely spaced contours should show quite definitely how the loudness of pure tones varies with level and frequency.

A schematic diagram of the apparatus used in the tests is shown in Fig. 2. It will be noted that the set-up consists of two symmetrical systems, which we have labelled *A* and *B*. The test tone was always furnished by the *A* oscillator. The filters in each case attenuated the first harmonic of the tone used about 75 transmission units. The thermocouples and galvanometers shown were used to measure the input currents of the attenuators. The resistance network attenuators which are calibrated to read the attenuation in transmission units could be readily connected by a switch to a special iron-clamped high impedance receiver.

The outline of the procedure in making tone balances was as follows: The *A* attenuator was placed in such a position that the observer could not see the dial; the dial of the *B* attenuator was covered with a cardboard screen, which prevented the observer from seeing the position of the pointer while making the adjustment. The 700 cycle test tone was set up on the *A* system and the frequency being compared with this on the *B* system. First three independent settings of the *A* threshold were made, then three for the *B* threshold. Next the experimenter set the *A* attenuator at one of the selected comparison levels and allowed the observer to adjust the *B* attenuator until when listening alternately to the two tones they seemed equally loud. The attenuator settings and the deflections of the meters

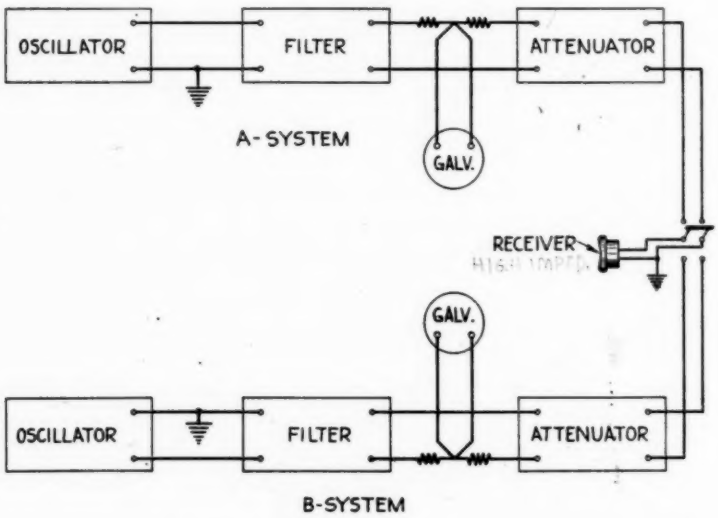

Fig. 2. Schematic diagram of apparatus.

were recorded for both systems. This process was repeated for the other fixed levels of the *A* tone, until three independent determinations had been made for each level. The order of taking the fixed levels of the *A* tone was made as random as possible and two successive determinations were seldom made at the same level. When the comparison of the two frequencies was finished, the *A* and *B* thresholds were once more secured.

From a calibration and check of the receiver and the input attenuator voltage, attenuator settings were reduced to the r.m.s. pressure in the ear canal in T.U. above or below one dyne/cm^2. It was found that r.m.s. pressures at the average *threshold of audibility* for this group coincided very closely with the values which represent the best estimates[1] for normal ears. Hence this threshold curve is taken as a datum from which all the other points on the diagram are to be reckoned.

[1] H. Fletcher, Useful Numerical Constants of Speech and Hearing, The Bell System Technical Journal, Vol. IV, No. 3, pp. 375, July, 1925.

In Fig. 1 were given the curves for the thresholds of feeling and audition. In Fig. 3, the data from loudness comparisons are plotted in a similar fashion

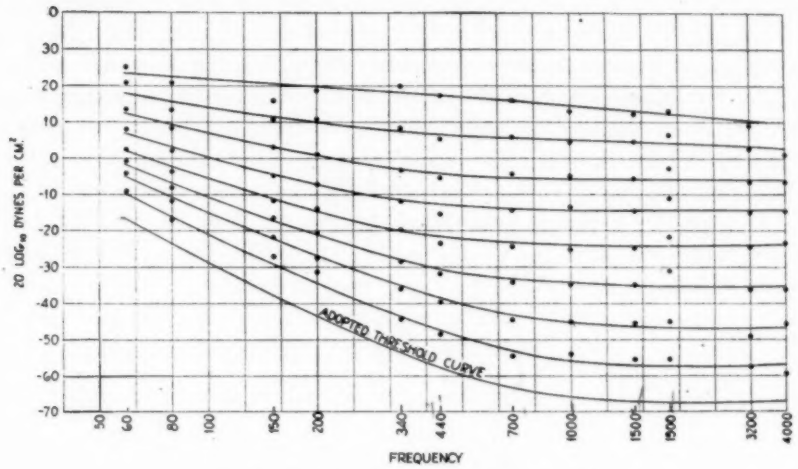

Fig. 3. Contour lines of equal loudness.

to demonstrate contour lines of equal loudness, the lowest curve being the threshold curve of audition.

These data may also be stated very conveniently in terms of *sensation level*, defined by the equation

$$S = 20 \log_{10}(P/P_0)$$

where P is the r.m.s. pressure of the sound wave and P_0 the minimum audible pressure for the average normal ear. That is, to get the sensation

TABLE I

SENSATION LEVEL (T. U.)

Each column represents 20 $\log_{10} P/P_0$ of equally loud tones
Threshold of audibility adopted for these data (P_0 in dynes/cm²).

Frequency:	60	80	150	200	340	440	700	1000	1500	1900	3200	4000
$20 \log_{10} P_0$:	−16.5	−23.0	−37.0	−43.6	−53.5	−57.5	−63.4	−65.5	−67.0	−67.4	−67.6	−67.5

Frequency	Thres	Sensation level ($20 \log_{10} P/P_0$)								
60	0	8.4	12.5	15.7	19.2	24.8	29.9	37.3	41.9	
80	0	6.6	11.4	14.9	19.6	25.1	31.7	36.1	43.9	
150	0	9.9	15.2	20.8	25.6	32.5	39.7	47.8	52.9	
200	0	12.7	16.4	23.2	29.9	36.5	44.8	54.4	62.2	
340	0	9.4	18.0	25.1	33.8	41.7	50.7	61.6	73.5	
440	0	9.3	17.7	25.7	33.8	42.2	52.5	62.9	75.3	83.4
700	0	9.3	19.3	29.3	39.3	49.3	59.3	69.3	79.3	89.3
1000	0	11.7	20.7	31.1	40.7	52.1	60.9	69.8	78.5	86.8
1500	0	11.6†	21.4	32.5	42.5	52.5	61.7	71.3	79.2	85.0
1900	0	11.9†	22.4	36.3	45.7	56.7	65.0	73.7	80.2‡	
3200	0	9.9	18.5	31.6	43.1	52.8	61.1	70.0	77.0	
4000	0	8.0	22.1	31.6	44.0	53.2	61.1	68.9		
Loudness*	0	8.5	20.3	39.0	60.0	83.5	107.0	130.0	151.5	172.0

* See 1000 cycle curve, Fig. 7.
† Average of 57 observations.
‡ Average of 63 observations.

level of any point in Fig. 3, it is merely necessary to notice how many T.U. the amplitude of the tone must be reduced to reach the threshold of audibility. In Table I, the data of Fig. 3 are expressed in terms of sensation level.

It has generally been assumed that loudness is a function both of the amplitude and frequency of the pressure wave, but the form of the function is not definitely known. The arbitrary levels of the 700 cycle tone had been chosen 10 T.U. apart, and loudness contours determined on this basis. At the level where the contours are closest together, the change in loudness for the same number of T.U. is greatest. The average interval between the contours was computed at each level, by adding together the intervals for each frequency and dividing by the number of frequencies. The first interval from the threshold was omitted since it was an irregular interval. The average interval between contours for each frequency was also computed. In Fig. 4 these data are plotted first with interval as a function of frequency and

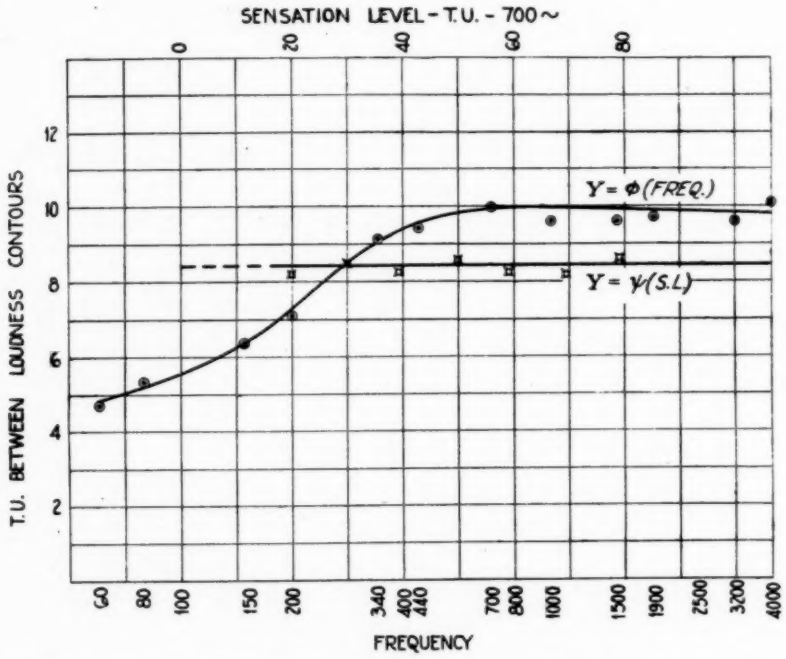

Fig. 4. Effect of sensation level and frequency upon sensation level increment between contours.

then with interval as a function of the sensation level of the 700 cycle tone. From these two curves it would appear that the interval between contours is about the same number of T.U. for all sensation levels, but that the loudness of low frequency tones increases much more rapidly than that of high frequency tones.

It seems desirable now to turn to another aspect of these results which should occupy a place of major interest in all hearing studies. This is the variation in observations which arises from the variability of an observer's judgment and the differences between ears. The usual procedure in reducing

data has been to take the arithmetic average of a number of observations and compute the standard deviation. In this case, because of the seemingly large importance of this variation, it appeared desirable to give it more careful treatment.

A particular value in Table I is the average of 66 observations, three of which were made by each of twenty-two observers. The deviation between any determination of an observer and his average can be readily calculated. The sum of the squares of these 66 deviations divided by 44 yields a quantity β which expresses the variance in observers' judgment. If X is an individual observation and $\overline{X}_p$ the average for that person this may be written: (Appendix I)

$$\Sigma(X-\overline{X}_p)^2/44=\beta$$

These variances, one for each value in Table I are included in Table II.

TABLE II

Variances of data averaged for values of Table I in (T. U.)²

$20 \log_{10} P_{700}$:		−63.4	−63.4	−54.1	−44.1	−34.1	−24.1	−14.1	−4.1	+5.9	15.9
Frequency		Thres$_A$	Thres$_B$								
60	α:	29.9	54.3	35.4	34.9	33.4	34.2	50.7	67.5	59.1	27.0
	β:	3.9	4.8	5.3	6.5	11.0	5.5	12.6	8.6	12.1	9.9
80	α:	23.4	24.8	20.1	26.5	21.4	28.3	37.4	36.8	21.5	17.8
	β:	4.1	8.3	4.8	8.5	8.8	17.6	14.2	13.4	15.6	10.1
150	α:	30.1	56.9	34.2	34.0	34.0	39.7	47.8	71.8	109.9	80.4
	β:	4.3	16.8	8.7	8.7	9.5	10.2	8.3	9.8	12.1	10.1
200	α:	32.6	36.7	11.4	40.7	27.0	33.7	34.8	64.5	67.4	26.2
	β:	3.3	8.0	8.3	7.3	11.7	12.6	13.0	18.3	11.1	14.1
340	α:	30.3	34.5	22.2	13.7	24.0	29.9	42.4	52.1	64.5	24.4
	β:	3.4	6.7	15.8	8.9	9.3	16.4	17.1	25.7	19.4	18.1
440	α:	31.7	54.3	21.8	22.6	31.0	38.9	43.8	48.9	41.5	31.3
	β:	3.3	9.5	11.0	10.5	20.1	7.9	12.6	14.7	14.5	8.5
700	α:*					1.1	0.2	2.0	1.1	.5	.8
	β:					2.2	1.4	1.6	3.	3.6	1.4
1000	α:	30.3	42.9		27.5	21.2	22.2	15.7	13.2	16.4	17.9
	β:	2.9	3.2		18.6	22.1	28.7	13.1	10.2	11.5	7.5
1500	α:	49.1	44.8		59.3	38.9	55.2	48.0	46.8	34.3	31.5
	β:	3.2	2.8		14.4	26.2	17.7	16.6	13.0	4.7	4.2
1900	α:	30.6	70.0		97.4	48.1	56.1	53.8	43.0	36.6	
	β:	2.9	7.0		11.4	27.5	28.0	16.8	11.6	10.8	
3200	α:	29.2	60.5		81.4	83.6	28.7	50.0	46.5	37.5	34.7
	β:	3.7	3.3		36.3	22.3	29.4	33.6	16.5	11.3	12.1
4000	α:	18.7	100.8		96.0	71.9	73.1	44.3	51.6	25.4	
	β:	2.5	5.2		26.8	27.4	31.2	24.4	12.5	8.9	

* From the observations of 20 observers comparing 700 cycles with 700 cycles.

In all this work, measurements were made to the nearest T.U. and arithmetic averages and variances computed to the nearest 0.1 T.U.

The other factor which contributes to variation is the variance between ears. Let us call this variance α. A particular value in Table I is the arithmetic average of 22 averages, each of which is the arithmetic average of an observer's three settings. Let the general average be $\overline{X}$. Then we can make the following equation define α and β: (Appendix I)

$$3\Sigma(\overline{X}_p - \overline{X})^2/21 = 3\alpha + \beta$$

Since the value of β is known, α can be computed. The values are also given in Table II.

The standard deviation of the observations whose average is an individual entry in Table I is defined by the relation: (Appendix I)

$$S.D. = (0.97\alpha + \beta)^{1/2}$$

If Z equals the ratio of the error of the average to the observed standard deviation, it is a function only of the number of observations. Choosing

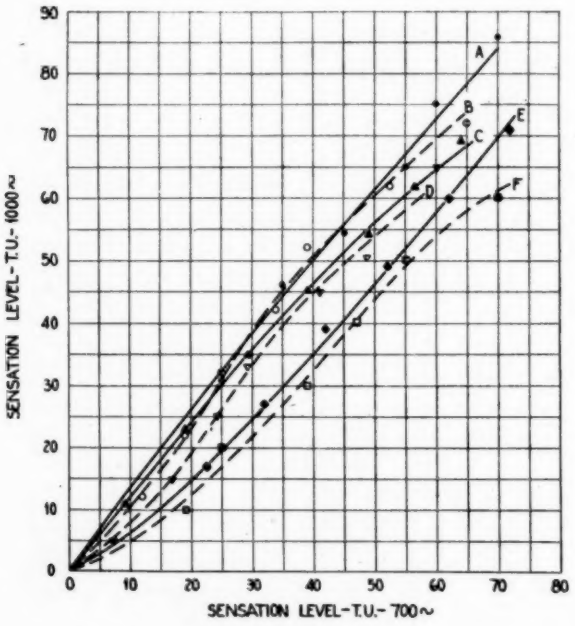

Fig. 5. Comparison of loudness balance methods.

the 95 percent error, a value in Table I will vary more than Z times its standard deviation only five times in a hundred, and another average outside of these limits would very likely be from another population of measurements. Z has in our case a value[2] of 0.25, and an entry in Table I is therefore determined to 1.5 or 2 T.U.

[2] W. A. Shewhart, Correction of data for errors of averages obtained from small samples, Bell System Technical Journal, **V**, No. 2, pp. 314, April, 1926.

All the experimental work up to this point had been carried on by making the levels of the A tone fixed and allowing the observer to adjust the B tone. In Fig. 5 are shown three pairs of representative comparisons, where each pair of curves A and B, C and D, E and F were made by the same individual. Every point shown is the average of 3 observations. A, C and E were made by fixing the level of the A tone as already described. For B, D, and F, the experimenter set the B tone and the observer adjusted the A tone for equal loudness. The results check rather closely; in fact two successive comparisons by the same method would not be more alike. The two comparisons were made about three months apart. It therefore seems reasonable in loudness comparisons to set the test tone at arbitrary levels.

In order to show conclusively that all points on a given contour represent equally loud tones, an additional simple check can be applied. If two B tones are compared directly will the result be the same as when each is compared with the A tone? To test this a direct comparison of 200 cycles and 3200 cycles was made by eleven male observers using 200 cycles as the A tone with fixed levels. Plotted in terms of 20 $\log_{10}$ (volts on receiver) the results of the two methods are shown in Fig. 6. The direct comparison is

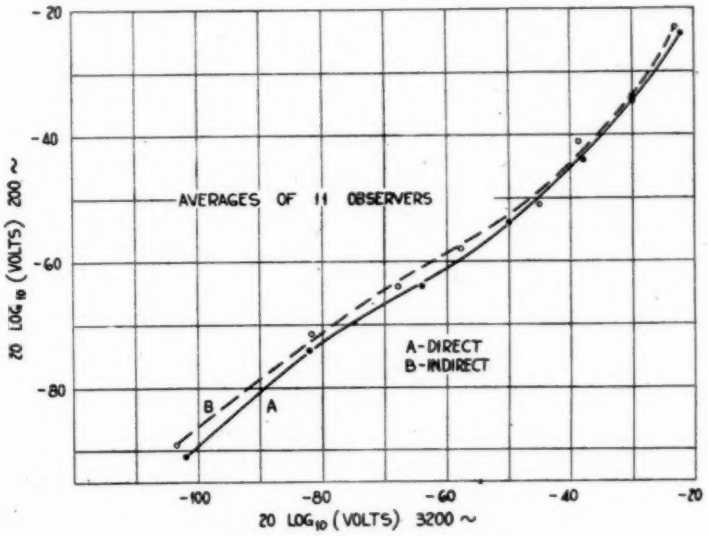

Fig. 6. Direct and indirect loudness comparisons.

the more accurate, since in the indirect comparison, variances are involved twice. In view of the values of α and β already given, the two curves do not appear significantly different.

Discussion of the Nature of Loudness

Since loudness is a subjective matter, it is rather difficult to determine what should be made the unit of loudness.[3] Of course, any arbitrary scale

[3] J. C. Steinberg, The Loudness of a Sound and Its Physical Stimulus, Phys. Rev., Second Series, Vol. 26, No. 4, pp. 507–523, October, 1925.

of loudness may be used provided that sounds which are equally loud have equal numbers on the scale and that loudness numbers vary progressively as we go from fainter to louder tones, but a system which recognizes some of the characteristics of loudness arising from the physical characteristics of audition would be preferable. Fig. 4 seems to show that in the ordinary range of hearing loudness is linear with sensation level if the Weber-Fechner Law holds. In light the unit of brightness has been made the least perceptible increment of brightness. Knudsen[4] has data for several pure tones which show the relation between the Fechner ratio $\Delta E/E$ and the r.m.s. pressure in dynes per cm² in the ear canal. This ratio, "intensity sensibility of the ear" expresses the ratio of the smallest perceptible difference in the energy of a tone to its total energy. At 1000 cycles from these data, we were able to plot a curve in which the Fechner ratio was a function of the 1000 cycle sensation level. This curve was then extrapolated to the threshold on the assumption that there the ratio was unity.[5] By making this ratio for the

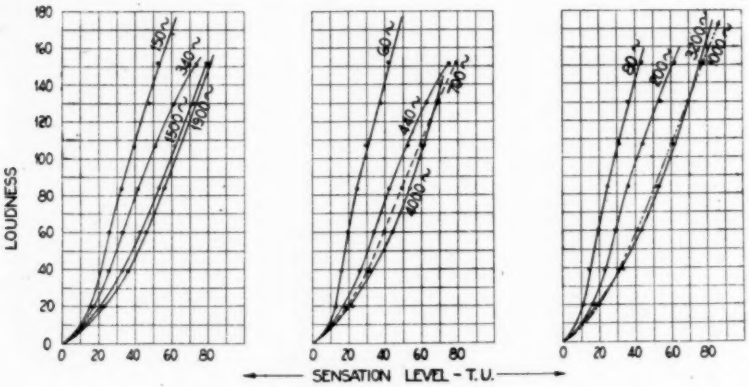

Fig. 7. Loudness of single frequency tones at various sensation levels.

1000 cycle tone our unit of loudness and calling the threshold of audibility zero loudness, it was possible to integrate from the above curve, a curve with the loudness of the 1000 cycle tone as ordinate and its sensation level as abscissa. That is, a 1000 cycle note just perceptibly above the 1000 cycle threshold has loudness unity; if it was just perceptibly louder than this its loudness is two and so on. This curve is marked 1000 cycles in Fig. 7.

The next step was to apply this unit to the data of Table I. Loudness numbers corresponding to the 1000 cycle sensation level given in this table were read from the 1000 cycle loudness curve. Each column in the table represented sounds which were equally loud in the ordinary sense, and the "loudness numbers" read from the 1000 cycle curve applied by the above definition to the other frequencies as well. Loudness for each frequency is thus numerically defined at several sensation levels. The remaining curves

[4] V. O. Knudsen, Sensibility of the Ear to Small Differences of Intensity and Frequency, PHYS. REV., Second Series, Vol. 21, pp. 84–103, January, 1923.

[5] P. G. Nutting, The Complete Form of Fechner's Law, Bulletin of the Bureau of Standards, Vol. 3, No 1, 1907.

of Fig. 7 were drawn up on this basis. A unit of loudness somewhat better for our purpose would have been the least perceptible increment of loudness of a 700 cycle tone compared with its sensation level, but data for such a unit are not available and there is reason to suspect that a curve of this kind between loudness and sensation level is much the same for 700 and 1000 cycles. Moreover, the unit used has been given a very definite quantitative value which makes it possible to compare it with any other unit. (Appendix II)

The Variability of the Data

An inspection of Table II fails to show any level of loudness where the similarity of ears is a maximum for all frequencies. In general the variances are smaller when the tones being compared are more nearly of the same frequency. Since α is usually greater than β, errors of judgment cause less variation than dissimilarity of ears. The differences in the values of α and β for the 700 cycle threshold are not significant. The statistical development on which these quantities rest makes them entirely independent quantities. If β is averaged for level, that is if the values in each column are added and the sum divided by the number in the column, it will be found that β reaches a maximum at about 40 T.U. above the 700 cycle threshold. The variance of judgment also varies with frequency being progressively smaller as we go from higher to lower frequencies. This makes it seem that the sensibility of the ear must be greater at low frequencies, which is equivalent to saying that the loudness sensation level curves will be steeper there.

The variability of ears does not seem to be correlated with frequency although it is somewhat less at the 1000 cycle comparison than elsewhere. The average α of equally loud tones below 700 cycles seems gradually to increase as loudness increases, while the average for equally loud tones above 700 cycles gradually decreases. In other words, at low frequency comparisons, ears are more alike for rather faint tones, while in the comparison of higher frequencies they are more alike at louder levels. This variability of ears is more nearly the same for all frequencies at about 40 T.U. above the 700 cycle threshold, but the error of judgment is here a maximum. It is therefore doubtful whether there is any best level for loudness comparisons. Practice seems to lower the 700 cycle threshold since it becomes lower in the same order as the balances were made. However, it appears probable that this effect is connected with other factors.

At 1900 cycles separate variances were computed from the observations made by the men and the women but no definite trend was found which would suggest sex differences in hearing.

Conclusion

When the amplitudes of single frequency tones are increased by equal ratios, high frequency tones increase in loudness more slowly than do low frequency tones. However, for frequencies above 700 cycles, the idea that tones are equally loud when they are an equal number of T.U. above the threshold is a very good approximation.

The study of the goodness of fit of regression lines which relate the sensation levels of equally loud tones may be made the subject of a later paper. An interpretation of such lines would be very much facilitated by a study of sensibility of the ear to intensity changes of pure tones because it is logical to suppose that in terms of this discrimination loudness matches are made.

Appendix I

In order to make the statistical analysis on which this paper rests easily available to the reader, a brief résumé[6] of the method is included here.

If in a group of measurements two factors cause variation an analysis of variance offers a good method of treatment. Let X be an individual measurement, $\overline{X}_p$ average of each class (determinations of each individual), $\overline{X}$ arithmetic average of all X's, k the number in each class and N' number of classes (observers). It can be shown that the following equation is true:

$$\sum_{1}^{kN'} (X-\overline{X})^2 = k\sum_{1}^{N'} (\overline{X}_p-\overline{X})^2 + \sum_{1}^{kN'} (X-\overline{X}_p)^2 \qquad (1)$$

Let β represent the variance within classes. Here there are $N'(k-1)$ degrees of freedom, and we may write:

$$\sum_{1}^{kN'} (X-\overline{X}_p)^2 = N'(k-1)\beta \qquad (2)$$

As twenty-two observers each making three observations were employed in determining the average values of Table I, we have, in this case, to put $k=3 \cdots N'=22$.

The mean of the observations in each class is affected by the variance β divided by k as there are k observations in each class, and also by a variance α related to the difference between classes. As there are here $(N'-1)$ degrees of freedom, we write:

$$\sum_{1}^{N'} (\overline{X}_p-\overline{X})^2 = (N'-1)(\alpha+\beta/k) \qquad (3)$$

where again for the special case of this paper $N'=22$ and $k=3$.

From (2) and (3) the value of α and β may be readily secured. It is only necessary to compute two of the three terms in Eq. (1). The usual procedure is to solve Eq. (1) for the summation on the left of Eq. (2) after evaluating the other two summations.

The standard deviation of our measurements from the general mean can be easily calculated from the above equations. The standard deviation is defined as:

$$(SD)^2 = \sum_{1}^{kN'} (X-\overline{X})^2/(kN'-1) \qquad (4)$$

[6] R. A. Fisher, Statistical Methods for Research Workers, 1925.

By the use of (1), (2) and (3) this reduces to:

$$(SD)^2=[1-(k-1)/(kN'-1)]\alpha+\beta$$
$$=.97\alpha+\beta \qquad (N'=22,\ k=3) \tag{5}$$

We define Z by the relation

$$Z=(\overline{X}-m)/(SD) \tag{6}$$

where m is the true mean of all observations.[2] Z then is a function of the number of observations made and its value for any particular error may be determined from statistical tables. When this has been done, $(\overline{X}-m)$ can be computed.

Appendix II

The primary effort in this paper has been to discuss the loudness of pure tones in a simple experimental fashion without much regard to formulas of loudness. The least perceptible increment in the energy of a 1000 cycle tone was made the unit of loudness in the consideration of the pure tone

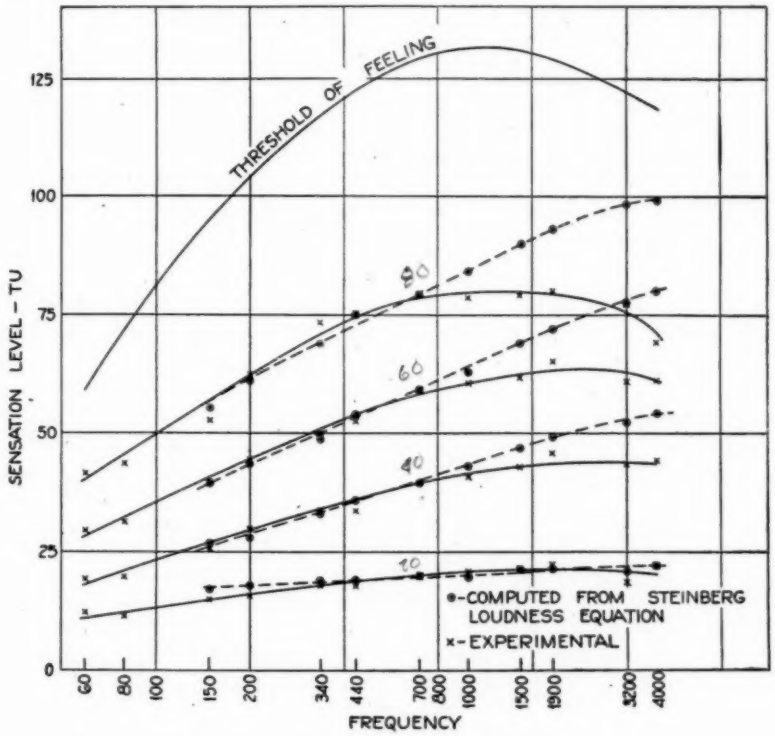

Fig. 8. Sensation levels of equally loud tones.

data because of its simplicity and direct application. However, this procedure did not justify the neglect of other methods of treating the data. Dr. J. C. Steinberg has developed a formula[3] for loudness with the primary purpose of computing the loudness of complex sounds when the frequency

spectrum is known. This method involves essentially the summation of the loudness of the various frequency components. It can be applied readily to the loudness of pure tones. The formula employs two factors, first a weight factor which depends on the sensation level of the sound and its frequency, secondly a root factor which depends only on the sensation level of the sound. Using the values of the weight and root factors given by Dr. Steinberg, the sensation levels of tones of the frequencies studied as loud as 700 cycles at 19.3, 39.3, 59.3, and 79.3 T.U. respectively above its threshold value were determined. The results of these computations and the experimental results of this study are shown in Fig. 8 as curves for the sensation levels of equally loud tones. Computations were not made at 60 and 80 cycles because these weight factors were not stated. The procedure employed makes the computed and experimental values for the sensation levels of the 700 cycle tone coincide. For the lower frequency tones the computed values fit the experimental data rather well. If the values of the root factor are considered known and independent of frequency, weight factors may be computed on the basis of the pure tone data in this report.

The justification of this formula as well as any other which attempts to express loudness, must be substantiated both by the study of pure tone loudness and the Fechner ratio. The accuracy with which weight factors calculated from these pure tone data fit measurements on complex sounds has not yet been determined.

BELL TELEPHONE LABORATORIES, INCORPORATED
December 1, 1926.

BOOK REVIEWS

Allgemeine Grundlagen der Quantenstatistik und Quantentheorie. ADOLF SMEKAL. This treatise is published both as a part of the Encyclopädie der Mathematischen Wissenschaften and as a separate volume. It is divided into three main sections, dealing respectively with the principles of classical and quantum statistics, the general foundations of quantum dynamics, and the application of the contents of the first two parts to particular problems of quantum statistics. The discussion in the first part centers on such topics as the ergodic and quasi-ergodic hypotheses, the structure of the phase space, the assignment of a priori probabilities, and adiabatic invariants, with frequent references to the older article in the Encyclopädie by P. and T. Ehrenfest. The application of the classical theory to gases, solids, heat radiation, and problems of fluctuations is taken up next, due consideration being given to the recent work of Fowler and Darwin. It is shown how the empirical facts regarding specific heats and heat radiation are incompatible with a continuous weight function and lead to the notion of a discrete structure of the phase space. The statistics for such a space is then investigated, as well as the radiation law which it leads to in conjunction with Einstein's assumptions about the processes of emission and absorption. After thus having shown the necessity of a modification in the classical view of atoms and molecules, the author proceeds with a very complete account of the basis of the older quantum theory—the Rutherford-Bohr atomic model, the correspondence principle for multiple periodic systems, the theory of perturbations, impacts, and optical phenomena (absorption, dispersion, scattering, and diffraction), with applications fully mentioned but not discussed at great length. Unfortunately, and quite without the author's fault, this part of the book is not up to date, because our knowledge of atomic phenomena has advanced by leaps and bounds since the time the article went to press (August, 1925). The undulatory mechanics of de Broglie and Schrödinger, the matrix formulation of atomic dynamics introduced by Born and Heisenberg, as well as the numerous applications of these developments to individual problems will therefore not be found in the book. Nevertheless, this second part retains a distinct value, as the reader is furnished with a profound discussion of the principal difficulties in the way of a satisfactory description of atomic phenomena and especially of the dual nature of radiation. In addition the very complete bibliography should be useful to any atomic specialist.

The last part falls into three sections; the specific heat of gases, dissociation equilibria in gases and chemical constants, and the statistics of impact phenomena. It is greatly to be regretted that Einstein's theory of the degeneration of gases evidently was published too late to be given more than a brief mention in some footnotes. For the same reason the remarkable connection between this theory, de Broglie's waves of phase, and Pauli's equivalence principle for spectra could not be taken up.

The volume should prove valuable, particularly as a work of reference, and it is to be hoped that Professor Smekal some day will undertake to write a new edition, with the recent advances treated in the same thorough and critical spirit which pervades the present pages. Pp. vi+362. B. G. Teubner, Leipzig, 1926. Price, bound, R.M. 16.00.

R. DE L. KRONIG

Abhandlungen zur Wellenmechanik. E. SCHRÖDINGER.—This book of 169 pages of text with a preface of 9 pages contains reprints of six papers by the author. All the papers are on wave-mechanics. They represent the origin and the most important developments of the subject. The fundamental thought is remarkably keen and simple. It is roughly as follows: Since classical mechanics can be thought of as geometrical optics in a properly chosen

medium (Hamilton), it is supposed that *true* mechanics is wave optics in the same medium. Stationary states of atoms are thought of as stationary oscillations of the medium. This is the first step towards doing away with the cabalistic nature of quantum conditions and forms a most fundamental advance. Even though Schrödinger's way should not prove to be the best and ultimately accepted one, the very fact that it has been conceived gives one hope of understanding physics in terms of fundamental principles and ideas rather than complicated restricting conditions.

The results of the theory have proved to be identical with those of the theory of matrices. The formal identity of the two is very elegantly presented in the fourth paper of the series. The first two papers show the evolution of the idea with applications to the hydrogen atom, the oscillator, the rotator, band spectra. The third paper discusses the transition from microscopic to macroscopic phenomena. The fifth paper develops the theory of perturbations and applies it to the Stark effect of the hydrogen atom. It also gives absolute intensities in the hydrogen spectrum. The sixth paper introduces modifications in the wave equation required for non-conservative systems, gives an interpretation of the charge density in terms of the wave parameter, eliminates thereby a part of the radiation difficulty, discusses dispersion, and gives the wave equation for relativity and for magnetic fields.

The series of papers is preceded by a short introduction expounding concisely and clearly the fundamental idea, stating what the theory is capable of doing and where it fails. The whole is written in a very lucid and attractive style. Pp. ix+169, 12 figures, 1927: 8°, Leipzig, Johann Ambrosius Barth. Price, unbound, R.M. 5.70; bound, R.M. 7.50.

G. BREIT

Outline of Physical Chemistry. GEORGE SENTER. Fourteenth Edition. The fact that this book has reached its fourteenth edition may be considered to be ample evidence that teachers and students of chemistry, especially in Great Britain, regard it as a highly successful introductory treatment of physical chemistry. To the student beginning the study of this branch of chemistry, this book should prove to be an excellent and stimulating guide. The reviewer is glad to recommend it heartily.

There are two points which seem to merit adverse criticism. On page 246, it is stated that in the electrolysis of sodium sulfate sodium ions and sulfate ions give up their charges to the electrodes and then react with water liberating hydrogen and oxygen. This view is in conflict with that expressed on page 399 where discussing a similar problem it is stated that "the gases are products of the primary decomposition of water." Again, on page 286 the author declares: "The reason why the law of mass action does not apply to strong electrolytes has not been satisfactorily elucidated." This is certainly a remarkable statement by a physical chemist in view of the fact that the paper by Debye and Hückel dealing with strong electrolytes appeared nearly four years ago. The reviewer does not necessarily object to the exclusion of the theory of Debye and Hückel from an elementary presentation of the theories of electrolytic solutions. He does object strongly to such a misstatement as is found in the sentence just quoted. Pp. 419, 46 figs. D. Van Nostrand Company, New York, 1927. Price $3.00.

F. H. MACDOUGALL

Das Element Hafnium. GEORG v. HEVESY. This monograph reviews the present state of our knowledge of the chemical and physical properties of the element hafnium. It is written by one of the discoverers of the element and one to whom we owe much of our information concerning it. After a brief description of the discovery of the element (the priority dispute is not discussed) the author details various methods for separating hafnium from zirconium. Following this is a statement of the properties of the element, its atomic weight, crystal structure, x-ray and optical spectra (with wave-length tables). The compounds discussed are the oxide, the double fluorides, the oxychloride, the phosphate and the acetylacetone derivative. There are chapters on the analytical chemistry of hafnium and on its occurence and abundance in the earth's crust. The last chapter is devoted to an interesting discussion of the reasons for

the striking similarity between hafnium and zirconium. The book will form a valuable addition to the library of the chemist and the physicist. Pp. 49, 23 figs. Julius Springer, Berlin, 1927. Unbound, price Reichsmark 3.60.

JOHN T. TATE

Lehrbuch der Physik, MÜLLER-POUILLET, 11 *Auflage, Zweiter Band, Lehre von der Strahlenden Energie (Optik), Erste Hälfte.* Edited by O. LUMMER in collaboration with H. ERGELET, F. JÜTTNER, A. KÖNIG, M. v. ROHR, and E. SCHRÖDINGER.—As indicated by the first half of the volume on optics, the eleventh edition of this well known text is being thoroughly revised and brought up to date. The principal revisions are mentioned in this review. In the first chapter there is a new treatment of the history of the conception of the ether, dealing with the changes brought about by the development of the electromagnetic theory, and later, of the special, and finally, of the general theory of relativity. New material on the propagation of light in moving media, on the Doppler effect, and the aberration of light, is introduced. There are two new chapters on the optical properties of glasses and other materials, and on their dependence on chemical composition. The chapters dealing with the eye and vision have been enlarged from 72 pages in the tenth edition to 167 in the present. The improvement here is noteworthy. The chapter on interference is nearly doubled in length by the introduction of material chiefly on interference spectroscopy. The chapter concerning images of objects which are not self luminous, which includes Abbe's theory of the microscope image, has been extended to three times its former length. In this revision, the subject of ultra-microscopy receives special emphasis. There has been, in fact, a decided improvement in this text. If the second half of this volume, which was not available to the reviewer, is as thoroughly revised in the light of modern knowledge as this half has been, the work will be most valuable for general reference or as a text in the field of optics. Pp. XVIII+928; 654 figs.+VII plates. Friedr. Vieweg & Sohn, Braunschweig, 1926. Price 50 M. unbound, 54 M. bound.

JOSEPH VALASEK

L'Energie Rayonnante, *Tableaux Synoptiques de l'echelle des Longueurs d'Onde et des principales caractéristiques du rayonnement électro-magnétique avec un résumé des théories actuelles.* A. FORESTIER.—This book contains tables of wave-lengths, together with formulas and constants having to do with radiation. Theories of radiation are summarized and various formulas for black body and spectral line radiation and for x-rays are given, with recent values of the constants appearing in them. The wave-length tables are historical in that they contain names and dates with most of the numerical data. The methods of investigation are also briefly summarized. The tables include wave-lengths from 30,000 meters to 0.0189 A. U. Cosmic rays are omitted. The recent work on joining the infra-red and Hertzian radiations and on gamma rays is summarized at the end of the book instead of being incorporated in the tables. Otherwise the selection and arrangement of material is very good. This volume will serve as a useful reference book for data on radiation.—Pp. 76. Librairie Scientifique Albert Blanchard. Paris, 1926. Price 20 f.

JOSEPH VALASEK

PROCEEDINGS

OF THE

AMERICAN PHYSICAL SOCIETY

MINUTES OF THE NEW YORK MEETING, FEBRUARY 25–26, 1927. JOINT MEETING WITH THE OPTICAL SOCIETY OF AMERICA.

The 143rd regular meeting of the American Physical Society was held in New York City in the new Physics Laboratories of Columbia University on Friday and Saturday, February 25 and 26, as a joint meeting with the Optical Society of America. The presiding officers were Karl T. Compton, President of the American Physical Society, and W. E. Forsythe, President of the Optical Society of America. The attendance was about 300 persons.

On Friday morning there was a general session of the Optical Society. The program of the Optical Society on Friday afternoon consisted of two invited papers, the first by Professor F. K. Richtmyer of Cornell University on "The Extension of the Classical Laws of Optics into the X-ray Region of the Spectrum," and the second by Professor R. W. Wood of Johns Hopkins University on "The Experimental Control of the Radiating States of Optically Excited Atoms."

The sessions of the Physical Society were held on Saturday morning and afternoon. Each session was divided into two sections.

On Saturday the members of the two societies were the guests of Columbia University at a complimentary luncheon served in the Physics Laboratories.

Special Business Meeting. A special business meeting of the American Physical Society was held at the end of the afternoon session on Saturday. Article I of the By-Laws was amended by adding a section as follows:

"5. The Council shall, however, have power, by a special vote in each case, to honor a member or fellow by placing him on a retired list with no dues, provided such a member or fellow is not less than 65 years of age, and has retired from active service in his professorial or other corresponding position. A member or fellow going on the retired list will waive the receipt of the journals from the Society."

At the regular meeting of the Council held on Saturday, February 26, 1927, twenty-four were elected to membership: Boyd W. Bartlett, J. G. Black, Ralph B. Blackman, C. J. Calbick, Preston B. Carwile, Frank W. Constant, Edgar D. Doyle, Theodore Dreier, Samuel O. Grimm, Newton S. Herod, Raynor C. Johnson, Nicolas de Kolossowsky, F. W. Lancaster,

Donald P. LeGalley, Bernard Lewis, Sunao Nakamura, Saburo Numakura, George F. Taylor, H. L. Van Velzer, George B. Welch, E. J. Workman, Bernard L. Worsnop, Ziro Yamauti, William A. Zinzow.

The titles and abstracts of papers presented before the Optical Society of America will be found in the Proceedings of that Society, published in the *Journal of the Optical Society of America and Review of Scientific Instruments*.

The abstracts of the forty-seven papers presented before the American Physical Society are given in the following pages. An **Author Index** will be found at the end.

HAROLD W. WEBB, *Secretary*.

ABSTRACTS

1. The intensity of scattered x-rays and the Compton effect. G. E. M. JAUNCEY, Washington University.—Williams (Phil. Mag. **2**, 657, (1926)) and Jauncey (Phys. Rev., **29**, 206, (1927)) have shown that the experimental intensity of x-rays reflected by crystals can only be calculated on theoretical grounds on the assumption that it is only the electrons in the U state (Phys. Rev., **27**, 687, (1926)) which take part in the Bragg reflection. In the present paper it is assumed that all the electrons in the U state in a given atom cooperate in the unmodified scattering. This requires that the unmodified scattering per atom varies as F^2 and the modified scattering as $(Z-F)$, where F is the atomic structure factor as calculated by Williams and Jauncey and Z is the atomic number. The ratio of the scattering in a given direction to the Thomson scattering in the same direction is then approximately (so long as $F>1$) given by $(F^2+Z-F)/Z$. Calculated and experimental values, the latter in parentheses, follow for $\lambda=0.41$ A scattered by copper: 40°, 4.1 (4.8); 60°, 2.58 (2.5); 80°, 1.88 (2.14); 100° 1.42 (1.45); 120°, 1.25; 180°, 1.12.

2. The measurement of x-rays used for therapy. HARRY CLARKE, Rockefeller Institute.—If it is desired to measure the dose at a well-defined point, a very small ionization-chamber must be used, and the current will then be so small that it must be measured by means of an electroscope or an electrometer. For accuracy of measurement, as well as for convenience, the meter has to be mounted rigidly at some distance from the tube. On the other hand, the chamber should be movable for convenience in use. The proper design of a conductor to connect the chamber with the meter has, heretofore, presented a difficult problem. The conductor must be well-insulated, and protected against both electrostatic induction and leakage due to ionization; it must also be flexible. The writer's apparatus consists of two separate units. The portable unit consists of a small chamber connected with a condenser; the fixed unit is an electroscope with a calibrated variable condenser. The chamber unit is connected with the electroscope for charging; it may then be taken to any part of the laboratory for exposure to the rays. After exposure, it is returned to the electroscope for measurement of the quantity of electricity lost.

3. Reflection of soft x-rays. ELIZABETH R. LAIRD, Mount Holyoke College.—The experiments on the reflection of soft x-rays reported earlier (Phys. Rev. **27**, 510, (1927)) have been repeated for copper, with slight changes in the apparatus, and the results confirmed; showing an absence of regular reflection at angles much above 5° at 950 volts and its presence at 340 volts. Also, at the lower voltage a fraction of the radiation is transmitted through fluorite, and the fluorite fluoresces; at the higher voltage the fluorite is quite opaque and does not fluoresce. It is inferred that the radiation at 950 volts does not include all that present at 340 volts. It is suggested that this may explain the different results obtained by Dauvillier

with the crystal reflection method using higher voltages and those of the critical potential method. A glass reflector with partially ground surface was used to show that the ground surface did not reflect.

NOTE: It has been found that glass reflects at large angles at 950 volts as at 340 volts. The phenomenon interpreted as a fluorescence of fluorite has not appeared on a later series of plates.

4. Further test of the theories of absorption of x-rays. F. K. RICHTMYER and L. S. TAYLOR, Cornell University.—At the Philadelphia meeting we reported measurements of the K discontinuity of Ag and Au in an attempt to decide between Kramer's theory of absorption and that of De Broglie. The uncertainty of the values of the mass scattering coefficients of Ag and Au made it impossible to decide between the two theories. The present measurements on Mo(42), Ag(47) and Sn(50) were made with the hope that the scattering coefficients for these three elements would not be far different and that the two theories might be thus tested. Assuming a reasonable value for σ/ρ, the data for the ratio of K absorption to L absorption are in better agreement with De Broglie's theory. But Kramer's theory gives a better value for the *absolute* magnitude of K absorption at the K limit.

5. The general radiation from a very thin target. WILLIAM DUANE, Harvard University.—Electrons, traveling horizontally with substantially the same velocity, pass through a hole in a block of iron. At its center, they meet the column of mercury moving downward in a mercury vapor pump. The mercury column acts as a very thin target, which continually renews itself. The radiation coming from the impacts of the electrons against the mercury column can be examined through suitable openings. Pin-hole camera photographs taken when the mercury pump is not running indicate some radiation coming from the interior walls of the apparatus. Such photographs taken with the mercury pump running show, in addition to the above, radiation coming from the space in which the electrons hit the mercury column. Measurements by means of an ionization chamber on the absorption of this radiation by aluminium indicate that it is not quite homogeneous, but much more nearly so than the radiation coming from a solid target. The average, or effective wave-length of the radiation is slightly longer than the short wave-length limit of the spectrum calculated from the constant (storage battery) voltage applied. Experiments with x-ray spectrometers on the distribution of energy in the spectrum are in progress.

6. An analysis of the arc and spark spectra of scandium. HENRY NORRIS RUSSELL, Princeton University, and WILLIAM F. MEGGERS, Bureau of Standards.—New measures of the arc spectrum (in which practically all the enhanced lines appear) have led to the classification of 337 lines of Sc I and 131 of Sc II leaving only a few weak lines outstanding. The spark spectrum is relatively simple. The lowest terms are ^3D, ^1D, arising from the electron configuration $3d \cdot 4s$. Next come $^3F'$, $^3P'$, ^1S, ^1D, ^1G from $3d \cdot 3d$. All these terms combine with ^3P, $^3D'$, ^3F, ^1P, $^1D'$, ^1F from $3d \cdot 4p$; and these again with ^3S, $^3P'$, ^3D, $^3F'$, ^3G, ^1D, from $3d \cdot 4d$, and ^3D, ^1D from $3d \cdot 5s$. The last are in series with the lowest terms, and indicate an ionization potential of 12.8 volts. A ^3P term arising from $4s \cdot 4p$ and a $^3P'$ from $4p \cdot 4p$ are also present The arc spectrum is much more complex. The lowest term is $^2D(3d \cdot 4s \cdot 4s)$; then $^4F'$, $^2F'$, ^2D, ^2G, ^4P $(3d \cdot 3d \cdot 4s)$. The configurations $3d \cdot 4s \cdot 4p$ and $3d \cdot 3d \cdot 4p$ give numerous "middle" terms combining with these. Higher terms have been identified as arising from $3d \cdot 4s \cdot 5s$; $3d \cdot 3d \cdot 5s$; $3d \cdot 3d \cdot 3d$; $3d \cdot 4s \cdot 4d$, and $3d \cdot 4p \cdot 4p$. The first two of these belong to series and give the ionization potential 6.7 volts for the neutral atom. There are strong intercombinations between the doublets and quartets in the red, and weak ones in the ultra-violet. All details of the structure of both arc and spark spectra are in complete agreement with Hund's theory.

7. Multiplets in the spectra of vanadium (III). R. C. GIBBS and H. E. WHITE, Cornell University.—Using the regular and irregular doublet rules as guides, it has been found possible,

from the corresponding known multiplets in Sc I and Ti II, to identify the triad of multiplets of V III designated as ${}^4F_{2,3,4,5}-{}^4G_{3,4,5,6}$; ${}^4F_{2,3,4,5}-{}^4F'_{2,3,4,5}$; and ${}^4F_{2,3,4,5}-{}^4D_{1,2,3,4}$. For these multiplets the initial state is given by one $4p$ electron and two $3d$ electrons. In the final state the $4p$ electron has shifted to a $4s$ orbit. The separations of the ${}^4F_{2,3,4,5}$ levels are found to be in the ratio 2.50:3.52:4.50, in very close agreement with Landé's interval rule which for these levels gives 2.5:3.5:4.5. The relative intensities of the lines in these multiplets conform to the usual rule. A comparison of the data for one, two, and three electron systems of Sc, Ti, and V shows that the addition of first one and then a second d electron causes not only an increase in the multiplicity but also successive shifts in the radiated lines toward the longer wavelengths by very nearly the same frequency interval. It has also been found possible to identify the ${}^4F_{2,3,4,5}-{}^4F'_{2,3,4,5}$ multiplet of Cr IV.

8. A quantitative test of Hund's theory of doublet bands of the OH type. E. C. KEMBLE and F. A. JENKINS, Harvard University.—According to Hund (Zeits. f. Phys. **36,** 657, (1926)) multiple electronic levels in molecules are due to different orientations of the electron spin vector relative to the internuclear axis. At low nuclear speeds the component of the spin vector parallel to the nuclear axis is quantized while at high speeds the component parallel to the resultant angular momentum is quantized. The consequent distortion of the molecule gives rise to bands in which each branch is composed of doublets or triplets with a maximum separation at the origin. In the case of doublets the effect of the distortion on the rotational term formula has been carried through quantitatively by one of the authors (Kemble) and the resulting equations have been tested on the data for NO beta bands by the other (Jenkins). The two levels involved have equal moments of inertia but different values of B in the empirical formula $E/h=A+Bj^2+Cj^3+\cdots$. The observations confirm the theory and in particular check the following formula for $B:B=(1\mp z)^2h/8\pi^2I\pm z^2\Delta_0$ where Δ_0=term difference for doublet at zero rotation and $z=h/(8\pi^2I\Delta_0-2h\pm 2h)$. The upper sign in each case goes with the lower level of the pair.

9. Vibrational levels in the blue-green band system of sodium. F. W. LOOMIS, New York University.—The lines in Wood's magnetic rotation spectrum of sodium vapor may, according to Kemble's theory of the Zeeman effect in band spectra, be considered as approximately representing band origins. Most of those in the blue-green region have been arranged into a band system and their frequencies formulated, in terms of the (integral) vibrational quantum numbers n' and n'', which can, by comparison with the fluorescent series, be unambiguously assigned, as follows:

$$\nu=20301.7+(124.13n'-0.84n'^2)-(158.5n''-0.73n''^2-0.0027n''^3).$$

The location of the n'' levels makes it possible to plot the fluorescent series in the manner used with iodine and to identify approximately the bands to which the fluorescent lines belong. Moreover, when n' and n'' are plotted for all the rotation lines identified, a wide open parabola-like figure appears, of a type which Condon (Phys. Rev. **28,** 1182 (1926)) has accounted for in terms of an hypothesis of Franck. This explains the effect on the fluorescent spectrum of varying the frequency of the exciting light, as reported by Wood (e. g. Physical Optics, Frontispiece, Fig. 8); since the separate patches in the blue and yellow which result from stimulation with blue light correspond to the two arms of the parabola, and the single green patch due to green stimulation corresponds to the vertex.

10. Equations for thermionic emission. W. R. HAM, Pennsylvania State College.—It has recently been shown that an equation of the form $i=A\epsilon^{-b\phi/T}$ applies as well as any other to experimental data on thermionic and photoelectric emission. The derivation of this equation from Richardson's general equation is now discussed. The value for ϕ assumed is $\phi=\phi_0-\frac{1}{2}KT-\int_0^\infty (dv/dx)dx$ where ϕ_0 is independent of T, K is the Boltzmann constant, and dv/dx the potential gradient in the space very near the surface of the thermionic emitter. The experimental and theoretical reasons for the assumption are stated. On substituting this

expression for ϕ in the general equation not only the first equation mentioned appears but also an equation $i = i_0 \exp[(e\int_0^x (dv/dx)dx)/KT]$, which may be used to explain lack of saturation observed in thermionic currents as the applied PD is increased indefinitely. A discussion of the upper limit X of the integral appearing in this last equation follows and it appears that assuming sufficient experimental confirmation of the equation, a variable value of the dielectric constant is indicated in the work function region and this in turn implies that the electrons in this region are still in their atomic orbits.

11. Evidence for collisions of the second kind in the rare gases. GAYLORD P. HARNWELL, Princeton University.—A positive ray apparatus was used to investigate the products of ionization by electron impact in mixtures of helium, neon, and argon. The variation with pressure of the ratio of the two types of positive ions present was investigated in detail for three cases.

Case 1. A mixture of half helium and half neon was investigated. The ratio He/Ne was found to decrease regularly between .03 mm and .15 mm. At .03 mm the mean free path is approximately equal to the dimensions of the apparatus. Case 2. A mixture of half neon and half argon was investigated throughout the same pressure range. The ratio Ne/A decreased regularly between .05 mm and .15mm, but this decrease was less rapid than in Case 1. Case 3. This mixture was half helium and half argon, and the pressure range was as above. The ratio He/A remained constant within experimental error, but as this mixture is least suited to analysis in a positive ray apparatus this result is the least conclusive. The observed effects are best explained by a type of collision of the second kind equivalent to ionization by positive ions. To account for the results obtained an electron must be transferred from an atom to an ion at a certain fraction of the collisions between an atom and an ion of lower ionizing potential.

12. Critical potentials of iron. RICHARD HAMER and S. SINGH, University of Pittsburgh.—The critical potentials of iron were investigated up to 132 volts. A long quartz tube enclosing two electrodes consisting of a central iron rod and a concentric iron cylinder was heated externally. Changes in potential could be made in practically equal or alternately large and small steps. Equal ones facilitated the plotting of differential curves. Alternate large and small steps facilitated observing differential deflections at desired potentials. Applied potentials were measured with a potentiometer. Repeatedly occurring breaks in the current potential curves were taken to indicate critical potentials. Many were checked by the differential methods. Those found are 3.7, 7.15, 11.2, 16.3, 19.4, 24.5, 29.0, 33.9, 38.8, 42.1, 45.7, 48.4, 51.4, 54.8, 61.6, 72.7, 89.6, 103.1, 111.6, 125.8 volts. Thomas and Compton did not find 38.8 and 45.7. Expect 72.7 and 89.6, all check with the observations of Thomas, usually within 0.3 volt. No marked break was, however, observed by us at 82.7. Possibly our 89.6 is an average effect corresponding to his 82.7 and 94.8. The method is being developed to differentiate multiple and fine structure potentials.

13. The ionization in HCl vapor. HENRY A. BARTON, National Research Fellow, Harvard University.—A mass spectrograph was used to study ionization in HCl vapor at low pressures, the resolving power being sufficiently good to distinguish between $(HCl)^+$ and Cl^+ and to separate the isotopes. The results show that in pure HCl the primary type of ion formed by electron impact is $(HCl)^+$. This is true from the ionizing potential of 13.8 volts to at least 75 volts. Cl^- ions were likewise observed but chiefly from near the filament where no electrons of more than three or four volts energy were available. Probably the HCl was dissociated at the filament, the Cl atoms then picking up electrons by virtue of their electron affinity. Further evidence of such dissociation was furnished by the observation of H_2^+, H^+, and Cl^+ ions from impact. These ions were most prominent shortly after evacuation suggesting that water vapor from the walls aided in the dissociation. Detection of $(H_2O)^+$ ions then confirmed the presence of water vapor. After some days the only ions at low pressures were $(HCl)^+$ and Cl^-, the latter probably not from impact. Thus the results are contrary to the previously held assumption that H^+ and Cl^- are the products of electron impact in HCl.

14. Ultra-ionization potentials of mercury. ERNEST O. LAWRENCE, National Research Fellow, Yale University.—By a method of magnetic analysis of the bombarding electrons it has recently been shown that there are a succession of distinct types of inelastic impacts in mercury vapor above the ionization potential. (Phys. Rev. **28,** 947 (1926)). Earlier measurements of the ionization of mercury by electron streams possessing Maxwellian velocity distributions by many investigators failed to bring out these critical potentials, although it seems that they should have been observed in a qualitative manner. The apparent discrepancy has been eliminated for the present investigation has shown that the ultra-ionization potentials are observable when using Maxwellian velocity distributions in the electron streams providing sufficient care is taken to insure constancy of conditions and the ionization is observed at intervals of 0.1 volt.

15. Ionization of mercury vapor by λ2537. PAUL D. FOOTE, Bureau of Standards.—Measurements of the photoelectric effect in Hg vapor were made by the method employed for caesium vapor. (Phys. Rev. **27,** 37 (1926)). Although the data were confined to a vapor pressure range and ratios of amplified photo-current to initial thermionic current, which were less than the corresponding values in caesium at which occur departures from the linear relation between photo-current and illumination, the relation for Hg vapor between illumination I and photo-current Δi was of the form $\Delta i = AI^2/(1+BI)^2$ where A and B are constants for a given vapor pressure. This law holds accurately in the range investigated, 25° to 60°C. Admixture of nitrogen greatly increases the effect while small amounts of hydrogen reduce the current rapidly to zero, as has been found by Houtermans. The above law approaches the relation $\Delta i = AI^2$ for small intensities, as found by Rouse and Giddings, showing that two separate excited atoms (since only the core of λ2537 is effective) are involved in the ionization process. The increase by nitrogen shows that the metastable state 2^3P_0 plays a role. Hydrogen at a pressure of 0.0002 mm reduces the current to half its initial value. Since the quenching of 2^3P_1 by hydrogen, as observed in resonance radiation, is inappreciable for such small pressures the concentration of the $^3P_0$ atoms exceeds by a large factor that of the $^3P_1$ atoms. The complete mechanism of the ionization process is considered in some detail.

16. The striated discharge in hydrogen and helium. JOHN ZELENY, Yale University.—The striated discharge between cold electrodes in hydrogen exhibits the remarkable property that the distance between the striae for constant current in the tube passes through a sharp minimum as the pressure is increased, and at a higher pressure passes through a maximum. The pressures at which these reversals occur and the magnitudes of the changes are dependent on the current through the tube and on some other factors. At pressures near that at which the minimum stria distance is observed, the Faraday dark space, which covers about 2 cm of length in most of the pressure region indicated, contracts and one or more striae leave the head of the positive column and move up to and surround the cathode. The stria distance in helium was measured between pressures of 2.7 mm and 9.7 mm, and for these two pressures was found to be 11.3 mm and 6.0 mm, respectively, with 6 m.a. current. Measurements made in argon, oxygen, and air under the same conditions are also given, but the range of pressures in which measurable striae was observed is much more limited.

17. Pressures in discharge tubes, Part I,—Long slim tubes. W. H. CREW and E. O. HULBURT, Naval Research Laboratory, Washington, D. C.—The pressure changes in a discharge tube 3 m long, diameter 10 mm, due to uncondensed discharges were measured by a striation gauge. The striation gauge consisted of a second discharge tube (joined to the first) excited by direct current calibrated so that the shift of the striations of the positive column with pressure was known. With helium the temperature increment above the temperature, with no discharge, about 300°K, calculated from the pressures, were, respectively, 4°, 13° and 21°C for 200, 600 and 1000 watts in the long tube. With wet hydrogen the pressure increments, corrected for temperature, gave for γ, the concentration of hydrogen atoms (i.e., the number of

atoms divided by the number of atoms plus molecules) values which increased rapidly with the power to about 400 watts, being thereafter appreciably constant; the values of γ for 150 watts in the tube decreased from about 70 to 50 percent as the pressure decreased from 0.6 to 0.15 mm of Hg. With dry hydrogen and with oxygen γ was less, with nitrogen γ was close to zero. Complete curves were obtained with air, CO_2 and CO. Observations were also made with condensed discharges.

18. Movements of striae in discharge tubes under varying pressures. L. H. DAWSON, Naval Research Laboratory, Washington, D. C.—The striae of the positive column of a discharge tube move along the tube when the pressure of the gas in the tube is varied. The curves of this motion have been obtained as a function of the pressure, the distance apart of the electrodes, the diameter of the tube and the density of the current for wet and dry hydrogen, helium, nitrogen, air, carbon monoxide and carbon dioxide. The pressures, measured by a McLeod gauge, ranged from 0.6 to 0.05 mm of mercury. With these curves the discharge tube may be used as a sensitive and quickly responding pressure gauge. The motion of the striations increased with the diameter of the tube being roughly ten times greater in tubes 30 mm in diameter than in tubes 16 mm in diameter. For tubes in which the distance between the electrodes was less than the maximum distance of motion of the striae, as the pressure was diminished the positive column marched into the anode without distortion and vanished.

19. The constancy of the flashing period of a neon glow-lamp. ELIAS KLEIN, Lehigh University.—The comparison of a neon-lamp frequency (operated on d.c.) with that of a standard clock is accomplished by the pendulum which cuts off a light-beam incident upon a photo-electric cell connected with the grid of a vacuum tube. The neon lamp is placed directly in the plate circuit, or in a separate circuit which is coupled to the plate circuit, of the vacuum tube. The period of the lamp is adjusted by capacitance and resistance associated with the lamp. Periodically, the pendulum admits light to the cell, the grid becomes negative and the space-current is reduced to zero thereby suppressing one or more lamp-flashes. While the cell is inoperative the lamp-frequency is again that which is characteristic of the circuit. Therefore, one pendulum cycle marks two clock-intervals during which the lamp completes a number of flashes. If the lamp-period is constant, each interval shows exactly the same number of flashes. Preliminary observations indicate the lamp-period constancy to a fair degree of precision. Replacing the pendulum by a tuning-fork-shutter yields similiar results. This is also a methods for subdividing intervals of time.

20. An absolute ionization vacuum gauge. THOMAS H. JOHNSON, Yale University.—The inconvenience of calibration has been eliminated in this new simply constructed gauge. The electrodes, which consist of a fine, straight incandescent filament between and parallel to two plane plates, are maintained at potentials which give a uniform electric field over the electron paths. The gauge constant, k, defined as the ratio of the pressure to the number of ions per electron, is obtained by means of the relation $k = V_+/(a\int_0^V P(\nu)d\nu)$ where a is the distance and V_+ the potential between the filament and the positive plate, and $P(\nu)$ is the ionization probability per centimeter at unit pressure expressed as a function of the electron energy. (See Compton and VanVoorhis, Phys. Rev. **27**, 724, (1926)). This method of obtalning the gauge constant assumes that all of the positive ions go to the negative plate. Ionization due to secondary electrons is neglected. Furthermore the effect of space charge on the electron paths and the potential distribution along the paths is not considered. However, measurements in mercury vapor in equilibrium with liquid mercury at 0°C, corrected for thermal effusion, show that the calculated constant is very nearly correct if V_+ is greater than 75 volts.

21. Post-arc conductivity and metastable states in mercury. M. L. POOL, University of Chicago (Introduced by A. J. Dempster).—For pressures from 0.3 to 10 mm current—potential curves have been obtained which suggest that around the collecting electrodes

there exist negative and positive space charge sheaths. Residual positive ions may, depending upon the size of the collecting electrodes, be made to persist as long as 1/10 sec. Galvanometric current—low potential curves have been obtained which can be explained by the diffusion of electrons from a region of high electron and positive ion concentration near the cathode. Cathode ray oscillograph curves which show (even in the presence of air, He, H_2, CO_2, or A) a critical potential of about +3.2 volts can be accounted for by the same assumptions. No convincing evidence of a long lived (1/20 sec.) metastable state has been found. The apparent long lived states deduced from absorption of certain spectral lines may be due to the continuous formation of metastable states of very short life as the positive ions recombine. Impurities may thus have a large influence on these short lived atoms while not, however, altering the slow process of their formation.

22. Excitation of mercury vapor by positive ions. ERNEST J. JONES, University of Minnesota.—Saturated mercury vapor at 90°C was bombarded with positive potassium ions from the source developed by Kunsman. The resulting radiation from a field free space was photographed by a quartz spectrograph. At 160 volts accelerating potential only the 2537 line appeared after six hours exposure, with an average ion current of 1.5×10^{-8} amperes. At 640 volts and four hours exposure with an ion current of 2×10^{-8} amperes the following lines were obtained; 2537 ($1S-2p_2$), 3126 ($2p_2-3d_2$), 3132 ($2p_2-3d_3$), 3650 ($2p_1-3d_1$), 4046 ($2p_2-2s$), 4358 ($2p_3-2s$). At 1200 volts and under the same conditions the above lines were again photographed. No new lines appeared. At the latter potential the intensity of lines originating from levels higher than the $2p_2$ was increased roughly 100% relative to that of the 2537 line. Comparison with the spectra excited by the electrons shows; (1) that the efficiency of excitation by positive ions is far less than by electrons; (2) that it increases with velocity at least up to 1200 volts; (3) that up to 1200 volts the probability of excitation to the $2p_2$ level is greater than to higher levels; (4) that up to 1200 volts the excitation to levels higher than the $3d_{1,2,3}$ is not observed with a four hour exposure and current of 2×10^{-8} amp.

23. Velocity selector for atomic rays. J. TYKOCINSKI-TYKOCINER, University of Illinois.—An atomic ray on its way towards a target is directed through two vibrating slits suspended in a magnetic field at a distance D apart. The vibrations are controlled by a piezoelectric oscillator. The emerging ray contains selected velocities. For small ratios of the width w of the slits to its amplitude a, the selected velocities are determined by $v_n=2Df/n$, where f is the frequency of the vibration and $n=0, 1, 2, 3$, etc. For larger w/a ratios velocity bands may be obtained each embracing a range

$$v'_n-v''_n=2Df[1/(n-w/2\pi a)-1/(n+w/2\pi a)]$$

When used in connection with Gerlach and Stern magnetic moment analyzer, spectrum-like images should be obtained consisting of n pairs of sharply defined lines each showing a deflection

$$S_n=[(Ml^2n^2/8mD^2f^2)\ (\partial H/\partial S)_0]\ [\tfrac{1}{2}+\{1/12+(\partial H/\partial S)_1/\tfrac{1}{6}(\partial H/\partial S)_0\}^{1/2}]$$

and a thickness

$$d_n=(\partial H/\partial S)\ (\tfrac{1}{2}+K)Ml^2nw/4mD^2f^2\pi a$$

The value for the magnetic moment M may be determined from either of these relations. For a selector, which is in the course of construction, the following data have been computed for rays of atomic hydrogen at 500°K ($f=9000$ and $n=2$): $v_n=1800$ m/sec; $S_n=1.5$ mm and $d_n=0.095$ mm.

24. Inelastic collisions in ionized gas mixtures. GAYLORD P. HARNWELL, Princeton University.—The variation with pressure of the ionization by electron impact in mixtures of the rare gases with hydrogen and nitrogen was studied using a positive ray apparatus. All the results described refer to mixtures of the gases concerned in equal proportions. Mixtures of hydrogen with helium, neon, and argon were investigated in turn. In each case the number of rare gas ions decreased rapidly after a pressure of about .05 mm was reached. At this

pressure the mean free path was approximately equal to the dimensions of the apparatus. H_2 decreased slightly with pressure but less rapidly than when the rare gas was not present. H_1 and H_3 increased, the latter very rapidly except in the case of the neon mixture where the increase was less marked. In mixtures of nitrogen and the rare gases the same type of effect was observed. At higher pressures the rare gas ions decreased at approximately the same rate as the N_2 ions. The N_1 ions increased, being present in slightly greater numbers when the rare gases were present than when they were not. These results definitely support the other evidence for the existence of a type of collision of the second kind resulting in ionizations by positive ions.

25. Note on "pendulum" orbits in atomic models. R. B. LINDSAY, Yale University.—"Pendulum" or straight line orbits in an atom are usually ruled out as physically impossible since they apparently involve collision of the electron with the nucleus. Nevertheless their value in fixing energy levels was suggested a few years ago by J. W. Nicholson, who sought to show that in the simple two body problem such orbits are possible with quantized energy values of the same form as those of the circular and elliptic orbits (viz., $W = -2\pi^2 Ne^2 m_0/n^2h^2$). Unfortunately in his quantum condition he used the rest mass m_0 throughout instead of the varying mass m. Correction of this error shows that his result is invalid without some modification of his premises. The present writer has been able to obtain quantized "pendulum" orbits with energies equal to the Balmer terms by the assumption that in addition to the inverse square force of attraction between nucleus and electron there is an inverse cube (or higher power) force of repulsion of such a character that it is effective only in the close vicinity of the nucleus, i. e. at a distance of the order of magnitude of 10^{-12} to 10^{-13} cm. It is believed that the result may be of interest in view of the possible utility of straight line orbits in atomic models with more than one electron.

26. Magnetic moments of iron in complex salts. L. A. WELO and O. BAUDISCH, Rockefeller Institute for Medical Research.—Although the moment of iron is 29 magnetons (Weiss) in the ferric ion and about 26 in the ferrous ion, it is known that the moment is nearly zero in the ferrocyanides, the pentacarboynl and the nitroprusside and that it is about 10 magnetons in the ferricyanides. The moment in the ferricyanides is probably the same as in the divalent copper ion. Possibly still other moments in iron may be found, and these may correspond to the ions of other transition elements. With this in view we have made a preliminary survey of 45 rare salts obtained from Professor Weinland of Würzburg. Twenty eight salts have the normal moment of simple ferric salts. Seven are hex-acetates of the type $[Fe_3(CH_3COO)_6(OH_2)]Cl$ and form a well defined group in which each iron atom has the same moment as the nickel ion with 16 magnetons. A hexa-benzoate $[Fe_3(C_6H_5COO)_6(OH)]ClO_4 \cdot C_6H_5COO$ also falls within this group corresponding to nickel. Two complex glycolates $(CH_2O \cdot COO)$ apparently correspond to the chromium ion with 19 magnetons. No correspondences are noted in remaining salts. It was assumed that the salts obey the simple Curie law. Experiments to test this question are under way.

27. A system of structures for atomic nuclei. WARREN W. NICHOLAS, National Research Fellow, Cornell University.—First, a neutron structure is assumed (proton inside electron) which may offer a simple basis for the "packing effect." Second, the known series of isotopes is discussed with reference to the postulate that evolution of light elements was from complex to simple, the nuclei losing units smaller than the α-particle. Third, a geometrical structure for the atomic nucleus (protons and neutrons on alternate cube corners in a cubic lattice) is assumed which shows some main features in common with the known nuclear series. Fourth, a specific structure is proposed for the nucleus of sulphur 32 which can be followed through consecutive disintegrations, thereby accounting for the known isotopes from sulphur 32 to helium 4. Several of the disintegrations seem rather arbitrary, but some of the results, especially concerning the symmetry of the abundant nuclei, are suggestive. The above theory

may be tested by (1) further experiments on artificial disintegration, and by (2) precision determination of isotope masses.

28. On the condition of validity of macromechanics. M. S. VALLARTA, Massachusetts Institute of Technology.—The problem considered in this paper is: Assuming the associated wave of de Broglie and Schrödinger, under what conditions do the trajectories orthogonal to the equiphase surfaces of the wave (i. e., the rays) coincide with the mechanical paths determined by the classical Hamilton principle? If $\alpha(xyz)$ is the amplitude of the associated wave, sufficient conditions are shown to be: (a) α satisfies Laplace's equation, i. e. there are no inhomogeneities in the "medium" where the wave propagates; (b) the frequency of the associated wave is infinite, i. e. Planck's constant vanishes. The necessary and sufficient condition is that the equiphase surfaces determined from the wave equation coincide with the (classical) surfaces of constant action. De Broglie's condition for the validity of macromechanics (Journal de Physique, **7,** 321, (1926)) is then examined and applications to the hydrogen atom are given. The Sommerfeld-Wilson quantum conditions and their generalization by Wentzel (Zs. für Physik, **38,** 518, (1926)) are studied in the light of the above criteria, and it is shown that an azimuthal quantum condition always has a meaning, not however a radial quantum condition.

29. A general proof of the Langevin-Debye formula and the susceptibilities of O_2 and NO. J. H. VAN VLECK, University of Minnesota.—Using the new quantum mechanics, the formula $\alpha+N\mu^2/3kT$ given by Langevin and Debye for magnetic and dielectric susceptibilities respectively is derived without specializing the model further than to assume that the precession frequencies of the moment vector are small compared to kT/h. These precessions may be due to temperature rotation, coupling of spin magnetic moment relative to axis of figure, etc. Thus the Debye formula for dielectric constants is applicable even to asymmetrical polyatomic molecules. Previous explanations of the paramagnetic susceptibilities of gaseous molecules involved the unreasonable assumption of a magnetic moment freely quantized relative to the magnetic field, but now it can be quantized either with reference to the figure or temperature rotation axis (Hund's couplings of types a and b). Quantitative results agreeing with experiment to within about 1% are obtained assuming ^3S normal levels in O_2 and Mulliken's suggestion of ^3P states separated by 122 cm^{-1} in NO. In NO the calculations include corrections for the fact that the contribution of the spin moment is somewhat diminished by its precession frequency (122 cm^{-1}) being comparable to kT/h, while the orbital moment precesses so fast that only its axial component $\sigma_k=1$ is effective.

30. On the calculation of changes of functions involving factorials as applied to entropy calculations. MORTON MASIUS, Worcester Polytechnic Institute.—In entropy calculations in connection with the kinetic theory of gases or the quantum theory the changes in functions depending on factorials have hitherto been calculated by a method depending on the replacement of factorials by continuous functions and differentiation. This method is neither simple nor logically satisfying. A new method of calculation is shown which depends on the direct evaluation, by simple well known processes, of

$$\Delta F = F(x+\Delta x,\ y+\Delta y,\ \cdots) - F(x,\ y,\ \cdots)$$

where F is a function involving the factorials of x, y, $\cdots$, and where x, y, $\cdots$ and $x+\Delta x$, $y+\Delta y$, $\cdots$ are taken as integers. The details of this method are illustrated by the treatment of two examples:

$$F_1 = \log\{\,[(n+p-1)!]/[(n-1)!p!]\}$$

and

$$F_2 = \log\{\,[n!]/[n_0!n_1!n_2!\cdots n_p!]\}$$

In F_1 the change in F_1 produced by some change Δp is found, and in F_2 the condition for making F_2 a maximum, subject to the additional restrictions that $\sum n_i = n$ and $\sum(in_i) = p$ is derived.

31. Properties of substances and mixtures in the condensed state at the absolute zero of temperature. R. D. KLEEMAN, Union College.—With the theoretical researches previously communicated to the Physical Society (Philadelphia meeting) as basis, a number of properties of a substance or mixture in the condensed state at the absolute zero of temperature have been deduced. The most important of these are: $c_v=0$, $(\delta c_v/\delta T)_v=0$, $(\delta^n c_v/\delta v^n)T=0$, $c_p=0$, $(\delta c_p/\delta T)_p=0$, $c=0$, $dc/dT=0$, $(\delta p/\delta T)_v=0$, $(\delta^2 p/\delta T^2)_v=0$, $dp/dT=0$, $d^2p/dT^2=0$, $(\delta v/\delta T)_p=0$, $(\delta^2 v/\delta T^2)_p=0$, $dv/dT=0$, $d^2v/dT^2=0$, where p denotes pressure, v volume, T absolute temperature, and c_v, c_p, c, the specific heats at constant volume, constant pressure, and under vapor pressure, respectively. The total differential coefficients refer to a substance or mixture under the pressure of its vapor. In the paper quoted it was shown directly that $c_v=0$, a result which is included in Nernst's Theorem. It is now shown that also $c_p=0$ and $c=0$, and that the specific heat possesses also the important properties expressed by $(\delta c_v/\delta T)_v=0$, $(\delta c_p/\delta T)_p=0$, and $dc/dT=0$.

32. On the surface heat of charging. LEWI TONKS and IRVING LANGMUIR, General Electric Co.—Two methods are available for calculating the theoretically necessary reversible heat development, or absorption accompanying the charging of the surface of a conductor. One method depends on a new relation $\eta_{s1}-\eta_{s2}=kTln(A_1/A_2)+\epsilon P_{21}$ between the surface heats, η_s of the two surfaces, the A'_s of electron emission equations of the type $i=AT^2e^{-b/T}$ and the Peltier heat at the interface between the conductors. The other method consists of a comparison of the cooling effect of electron emission and the latent heat calculated from the temperature variation of emission. Experimental evidence points to $\eta_s=0$ (nearly), $A=60.2$ amps/cm^2 deg^2 (nearly) for all pure metals. Published cooling effect measurements on an oxide coated filament give $\eta_s=0$ whereas the value of A gives η_s not equal to zero. This leads to no contradiction if only part of the surface is emitting electrons. For monatomic films cooling effect measurements are lacking but the values of A give both positive and negative surface heats of charging.

33. Thermal agitation in conductors. H. NYQUIST, American Telephone and Telegraph Company.—At the December, 1926, meeting of the American Physical Society, J. B. Johnson reported the discovery and measurement of an e.m.f. due to the thermal agitation in conductors. The present paper outlines a theoretical derivation of this effect. A non-dissipative transmission line is brought into thermodynamic equilibrium with conductors of a definite temperature. The line is then isolated and its energy investigated statistically. The resultant formula is $E_\nu^2 d\nu=4kTRd\nu$ for the r.m.s. e.m.f. E_ν contributed in a frequency range one cycle wide by a network whose resistance component at the frequency ν is R. T and k are the absolute temperature and the Boltzmann constant. Experimental data are available for the audible range and there the agreement between the formula and the data is good. It will be observed that neither the charge nor mass nor any other property of the carrier of electricity enters the formula explicitly. They enter indirectly through R. The formula above is based on the equipartition law. If the quantum distribution law is used the expression becomes

$$E_\nu^2 d\nu=[4h\nu R/(e^{h\nu/kT}-1)]d\nu.$$

The two expressions are indistinguishable in the range of the measurements.

34. Temperature variations in wires heated by alternating current. L. SMEDE, Westinghouse Elec. and Mfg. Co., East Pittsburgh.—Corbino, in 1910 and 1911, gave a solution of the problem of the temperature variation of a wire heated by alternating current. In this solution it is assumed that the temperature variation is small compared to the average temperature of the wire. Certain terms are neglected in order to simplify the solution, which seem too large to neglect. In the present paper it is assumed that, for small temperature variations, the radiation is proportional to the first power of the absolute temperature, and that the resistance remains constant. On these assumptions an equation is derived which gives the same temperature variation as derived by Corbino.

35. The potential of photoactive cells containing fluorescent electrolytes. H. W. RUSSELL, Cornell University.—The variation of the potential of a photoactive cell containing a fluorescent electrolyte with time of illumination has long been a subject of dispute. Goldmann in particular, having noted that the potential approached a maximum which was independent of the intensity of the exciting light, arrived at a potential-time law on a theory involving the Hallwachs photo-electric effect. Measurements on cells with sputtered platinum electrodes containing Rhodamin B in absolute alcohol have been made. The potential has been measured with a string electrometer of small capacity and short period. Goldmann's limiting potential was not found. The magnitude of the effect does not vary with the frequency of the exciting light in accord with the true photo-electric effect, yellow light being more effective than blue light of the same intensity. A theory has been developed on the assumption that the exciting light causes a permanent chemical change in the electrolyte. Diffusion plays an important part in the potential-time relation. This theory predicts the shape of the potential-time curve and its variation with the intensity of the exciting light.

36. Optical absorption and photo-electric conductivity of sulphur crystals. B. KURRELMEYER, Harvard University.—The optical absorption and photo-electric conductivity of single crystals of rhombic sulphur have been measured over the visible spectrum. The absorption is complete in the violet, but is relatively low from 500 to 650 mμ. The photo-electric conductivity is measurable between 400 and 650 mμ; its maximum, referred to unit incident energy, lies at 470 mμ. There is strict proportionality between photocurrent and light intensity and between photocurrent and electric intensity throughout the ranges used. If there is a saturation value of the electric intensity it probably lies above 30,000 volts per cm, and is therefore very much higher than the saturation electric intensity in the diamond and in zincblende. This fact may be connected with the relative magnitudes of the refractive indices. The conductivity referred to unit absorbed light energy does not seem to obey the linear relation demanded by the quantum mechanism usually assumed for its production.

37. The periodicity of photo-electric thresholds. GEORGE B. WELSH, Cornell University.—Considering the photo-electric threshold as a measure of the energy taken from the incident radiation in order to detach one of the outer electrons from its atom, the elements having the most loosely bound electrons should permit detachment with the expenditure of minimum amounts of energy. Using the present available data, the curve showing the relation between photo-electric thresholds and atomic numbers exhibits a certain periodicity with strong maxima for the alkali metals and decreasing values as one proceeds towards the more electonegative elements. The curve also shows minor peaks for Cu and Ag, but none for Au, where it might have been expected. When the widely varying conditions of observation are considered the amount of agreement is surprisingly good. A new measurement for the threshold of Ge (2590 A) and a tentative one for Be are included; both of these assume their expected positions on the curve.

38. Tests of a New Selective Radiometer of Molybdenite. W. W. COBLENTZ, Bureau of Standards.—The radiometers were lamina of molybdenite having a resistance of about 40,000 ohms, and spots of only one actinoelectric polarity. A 10-ohm Thomson galvanometer was used. Focusing an artificial star (pinhole in front of a flat incandescent tungsten filament) on a vacuum stellar thermocouple (non-selective) gave a deflection of 232 cm; and 45 cm on the molybdenite receiver. The latter deflection would be increased about 60-fold (2500 cm) by using a high-resistance galvanometer. Measurements by Coblentz and Stetson at Benkoelen, Sumatra, Jan. 1, 1926, using a high resistance d'Arsonval gave a deflection of 2mm in moonlight of 0.008 foot candle normal intensity. This could be magnified by using a lens or mirror. Settings on the star Vega (mag. 0.14) by Coblentz and Lampland, Oct. 1926, using the 42-inch Lowell reflector and a 5-ohm Thomson galvanometer gave deflections of 4 to 5 mm. With an electrometer or a suitable galvanometer the deflection would have been increased about 100-

fold (40 to 50 cm) which is 10 times that observed with a stellar thermocouple. A patient examination of molybdenite from various sources may reveal samples even more sensitive than those just described.

39. Thermal conductivity of fused quartz as a function of temperature. HERMAN E. SEEMANN, Cornell University.—Preliminary measurements of the thermal conductivity of a specimen of clear fused quartz indicate that this property increases linearly with the temperature, within experimental error, from .0026 cal./cm. deg. sec. at −25°C to .0064 cal./cm. deg. sec. at 950°C. The specimen was in the form of a hollow cylinder, closed at one end with a hemispherical cap. Energy to maintain a steady temperature gradient was supplied by means of an electrically heated filament mounted axially inside the specimen. Thermal contact with the specimen was made with mercury inside and outside at the lower temperatures and with the tin-lead eutectic at the higher temperatures. Inside and outside temperatures were obtained with thermocouples. A guard ring scheme was used to prevent heat loss or gain at the open end of the cylinder and correction was made for the heat flow through the hemispherical end cap.

40. Thermal expansion of beryllium. PETER HIDNERT and W. T. SWEENEY, Bureau of Standards.—Data on the linear thermal expansion of beryllium between −120 and +700°C have recently been obtained. The rod investigated was prepared by the Beryllium Corporation of America, and was found to have a density of 1.835 grams per cubic centimeter at 20°C. The coefficient of expansion increases rapidly with temperature. The coefficients or rates of expansion at −110 and +650°C are 5×10^{-6} and 20×10^{-6} respectively. Beryllium expands considerably less than the other elements of sub-group II B (Mg, Zn, Cd and Hg). Average coefficients of expansion for various temperature ranges are given in the following table.

Temperature Range: °C	Coefficient of Expansion $\times10^6$	Temperature Range: °C	Coefficient of Expansion $\times10^6$
−100 to − 50	7.0	20 to 300	14.0
−120 " + 20	8.1	20 " 400	14.8
− 50 " 20	9.8	20 " 500	15.5
+ 20 " 100	12.3	20 " 600	16.1
20 " 200	13.3	20 " 700	16.8

41. Internal friction in solids. A. L. KIMBALL and D. E. LOVELL, General Electric Co.—The internal friction of seventeen different solids is studied by a method previously described before this society (Phys. Rev. **25,** 899 (1925)). By this method it was found that in every case the dissipative forces were the same whatever the speed of deformation, contrary to the assumption of many investigators that the forces are greater the more rapid the deformation. A simple approximate law of internal friction in solids which in general best fits the facts is $F=\xi f_m^2$ where F=frictional loss per unit volume per cycle of stress at a point in the solid f_m=maximum value of the stress amplitude at that point during a stress cycle. ξ=proportionality factor which may be called the internal friction constant. Values of ξ are tabulated for a number of different solids.

42. The nodal lines of bells. ARTHUR TABER JONES, Smith College.—Two systems of nodal lines are generally recognized for bells: A system of circles parallel to the mouth, and a system of vertical meridians. In the present work the number and position of these lines are checked for the lower modes of vibration and are determined for higher modes than those for which they have previously been known. The work was done as part of another investigation on the ten bells of the Harkness Memorial Chime at Yale University. The method was similar to that described in the Physical Review, **16,** 247 (1920). On all of the Harkness bells the first ten partials have respectively the following numbers of nodal meridians: 4, 4, 6, 6, 8, 8, 10, 8, 10, 12. The nodal circles are more difficult to determine. For the first seven partials

the numbers of nodal circles are: 0, 1, 0, 1, 1, 2, 2. The nodal circle for the second partial lies about 1/3 of the way up the bell, and for the fourth and fifth partials the corresponding fractions are about 1/6 and 1/2. Surfaces of minimum intensity in the air close to the bells spread away from the metal in different directions for different partials.

43. Determination of the surface area of adsorbers. KARL HOROVITZ, International Research Fellow, Rockefeller Institute.—It is known that certain fatty acids or their compounds form mono-molecular layers covering the available surfaces (Langmuir, Harkins, a.o.). Extensive experiments on surface tension of sodium oleate solutions under various conditions (DuNouy) lead to the conclusion that sodium oleate is also adsorbed in a mono-molecular layer at the interface of two phases. Assuming that this mono-molecular layer of sodium oleate is formed on every adsorber it is possible in an exceedingly simple manner to determine the surface area of the adsorber from the quantity of sodium oleate adsorbed and the known dimensions of the sodium oleate molecule. The adsorption of the sodium oleate was determined from the change in the static values for the surface tension of the sodium oleate solutions at different concentrations, using the ring method (DuNouy tensiometer). The surface of different charcoals determined by this method was found to be of the order of magnitude of some 100 per sq. m.g. charcoal, the comparative surface areas for charcoals of different origins being in good agreement with the determination by other methods and other investigators.

44. A type of oscillation hysteresis. LAURISTON TAYLOR, Cornell University (Introduced by E. Merritt).—A simple triode oscillator was modified by placing a high resistance (.5–1.0 meg) shunted by a capacity of $1/10\mu$f, in series with the grid. The circuit then oscillates intermittently, the period during which oscillation occurs being called a zule. Over a wide region the zule frequency F is found to obey a simple relation to the constants of the circuit, i. e., $F=A \exp [(L_2-kC_2)/2L_1]$, where A and k are constants. At the borders of these regions F is extremely sensitive to very small changes in L_2 and C_2. A theory is given for the zule formation showing how they are related to the state of depression of the grid potential. Their finite length is due to a type of oscillation hysteresis, where oscillation ceases at one value of E_g and is resumed at a higher value. At the end of a zule, the mean of E_g is equal to the dynamic cut-off potential, and at the start of the next zule is several volts higher, increasing exponentially between these values. The variations of E_g were later studied by means of a synchronized oscilloscope, and all points of the theory were checked. Oscillation within the main circuit showed the same formation except that the potential between zules was constant.

45. A shear mode of crystal vibration. W. G. Cady, Wesleyan University.—In the various applications of piezo-electric quartz plates, it has until recently been customary to cut the plates with their faces perpendicular to an electric axis. The vibrations of such plates are then longitudinal, *i. e.*, stationary waves of compression and rarefaction. Various observers have recently found that plates cut *parallel* to the electric and optic axes (*i.e.*, parallel to a natural prismatic face of the crystal) are good piezo-electric oscillators, but hitherto no explanation has been offered. According to Voigt's theory of piezo-electricity, an electric field perpendicular to the electric and optic axes causes a shearing stress about the optic axis. Hence the deformation of a plate cut as indicated, when in a field normal to its surface, is a shearing strain, and under an alternating impressed field vibrations are to be expected, whose resonant frequency is determined by the shear-inertia of the plate and by the elastic force of restitution. Computed and observed values of the natural frequency are in satisfactory agreement.

46. Theory and application of low frequency piezo-electric vibrations in quartz plates. J. R. HARRISON, Wesleyan University.—Further study of the phenomena described at the December meeting (Phys. Rev. 29, p. 366, 1927) indicates that the observed frequencies of vibration are sufficiently in accord with those calculated from the formula for flexural vibrations to make it fairly certain that the vibrations are of this type. In general, agreement between

MAY 10 1927

theory and observation is best for relatively long plates as would be expected. With relatively long rods the second mode of vibration having three nodes has also been observed. These facts are illustrated by numerical data and curves. An empirical formula has been derived which fits the observed data better than the theoretical equation for flexural vibrations. A plate $30\times10\times1$ mm vibrating at 60 kc was placed in the circuit of a type UX-210 tube as a power oscillator. The observed output power was about $\frac{1}{2}$ watt, which considering the low frequency compares favorably with the output from a high frequency quartz oscillators.

47. Theory of the magnetic nature of gravity and the Balmer series. CORNELIO L. SAGUI, Castelnuovo dei Sabbioni, Italy.—In a preceding paper dealing with a corpuscular conception of energy the equation $(x^2+x)/2=y$ was found for the variation of the gravitational potential of physical nature, at least for an atomic space. The geometrical variation due to the Newtonian law is here not considered. With the same equation the Balmer lines are now studied and a physical meaning found for doublets, triplets and other groups of this kind. The stark effect is also considered. The radiation of energy is also investigated and it is supposed to be due to a magnetic depression on the front of the traveling ray. Suggestion is given as to the astronomical verification of such a fact.

AUTHOR INDEX

Barton, Henry A.—No. 13
Baudisch, O.—see Welo
Cady, W. G.—No. 45
Clarke, Harry—No. 2
Coblentz, W. W.—No. 38
Crew, W. H. and E. O. Hulburt—No. 17
Dawson, L. H.—No. 18.
Duane, William—No. 5
Foote, Paul D.—No. 15
Gibbs, R. C. and H. E. White—No. 7.
Ham, W. R.—No. 10
Hamer, Richard and S. Singh—No. 12
Harnwell, Gaylord P.—Nos. 11, 24
Harrison, J. R.—No. 46
Hidnert, Peter and W. T. Sweeney—No. 40
Horovitz, Karl—No. 43
Hulburt, E. O.—see Crew
Jauncey, G. E. M.—No. 1
Jenkins, F. A.—see Kemble.
Johnson, Thomas H.—No. 20
Jones, Arthur Tabor—No. 42
Jones, Ernest J.—No. 22
Kemble, E. C. and F. A. Jenkins—No. 8
Kimball, A. L. and D. E. Lovell—No. 41
Kleeman, R. D.—No. 31
Klein, Elias—No. 19
Kurrelmeyer, B.—No. 36
Laird, Elizabeth R.—No. 3
Langmuir, Irving—see Tonks
Lawrence, Ernest O.—No. 14
Lindsay, R. B.—No. 25
Loomis, F. W.—No. 9
Lovell, D. E.—see Kimball
Masius, Morton,—No. 30
Meggers, William F.—see Russell
Nicholas, Warren W.—No. 27
Nyquist, H.—No. 33
Pool, M. L.—No. 21
Richtmyer, F. K. and L. S. Taylor—No. 4
Russell, Henry Norris, and William F. Meggers—No. 6
Russel, H. W.—No. 35
Sagui, Cornelio L.—No. 47
Seemann, Herman E.—No. 39
Singh, S.—see Hamer
Smede, L.—No. 34
Sweeney, W. T.—see Hidnert
Taylor, Lauriston—No. 44
Taylor, L. S.—see Richtmyer
Tonks, Lewi, and Irving Langmuir—No. 32
Tykocinski-Tykociner, J.—No. 23
Vallarta, M. S.—No. 28
Van Vleck, J. H.—No. 29
Welch, George B.—No. 37
Welo, L. A. and O. Baudisch—No. 26
White, H. E.—see Gibbs
Zeleny, John—No. 16